PROTEIN ARGININE METHYLTRANSFERASE 5 IN CASTRATION-RESISTANT AND NEUROENDOCRINE PROSTATE CANCER

by

Elena Wild

A Dissertation

Submitted to the Faculty of Purdue University

In Partial Fulfillment of the Requirements for the degree of

Doctor of Philosophy

Department of Medicinal Chemistry and Molecular Pharmacology

West Lafayette, Indiana

December 2020

THE PURDUE UNIVERSITY GRADUATE SCHOOL
STATEMENT OF COMMITTEE APPROVAL

Dr. Chang-Deng Hu, Chair

Department of Medicinal Chemistry and Molecular Pharmacology

Dr. Ourania Andrisani

Department of Basic Medical Sciences

Dr. Emily Dykhuizen

Department of Medicinal Chemistry and Molecular Pharmacology

Dr. Michael Wendt

Department of Medicinal Chemistry and Molecular Pharmacology

Approved by:

Dr. Zhong-Yin Zhang

This dissertation is dedicated to my parents, Vladimir Beketov and Dr. Nina Beketova, and to my husband Todd Wild.

Always with love.

ACKNOWLEDGMENTS

First and foremost, I want to thank my thesis advisor and mentor, Dr. Chang-Deng Hu, for the endless support and enthusiasm for research. His determination and guidance helped me so much that I cannot find words to express my gratitude. I am deeply thankful to my thesis committee members, Dr. Ourania Andrisani, Dr. Emily Dykhuizen, and Dr. Michael Wendt, for the insightful discussions of my research and encouragement. I am also deeply thankful to my former thesis committee member Dr. Alice Chang, who also was the head of my preliminary examination committee, for all the helpful suggestions and discussions. I am also very thankful for the help of the great collaborators of our lab, Dr. Wan, Dr. Jiang, and Dr. Huang, and their lab members.

I want to thank all past and present members of Dr. Hu's lab, especially Sarah Kelsey, Dr. Jake Owens, Sam Tinsley, and Andrew Asberry. Their support and friendship were incredibly valuable throughout my studies. I would also like to thank all the other – so many! – friends I made at Purdue, particularly "Lab Savages" crew and the Purdue Night Train Swing and Blues dance club members. Making friends overseas was one of the best parts of my graduate journey. Blues and swing dancing quickly became a huge part of my life and was a perfect way to have a small break from the lab to meet people, have fun, and stay sane.

I am endlessly grateful to so many professors and instructors at the Lomonosov Moscow State University, particularly to Dr. Nikolay Gusev, the head of my home Biochemistry Department. His devotion to mentoring students and passion for biochemistry is an inspiration for me. I am also very thankful to my research mentor Dr. Alexey Katrukha who gave me an opportunity to begin my journey as a researcher. I also want to sincerely thank all my friends whom I left in Russia and who still supported me from overseas, especially Dr. Maria Savvateeva and Dr. Julia Sukhanova. I am incredibly glad we can stay in touch while being thousands of miles and even more thousands of kilometers away.

My very special thanks to my parents Vladimir Beketov and Dr. Nina Beketova, for the endless love, support, and encouragement. I miss seeing them in person very much. I am incredibly lucky that the first people I ever knew – my parents – are scientists. Both as loving parents and devoted researchers, their example and support were a deciding factor for choosing my path.

My very big thank you is to my husband, Todd Wild. I cannot imagine making it through the graduate studies without your support, particularly in the latest months of thesis writing. I

would not be the person I am now without you. I cannot wait to see where the next adventures with you and our puppy Tesla will bring us.

I would also like to acknowledge many funding sources that allowed me to work on the following research. This work was supported by the grants: U.S. Army Medical Research Acquisition Activity (W81XWH-16-10394), NCI RO1CA212403, Purdue University Center for Cancer Research Small Grants, Purdue Research Foundation Research Grant, Indiana University Simon Comprehensive Cancer Center (P30CA082709), Purdue University Center for Cancer Research (P30CA023168), Walther Cancer Foundation, and Indiana University Precision Health Initiative (PHI). I was also a recipient of the College of Pharmacy PRF Graduate Research Fellowship, Purdue University Center for Cancer Research SIRG Graduate Fellowship, and Bilsland Dissertation Fellowship.

TABLE OF CONTENTS

LIST OF FIGURES

LIST OF ABBREVIATIONS

aDMA:	asymmetrically dimethylated arginine
ADT:	androgen deprivation therapy
AKT:	protein kinase B
AML:	acute myeloid leukemia
ANOVA:	analysis of variance
AP:	anterior (lobe of) prostate
AR:	androgen receptor
AR-FL:	androgen receptor full length
AR-V:	androgen receptor variant
ARE:	androgen response element
ASI:	androgen signaling inhibitor
BiFC:	bimolecular fluorescence complementation
bp:	base pair
BPH:	benign prostate hyperplasia
BRCA1/2:	breast cancer (gene) 1/2
cAMP:	cyclic adenosine monophosphate
CBP:	CREB-binding protein
cDNA:	complementary DNA
CDS-FBS:	charcoal-dextran stripped FBS
CFP:	cerulean fluorescent protein
CgA:	chromogranin A
ChIP:	chromatin immunoprecipitation
ChIP-seq:	chromatin immunoprecipitation (with) sequencing

CITED2:	CBP interacting transactivator glutamine/asparagine rich C-terminal domain 2
COPR5:	cooperator of PRMT5
CREB:	cAMP response element-binding protein transcription factor
CRPC:	castration-resistant prostate cancer
CYP17A1:	cytochrome P450 family 17 subfamily A member 1
Da:	Dalton
DAB:	3,3'-diaminobenzidine
DAVID:	database for annotation, visualization and integrated discovery
DEG:	differentially expressed gene
DET:	differentially expressed transcript
DHT:	dihydrotestosterone
DLP:	dorso-lateral (lobe of) prostate
DMSO:	dimethylsulfoxide
DNA:	deoxyribonucleic acid
DNMT:	DNA methyltransferase
Dox:	doxycycline
DTT:	dithiothreitol
EDTA:	ethylenediaminetetraacetic acid
EGFR:	epidermal growth factor receptor
EMT:	epithelial-mesenchymal transition
ERG:	ETS-related gene
ETS:	erythroblast transformation specific
EZH2:	enhancer of zeste homolog 2
FBS:	fetal bovine serum
FDA:	(US) Food (and) Drug Administration

FDR:	false discovery rate
GAPDH:	glyceraldehyde 3-phosphate dehydrogenase
GEM:	genetically engineered mouse
GEO:	Gene Expression Omnibus
GO:	gene ontology
HDAC:	histone deacetylase
HE:	hematoxylin (and) eosin
HNPC:	hormone-naïve prostate cancer
IHC:	immunohistochemistry
IP:	immunoprecipitation
IVL:	involucrin
KEGG:	Kyoto Encyclopedia of Genes and Genomes
KLK:	kallikrein
LBD:	ligand binding domain
LHRH:	luteinizing hormone-releasing hormone
MEP50:	methylosome protein 50
MLL:	mixed lineage leukemia
MMA:	monomethylarginine
mRNA:	messenger RNA
MTAP:	S-methyl-5'-thioadenosine phosphorylase
NE:	neuroendocrine
NED:	neuroendocrine differentiation
NEPC:	neuroendocrine prostate cancer
NES:	nuclear export signal
NLS:	nuclear localization signal

NRG: non-obese diabetic-Rag1(null)-γ chain(null)

NSE: neuron-specific enolase

PARP: poly (ADP-ribose) polymerase

PB: probasin

PBS: phosphate buffered saline

PCR: polymerase chain reaction

PIN: prostate intraepithelial neoplasia

PMSF: phenylmethylsulfonyl fluoride

PNPP: para-nitrophenylphosphate

PPI: protein-protein interaction

PRC2: polycomb repressive complex 2

PROTAC: proteolysis targeting chimera

PRMT: protein arginine methyltransferase

PSA: prostate-specific antigen

PSMA: prostate-specific membrane antigen

PTEN: phosphatase and tensin homolog

qPCR: quantitative PCR

RB1: retinoblastoma (protein) 1

RIOK1: right open (reading frame serine/threonine-protein) kinase 1

RNA: ribonucleic acid

RRID: research resource identifier

RT: reverse transcription

SAM: S-adenosylmethionine

SC: scramble control

shRNA: short hairpin RNA

snRNP:	small nuclear ribonucleoprotein
TMA:	tissue microarray
TMRSS2:	transmembrane protease, serine 2
TSS:	transcription start site
VC:	Venus fluorescent protein C-terminal part
VN:	Venus fluorescent protein N-terminal part
VP:	ventral (lobe of) prostate
WDR5:	WD repeat domain 5 (protein)
WHO:	World Health Organization
WT:	wild type
YFP:	yellow fluorescent protein

ABSTRACT

Prostate cancer is one of the most frequently diagnosed cancers and the second leading cause of cancer-related deaths in male population. While localized prostate cancer can be successfully treated with surgery or radiation therapy, the metastatic disease has no curable options. Metastasis can be developed as a result of failed therapy of localized cancer or present at initial diagnosis. As metastasis is the most common cause of prostate cancer-related death, developing novel approaches and improving the efficiency of existing therapies for the metastatic prostate cancer treatment will significantly improve patients' survival.

The first-line treatment option for metastatic prostate cancer and localized prostate cancer with high risk of recurrence is androgen deprivation therapy (ADT) that decreases androgen receptor (AR) signaling. However, targeting AR signaling inevitably leads to AR reactivation and cancer progression to the castration-resistant prostate cancer (CRPC) that has no curable treatment options. Moreover, about 30% of CRPC cases progress to neuroendocrine prostate cancer (NEPC), highly aggressive and lethal type of prostate cancer.

Recently my group has shown that protein arginine methyltransferase 5 (PRMT5) functions as an activator of AR expression in hormone-naïve prostate cancer (HNPC). In this dissertation, I demonstrate that PRMT5 also functions as an epigenetic activator of *AR* transcription in CRPC via symmetric dimethylation of H4R3 at the *AR* promoter. This epigenetic activation is dependent on pICln, a PRMT5 interaction partner involved in spliceosome assembly, and independent of MEP50, the canonical cofactor of PRMT5. PRMT5 and pICln, but not MEP50, were required for the expression of AR signaling pathway genes. In clinical samples of both HNPC and CRPC, nuclear PRMT5 and pICln protein expressions were highly positively correlated with nuclear AR protein expression. In xenograft tumors, targeting PRMT5 or pICln significantly decreased tumor growth and AR expression.

Overall, this work identifies PRMT5/pICln as a therapeutic target for HNPC and CRPC treatment that needs to be further evaluated in clinical setting.

CHAPTER 1. INTRODUCTION

Fragments of the following chapter were submitted for publication in *Cancer Gene Therapy* as a part of review article but were not published at the time of dissertation deposit.

1.1 Prostate in normal organism

1.1.1 Prostate function and structure

Prostate is a male reproductive gland that contributes to the production of seminal plasma via secretion of alkaline fluid containing proteins such as prostate specific antigen (PSA) and other kallikreins, metabolites such as citrate and spermine, trace elements such as zinc, and other factors [1]. Prostatic secretion alongside with the secretions of other male accessory glands (seminal vesicles and bulbourethral glands) is necessary for the sustaining of proper function of sperm cells and male fertility [1].

The prostate gland surrounds the proximal urethra close to the base of the bladder and is often described as "walnut-shape" organ [2]. Normal healthy prostate has size of approximately 3 × 3 × 5 cm. There are three glandular zones in the prostate that differ by the embryological origins and can be defined via histological and anatomical markers: central, transitional, and peripheral zones [2,3]. Peripheral zone makes up approximately 70% of the prostate organ volume while the rest 20% and 10% of volume contain transitional and central zone, correspondingly. The importance of the distinction of these three zones is underscored by the differential emergence of prostate-associated diseases: benign prostatic hyperplasia (BPH, the common age-associated benign enlargement of the prostate) arises exclusively in the transitional zone while the prostate carcinoma mostly arises in the peripheral zone [3].

In terms of microscopic anatomy and cell types composition, prostate consists of epithelial cells that form glands and perform secretory function, and stromal cells that support the epithelial cells via paracrine signaling and are critical for the normal prostate development [4]. Stroma consists of resident mesenchymal cells, several types of immune cells, nerves, and extracellular matrix proteins [5].

Within the epithelial compartment, there are three major cell types: basal (expressing cytokeratin 14 and p63), luminal (expressing cytokeratin 8 and prostate-specific markers such as

Nkx3.1), and neuroendocrine (NE, expressing markers chromogranin A (CgA) and neuron-specific enolase (NSE) among others) [6]. Luminal cells are the major secretory compartment of the prostate, while basal cells support luminal cells phenotype and gene expression [6]. NE cells make up to less than 1% of normal prostate cellular content and possess hybrid features of epithelial, neural, and endocrine nature. These cells secrete various products, including, but not limited to, serotonin, chromogranin peptides, calcitonin, neuropeptide Y, somatostatin, and bombesin/gastrin releasing peptide [7]. NE cells cannot be identified via conventional hematoxylin and eosin staining (HE), instead, they can be detected with immunochemistry staining. NE cells bear long dendrite-like projections that extend to the nearby epithelial cells. Thus, it was hypothesized that NE cells perform regulatory function to support luminal cells via paracrine mechanism [7].

Interestingly, prostate epithelium cells produce energy via glycolysis, the property usually attributed to cancer cells and not cells of the healthy organism. Thus, prostate epithelium and blood cells are the only cells of healthy organism to produce energy using glycolysis pathway [1].

1.1.2 Hormonal signaling in normal prostate

Androgen/androgen receptor (AR) signaling is crucial for the prostate development and the maintenance of prostate epithelium in adult prostate [8]. Luminal epithelium and stromal cells express AR while basal epithelium cells are mostly AR-negative [8].

In mammals, there are two naturally occurring agonists of AR: testosterone, which is the primary androgen produced by testes, and dihydrotestosterone (DHT), which is more potent in terms of AR activation [9]. Testosterone is converted to DHT by the enzyme 5α-reductase in the prostate. During the prostate development, activated by the DHT AR in the stroma of embryonic urogenital sinus initiates prostatic development via paracrine signaling [10]. The lack of functional 5α-reductase in urogenital sinus results in the abnormal development of extremely small prostate that does not have prostate epithelium [11] while inactivating *AR* mutations or *AR* knockout completely abolish the formation of prostate [12].

In the adult prostate, AR signaling promotes maintenance of the prostate epithelium [13]. Normally, about 2% of prostate epithelium cells die every day, and this rate of cell death has to be compensated by cell proliferation [14]. Castration, leading to drastic reduction of serum testosterone and DHT, results in apoptotic death of approximately 70% of prostate epithelium

luminal cells although stromal and basal epithelium cells survive, and notably, stromal cells express AR indicating that androgens are not required for the maintenance of stroma [13]. Thus, prostate epithelium maintenance requires AR-dependent signaling from stromal cells, and in the epithelial cells AR signaling activates secretion of metabolites and proteins described above [15].

AR belongs to a superfamily of nuclear steroid receptor transcription factors. In the absence of agonists, AR is inactive and bound to the cytoplasmic chaperone proteins such as heat shock protein 90 [16]. The binding of agonists causes conformational change resulting in the dissociation of chaperones, exposure of nuclear localization signal (NLS), dimerization of AR, and nuclear transportation of the dimer [17]. In the nucleus, AR dimer binds to the regulatory elements of genes (androgen response elements, ARE) to regulate the transcription of its target genes [18] such as PSA and TMPRSS2.

Structurally, AR protein has three functional domains: (1) N-terminal domain required for transcriptional activation by AR; (2) a zinc finger DNA-binding domain; and (3) C-terminal ligand-binding domain that are encoded by 8 exons of the *AR* gene located on the X chromosome [19]. Ligand binding to the ligand-binding pocket of AR changes the conformation of receptor to simultaneously promote interaction between N- and C- termini and DNA-binding domains of two AR molecules, expose the NLS located next to DNA-binding domain, and allow binding of co-activators such as p300 to the N-terminal domain. Interaction with co-activators causes chromatin to shift into more open conformation at target genes regulatory elements thus facilitating the transcription of target genes [20]. Although the mechanism of gene transcription activation by AR is well characterized, AR can also facilitate transcriptional repression through a less described mechanism [15]. Understanding of the mechanism of AR function both in healthy prostate and disease stimulated development of AR-targeted therapies for the treatment of prostate cancer.

1.2 Prostate cancer

1.2.1 Prostate cancer statistics

Prostate cancer is the most frequently diagnosed non-skin cancer in males in United States [21]. In American men population, prostate cancer is diagnosed in 1 out of 5 of all new cancer cases [21]. Prostate cancer disproportionally affects people of African descent: Black people have the highest prostate cancer mortality rate among all races [22]. Other risk factors for prostate cancer

include age (majority of prostate cancer cases is diagnosed in men over 65 years old), family history, and to less extent factors like diet, obesity, and smoking [23,24]. Although significant progress of prostate cancer treatment has been made over the past 20 years decreasing the death rate by approximately 52% (compared to 1993), the 5-year survival rate for patients with distant metastasis is only 30%, and prostate cancer remains a second-leading cause of cancer death in men in US [21]. In contrast, the 5-year survival rate for localized and regional prostate cancer among all the races is over 99%. Thus, understanding the molecular mechanisms underlying the development and survival of metastatic prostate cancer and improving the efficiency of existing treatments and developing novel approaches for metastatic disease are urgently needed.

1.2.2 Prostate cancer diagnosis

Prior to 1980s, prostate cancer was mainly diagnosed through the observation of clinical symptoms such as local pain, urinary and sexual dysfunction combined with digital rectal exam. Lack of robust diagnostic system often caused a late diagnosis. Discovery of PSA presence in the serum of prostate cancer patients in 1980 [25] led to the development of PSA test systems that are widely used nowadays for early prostate cancer diagnosis. In case of healthy prostate, PSA can be detected mostly in prostate tissue and seminal plasma with serum concentration typically below 2.5 ng/mL. For PSA levels 2.5 ng/mL to 4 ng/mL, it is usually up to a healthcare provider to assign further testing based on the patient's condition. PSA level of 4 ng/mL and higher usually indicates a need for more detailed testing possibly including biopsies, imaging, genetic tests and others. PSA level of >10 ng/mL indicate ~50% probability of prostate cancer presence [26].

If a biopsy is recommended, the prostate tissue gets examined, and in case of prostate cancer detection, a grade will be assigned to determine further treatment option. Since the development by Donald Gleason in 1966, Gleason scoring system (with modifications) remained a cornerstone of prostate cancer management. In this system, the grade is assigned to the prostate cancer tissue based on the glandular morphology and a level of differentiation within the tissue [27]. Tissues with the score of 6 and below are well-differentiated (low-grade), 7 is moderately-differentiated, and 8 to 10 are poorly differentiated. However, Gleason score cannot be applied to the samples from distant metastasis of prostate adenocarcinoma. If there is a chance of prostate cancer spreading outside of prostate, additional imaging (ultrasound, magnetic resonance imaging,

bone scans, etc.) can be performed to determine the TNM score of cancer. TNM score describes the primary tumor (T), spread to closely located lymph nodes (N), and presence of metastasis (M).

Prostate cancer progresses from clinical stage from I to stage IV. Stage I prostate cancer is located in a part of the prostate, stage II tumors typically spread in more than one part of prostate, stage III indicates cancer growth in nearby tissues but not the lymph nodes, and stage IV means cancer growth in lymph nodes and other organs. Most common sites for prostate cancer metastasis are bones, lungs, and bladder. Clinical staging combined with other factors will largely determine the necessary treatment for the prostate cancer.

1.2.3 Prostate cancer treatment

The choice of treatment for every stage of prostate cancer is based on the risk of recurrence. "High-risk" tumors have a high probability to recur even after the successful local therapy [28]. The updated The National Comprehensive Cancer Network guideline stratifies following risk groups: very low, low, intermediate favorable, intermediate unfavorable, high, and very high. Stratification of patients into risk groups is based on combination of TNM score, Gleason score, and PSA level.

Clinical stages of prostate cancer I to III (localized disease) are usually managed using active surveillance (for "low-risk" prostate cancer), or radical prostatectomy and radiation therapy, often combined with androgen deprivation therapy (ADT) for "high-risk" prostate cancer [28,29]. Localized prostate cancer recurs in ~35% of cases and progresses to metastatic disease, which is treated with ADT.

The effect of androgen deprivation on the prostate cancer was first described by Charles Huggins and his student Clarence Hodges at the University of Chicago in 1941. Huggins and Hodges treated prostate cancer patients with either surgical castration or estrogen injection and observed a reduction of the tumor growth [30]. Twenty-five years later, for this landmark discovery Charles Huggins was awarded a Nobel Prize in Physiology and Medicine. At the time, the discovery was particularly important as the PSA test was not developed yet, and majority of patients were present at late stage, often with metastatic disease. Since this breakthrough, various methods for the suppression of circulating androgens production were developed in addition to initially used surgical castration and estrogens treatment, both of which cause significant adverse effects and decrease patients' quality of life.

Testosterone is mainly synthetized in testes (much smaller portion is produced in adrenal cortex) in response to luteinizing hormone, production of which by pituitary gland is controlled by luteinizing hormone-releasing hormone (LHRH) produced in hypothalamus. Both LHRH agonists and antagonists are used to suppress the production of testosterone. The use of LHRH agonists for the suppression of androgen production by testes is possible because of the negative feedback loop regulation: high levels of testosterone reduce production of LHRH and luteinizing hormone. In case of this therapy, androgen suppression is delayed by nearly 2 weeks. Additionally, about 10% of patients treated with LHRH agonists experience sharp increase of testosterone level (so called "flare") due to the initial increase of luteinizing hormone level. Flare causes patients to experience bone pain and troubles with urinating [31]. Patients with high risk of clinical complications due to the androgen flare are typically treated with LHRH antagonists: LHRH antagonists are able to decrease androgen production within hours [32]. Nonetheless, both LHRH agonists and antagonists do not affect production of androgens by the adrenal cortex thus decreasing the efficiency of androgen level suppression.

Another approach to decrease the level of circulating androgens involves direct inhibition of enzymes that participate in the cascade of reactions converting cholesterol to testosterone. Steroid 17-[alpha]-hydroxylase/17,20 lyase (CYP17A1) is an enzyme involved in the critical step of androgen biosynthesis and thus is a prominent target for the androgens level control [33]. Abiraterone acetate, a potent CYP17A1 inhibitor, was first approved by FDA for the prostate cancer therapy in 2011. Notably, abiraterone acetate treatment blocks both testicular and adrenal cortex production of androgens.

Finally, androgen signaling can be decreased by directly preventing binding of androgens to AR and preventing AR translocation to the nucleus. These compounds are often called "anti-androgens"; several generations of anti-androgens have been developed to date [34]. Although bilateral orchiectomy remains in use worldwide, medical castration is used instead if possible, due to the psychological effect and impact on the quality of life of surgical castration [35].

Beyond ADT, treatment options for metastatic disease are limited due to the emergence of cancer resistance that I will discuss below. Often existing therapies for prostate cancer post-ADT step will include cytotoxic agents for chemotherapy. The most commonly used agents are taxanes docetaxel and cabazitaxel that stabilize microtubules and thus disrupt cell division, topoisomerase inhibitor mitoxantrone that intercalates into DNA and cross-links it, and estramustine that disrupts

microtubules [36]. However, chemotherapeutics often cause multiple significant adverse effects, such as hair loss, nausea, diarrhea, and fatigue, among others, and provide improvement of overall survival by only a few months [36].

Additionally, Sipuleucel-T, radium-223 dichloride, and PARP inhibitors are used for certain patients alone or in combination with ADT or chemotherapy. Autologous cellular immunotherapeutic vaccine Sipuleucel-T is used for prostate cancer that is post-ADT but does not show significant cancer-related symptoms [37]. It should be noted that, overall, prostate cancer cells express relatively low amount of tumor neo-antigens thus causing prostate cancer cells to be less responsive to the immune checkpoint therapy [38]. Radium-223 dichloride is used for the treatment of patients with only bone metastasis (no signs of visceral metastasis) as this radioactive compound is selectively accumulated in bones similarly to calcium [39]. Poly (ADP)-ribose polymerase (PARP) inhibitors olaparib and rucaparib are most beneficial for patients with mutations in genes involved in the repair of DNA such as BRCA1 and BRCA2 and other defects in DNA damage repair system. In fact, in May 2020 FDA approved the use of PARP inhibitors for patients with metastatic disease post-hormonal therapy. Olaparib was approved for patients with mutations in any out of 14 homologous recombination genes, and rucaparib was approved for patients with mutations in BRCA1 or 2 [40].

Overall, ADT is the mainstay of prostate cancer therapy, being the first-line treatment option for metastatic disease and used in combination with radiation or surgery for high-risk non-metastatic disease. Thus, improving ADT outcomes and reducing side effects will have a major impact on prostate cancer patients' quality of life and survival.

1.3 ADT leads to the deadly terminal stage of prostate cancer

ADT exploits the unique dependence of prostate cancer cells on the androgen/AR signaling. Decreasing the serum levels of circulating androgens to the <50 ng/dL (1.74 nmol/L), the level achieved by surgical castration, significantly slows the tumor growth and alleviates cancer-related symptoms, although patients can experience decreased bone density, sexual dysfunction, and hot flashes. In spite of initial response, in 18-35 months prostate cancer inevitably progresses despite the castrate level of serum androgens [41]. At this stage, the disease is called "castration-resistant prostate cancer" (CRPC) and is incurable. This is opposed to the prostate cancer pre-ADT that responds to the ADT well. At this pre-ADT stage prostate cancer is called

"hormone-naïve prostate cancer" (HNPC). CRPC was also historically referred to as "hormone-refractory" or "androgen-independent", based on the presumption that tumors maintain androgens level as low as serum. Later discoveries suggest that CRPC tumors often maintain active AR signaling lead to revision of this concept and corrected disease name.

1.3.1 AR signaling in therapeutic resistance during CRPC progression

Prostate cancer cells are able to overcome low levels of androgens and continue to proliferate. Often tumors maintain active AR signaling even with the low level of serum androgens while a smaller fraction of tumors evade ADT through non-AR related mechanisms [42]. This maintenance of active proliferation in prostate cancer cells is possible due to AR signaling reactivation that can occur via multiple mechanisms.

CRPC tumors tend to maintain higher expression of AR protein compared to normal prostate tissues and HNPC tumors [43]. This, in turn, is also possible due to several mechanisms. First, *AR* gene amplification is observed in 50-70% of CRPC cases and is extremely rarely observed in HNPC tumors [44,45]. Second, long-term androgen depletion can lead to the upregulation of AR mRNA resulting in increased AR protein expression [46]. Several authors proposed alteration of miRNAs regulating AR mRNA in CRPC, also leading to increased AR mRNA and protein expression [47–49]. Overall, high levels of AR protein hypersensitizes CRPC cells to the low castrate serum levels of androgens [46].

In addition to alterations leading to increased AR protein, CRPC tumors often bear activating point mutations of *AR* causing AR protein to be activated by weaker ligands such as testosterone and other steroid hormones (estrogen, progesterone, and glucocorticoids among others) or even get activated by antagonists (enzalutamide and bicalutamide). Activating AR mutations can be found in up to 20% of CRPC tumors [50]. The most common activating AR mutations include T878A or S, H875Y and L702H; these mutations can be observed in patients treated with abiraterone and anti-androgens, and these mutations cause AR responsiveness to antagonists and mentioned above ligands [51].

The function of AR as transcription factor is modulated by the interaction of AR with co-activators and co-repressors. Over 150 of such co-regulators were identified for AR, and dysregulation of co-activators and co-repressors has been implicated in the CRPC progression

[20,52]. Often, AR co-activators are upregulated while co-repressors are downregulated, thus allowing AR to continue signaling in the low level or androgens [53].

While serum testosterone level in patients post-ADT drops drastically, the prostate and metastatic tumor levels of androgens may remain as high as 20% of androgens level before treatment [54]. Prostate cancer cells are able to synthetize androgen precursors and convert them to DHT. CRPC cells have several folds elevated levels of enzymes required for these reactions compared to HNPC cells [55]. Although abiraterone treatment inhibits the key enzyme of androgen synthesis, CYP17A1, CRPC cells can bypass this inhibition via expression of AR with gain-of-function mutations, elevated levels of CYP17A1, and expression of ligand-independent alternatively spliced variants of AR.

The alternatively spliced variants of AR (AR-Vs) lack ligand-binding domain and are able to remain in active state in terms of nuclear translocation and transcription activation even in the absence of androgens. Currently, over 20 of AR-Vs were described in prostate cancer cell lines, xenograft tumors, and patients samples [56,57]. Some of these variants have disruptions in NLS (mapped to exon 3 and 4) and tend to remain cytoplasmic [58]. However, other variants are able to translocate into the nucleus and function as transcription factor. Very low levels of mRNA for these variants can be detected in HNPC samples, but CRPC samples contain high levels of AR-Vs mRNA and protein [44,59].

Out of the AR variants, AR-V7 (also sometimes referred to as AR3) has particular clinical significance. AR-V7 can be detected in 18-28% of CRPC tissues [60], and AR-V7 high expression indicates poor patients' prognosis [60]. Tumors that express AR-V7 are more resistant to the anti-androgen treatment. Although AR-V7 lacks NLS from exons 3-4, it actively gets translocated to nucleus. It was suggested that unique C-terminus of AR-V7 translated from cryptic exon 3 of AR gene contains NLS-like sequence [61]. It is still debated whether AR-V7 and other AR-Vs activate unique sets of genes, or the same as full-length AR (AR-FL), or both [62–64].

Given that targeting LBD of AR is ineffective for prostate cancer tumors with AR-Vs expression [65], there is a need for novel therapeutic approaches to target all AR variants. One possible approach is targeting AR expression via AR protein degradation; such targeting suppressed prostate cancer cell growth in several pre-clinical studies [66,67]. An AR degrader utilizing proteolysis targeting chimeras (PROTAC) technology is currently in a Phase I clinical

trial [68]. However, targeting AR signaling can be hampered by emergence of neuroendocrine differentiation (NED).

1.3.2 Neuroendocrine differentiation (NED) in therapeutic resistance of prostate cancer

NED allows prostate cancer cells to bypass suppression of AR signaling during ADT and to maintain cell proliferation and survival. During NED, prostate cancer cells that usually demonstrate prostate luminal features [69] lose characteristic for prostate luminal cells AR/PSA expression and acquire features that can be observed in normal NE cells such as expression of CgA and NSE [7]. Due to this similarity, prostate cancer cells that acquired NE features are often called NE-like cells. But, as opposed to normal prostate NE cells expressing basal markers such as cytokeratin 5, prostate cancer NE-like cells express luminal cytokeratin 18 and other luminal markers but lack basal markers [7]. These observations, along with genetics studies in prostate cancer tumors showing that genetic aberrations are conserved between adenocarcinomas and prostate tumors with NED, demonstrate that NE-like cells of prostate cancer might have luminal origin [70].

However, the cellular origin of both NE-like cells and adenocarcinoma is still being heavily debated [71,72] with evidences suggesting that both luminal and basal cells can serve as cells or origin for adenocarcinoma or NE-like cells as demonstrated in genetically-engineered mouse (GEM) models [73,74] and organoid culture [75,76].

As NE-like cells do not express AR and are not dependent on the AR signaling, they can survive ADT and function at the castrate level of androgens. Furthermore, NE-like cells, due to the endocrine ability, can maintain proliferation of tumor cells in paracrine manner. This ability is highlighted by the observation that NE-like cells grafted in the flank of castrated mice stimulated the growth of LNCaP xenografts in the opposite flank [77]. Additionally, NE-like cells are resistant to apoptosis [78] and promote apoptotic resistance in the surrounding cells [79]. Thus, emergence of NE-like cells and associated neuroendocrine prostate cancer (NEPC) presents a significant therapeutic challenge.

1.3.3 NEPC is the most aggressive form of prostate cancer

NEPC is a broad term used to describe a spectrum of prostate cancer conditions with NE-like cells presence which can get confusing. According to the World Health Organization (WHO), NEPC tumors can be classified into five subtypes: (1) adenocarcinoma with NE features (positive for AR and PSA as normal adenocarcinoma but with elevated presence of NE-like cells); (2) adenocarcinoma with Paneth-like cells NED (characterized by the presence of cells demonstrating NE-like features and at the same time resembling Paneth cells of small intestine due to the presence of eosinophilic granules); (3) carcinoid tumor (true "pure" NE tumor); (4) small cell carcinoma (characterized by the presence of small cells with high nuclear to cytoplasmic ratio and nuclear fragility); and (5) large cell NE carcinoma (rare type characterized by the presence of large groups of cells with abundant cytoplasm and high mitotic rate) [80]. In practice, patients can be present with tumors that do not exactly fit in the WHO classification such as mixed NE carcinoma/adenocarcinoma and demonstrate a spectrum of both usual adenocarcinoma and NE features often with distinct boundaries for each tumor type [81,82].

NEPC can develop spontaneously but these cases of carcinoid tumors are extremely rare, representing less than 2% of prostate cancer cases, and tend to be extremely aggressive with overall patients survival of less than a year [83]. Most often NEPC develops after the course of ADT, with estimation of up to 30% of CRPC cases showing NED [84]. As NEPC cells express low levels of AR and PSA, the prostate cancer progression to NEPC is easy to overlook when using PSA test. Furthermore, it was suggested that increased use of androgen signaling inhibitors (ASIs) abiraterone acetate and enzalutamide may promote NED and NEPC progression [85,86].

NEPC is the most lethal subtype of prostate cancer [87]: compared to adenocarcinoma with median survival of about 10 years (often attributed to old age and not to the disease itself), the median survival length for NEPC patients is only 7 months [88,89]. There are no curative treatment options available for NEPC patients. Current therapeutic approaches include taxanes (cabazitaxel and docetaxel) and platinum-based chemotherapy regimen, however, these treatment options prolong patients' survival by only 3-5 months and are associated with high toxicity [90].

Interestingly, ADT is not the only way to induce NEPC in prostate cancer. Previously, my group has demonstrated that prostate cancer cells can transdifferentiate into NE-like phenotype when exposed to ionizing radiation mimicking radiation therapy [91,92]. It was also shown that multiple agents can induce NED in prostate cancer cell culture [93]. Importantly, NED is not

exclusive for prostate cancer: for example, lung cancer cells post-EGFR inhibitors therapy are able to undergo shift to a small cell phenotype which is also associated with mutations and downregulation of EGFR [94]. Taken together, these evidences suggest that NED can be a common mechanism of therapeutic resistance in cancer.

1.3.4 Genetic aberrations in CRPC and NEPC

As I mentioned above, genetic studies of AR-driven CRPC tumors and NEPC tumors indicate the divergent evolution of NEPC cells from CRPC cells [95]. That is, NEPC cells share multiple genetic aberrations with CRPC cells but have distinct epigenetic landscapes [96].

Phosphatase and tensin homologue (PTEN) tumor suppressor inactivation is one of the most common alterations for primary prostate cancer, CRPC, and NEPC [97]. Most often, PTEN inactivation is mediated by *PTEN* gene loss, however, in some cases inactivation is connected to *PTEN* mutations and epigenetic silencing (Cancer Genome Atlas). Frequency of PTEN inactivation is positively correlated with the tumor Gleason score and prostate cancer stage [98], and homozygous PTEN deletion is often observed in metastatic prostate cancer [99]. Inactivation of PTEN leads to the activation of PI3K/Akt signaling pathway and bypass of G_1 cell cycle check-point [100]. In GEM model, prostate-specific deletion of *PTEN* led to the quick development of metastatic prostate cancer [101].

PTEN inactivation is often associated with ETS fusions [45]. Fusions of genes of ETS family with androgen-regulated genes are very common in all types of prostate cancer [102]. Out of these rearrangements, fusion of prostate-specific androgen-regulated gene *TMPRSS2* and *ERG*, transcription factor from ETS family, is present in nearly 50% of all prostate cancer cases [102]. Mechanistically, presence of this fusion leads to aberrant androgen-dependent activation of ERG, promoting prostate cancer cells proliferation. At the same time, ERG overexpression suppresses NED and promotes AR signaling in GEM [103]. Interestingly, ERG rearrangements are unique for prostate cancer and can be used for the identification the origin of metastatic tumor [104].

Another tumor suppressor often lost in advanced prostate cancer is *TP53*; this loss is detected in 66.7% of NEPC and 31.4% of CRPC [105]. In GEM model, inactivation of p53 alone led to the development of prostate intraepithelial neoplasia (PIN, the first step of prostate cancer development) [106] suggesting that additional genetic rearrangements are required to initiate prostate cancer. Notably, double inactivation of PTEN and p53 in GEM model led to the

development of prostate tumors with spectrum of NE-like features which was not observed in mice with PTEN inactivation only [107].

Loss of tumor suppressor *RB1* is detected concurrently with *TP53* loss in over 50% of NEPC cases and only 13% of CRPC cases [105]. Moreover, concomitant inactivation of RB1 and TP53 promoted formation of tumors with NE-like features in GEM model [108] suggesting cooperative loss of these tumor suppressors in NED.

MYC and N-Myc were both implicated in the prostate cancer progression and lineage plasticity [109]. MYC is a positive regulator of *AR* transcription and a prominent oncogene in prostate cancer [110]. *MYC* is frequently amplified in both CRPC and NEPC, indicating that this transcription factor is required in the earlier progression of prostate cancer [109]. On the opposite, expression of N-Myc (encoded by *MYCN* gene) is higher in NEPC compare to non-NE-like tumors of prostate [111]. N-Myc simultaneously interacts with AR and EZH2 to promote transcriptional repression of AR target genes during prostate cancer neuroendocrine differentiation [111].

Overall, a plethora of studies attempted to described the role of PTEN, RB1, p53, Myc family factors, and the combinations in progression of prostate cancer [106,108,111–113] showing that as little as two of these factors can be required for some induction of NED. One recent study examined in details the role of all 4 of these factors by “one-out” principle [76]. This study has shown that MYC overexpression and PTEN inactivation are required for tumor formation while RB1 and TP53 inactivation are required for NED. Combination of MYC overexpression, PTEN, RB1, and p53 inactivation led to induction of tumors with strong NE-like features, and this is common for NED in prostate and lung cells. Interestingly, MYC overexpression led to more robust induction of NED than N-Myc overexpression (from a personal conversation at the SBUR meeting, unpublished).

Discovery of master regulators of mentioned above aberrations will allow to design novel therapeutic approaches for NEPC and CRPC treatment. Importantly, as many genetic aberrations are shared between CRPC and NEPC while these two cancers demonstrate distinct phenotypes, it is likely that epigenetic regulation plays critical role in progression of CRPC to NEPC.

1.4 Protein arginine methyltransferase 5 (PRMT5) in healthy organism and cancers

1.4.1 PRMT5 enzymatic function

PRMT5 belongs to a family of protein arginine methyltransferases (PRMTs), the enzymes catalyzing transfer of the methyl group from S-adenosylmethionine (SAM) donor on the arginine residues of various proteins [114]. Methylation of the arginine residue does not change the charge of the residue but increases hydrophobicity and the size of the residue, decreases the potential of the arginine guanidyl group to form hydrogen bonds with its partners, thus affecting protein-protein, protein-DNA, and protein-RNA interactions of the substrate protein [115].

Guanidine group of the arginine residue has two terminal (ω) nitrogen atoms and one δ atom available for methylation resulting in total 5 possible positions for methylation. Based on the ability to methylate certain nitrogen atoms in the arginine, PRMTs are classified into 4 types: (1) type I PRMTs catalyze formation of ω-N^G-monomethylarginine (MMA) and ω-N^G,N^G-asymmetric dimethylarginine (aDMA); (2) type II PRMTs catalyze formation of MMA and ω-N^G,N^G-symmetric dimethylarginine (sDMA); (3) type III PRMTs catalyzes only formation of MMA; and (4) type IV PRMTs catalyze formation of δ-N-monomethylarginine [116]. Type IV PRMTs can be found only in yeasts. In humans, 9 PRMTs were identified: PRMT1, 2, 3, 4, 6, and 8 are type I, PRMT5 and 9 are type II, and PRMT7 is the only type III PRMT.

In terms of substrate preference, sequences rich in glycine and arginine (RG/RGG motifs) are most commonly identified for PRMTs [117] with the exception of PRMT4 preferring proline, glycine, and methionine-rich motifs, and PRMT7 preferring arginine-any aminoacid-arginine motifs in lysine-rich surroundings [118]. PRMT5 is a distributive (non-processive) enzyme which means that after the first methylation reaction monomethylated product is released, and dimethylated product is formed in the second independent reaction [119].

1.4.2 PRMT5 regulates various cellular processes

PRMT5-driven methylation is implicated in a variety of processes related to development, healthy organism homeostasis, and disease state. PRMT5 homologues can be found in all eukaryotic species [120]. PRMT5 knockout in mice is embryonic lethal, indicating significant role of PRMT5 in developing organism. It was demonstrated that PRMT5 is important for embryonic stem cell pluripotency [121]. Tissue-specific knockout identified role of PRMT5 in nervous,

muscular, and reproductive system and hematopoiesis [122]. PRMT5 expression is higher during the embryonic developmental stages and lower in most normal tissues in adults [121]. PRMT5 has been linked to multiple cancers, including breast cancer, colon cancer, leukemia, lung cancer, lymphoma, melanoma, pancreatic, and prostate cancer [122,123], and high PRMT5 expression correlates with worse patient overall survival prognosis and clinical outcomes [124,125].

Through the symmetric dimethylation of histones [114,120,126] and multiple signaling molecules [126] PRMT5 epigenetically and post-translationally regulates cell proliferation and differentiation, cell cycle progression, DNA damage response (DDR), and cell death [114,120,126]. PRMT5 methylates histones H2AR3 (H2AR3me2s), H3R2 (H3R2me2s), H3R8 (H3R8me2s), and H4R3 (H4R3me2s), and various signaling molecules such as NF-κB, EGFR, p53, and others.

In general, PRMT5 is considered an epigenetic repressor of target gene transcription via symmetric dimethylation of histones H4R3, H3R8, and H2AR3 [114,120,126], however, recent studies demonstrate that PRMT5 can function as activator of gene transcription via symmetric dimethylation of H3R2, H3R8, and H4R3 [127–129].

1.4.3 Regulation of PRMT5 activity and target gene expression by interacting proteins

PRMT5 enzymatic activity is low in the absence of its interacting proteins. Methylosome protein 50 (MEP50) is believed to be a critical PRMT5 cofactor facilitating substrate recognition and positioning of substrate peptide via interaction with the N-terminal region of PRMT5 [119,130]. PRMT5 and MEP50 form a unique heterooctameric complex with 4 PRMT5 and 4 MEP50 molecules [119].

PRMT5 can interact with several proteins in addition to MEP50, and these interacting proteins may regulate the enzymatic activity and substrate specificity [131–135]. Studies utilizing purified recombinant proteins suggest that MEP50 is an obligate cofactor of PRMT5 required for methyltransferase activity while proteins such as RioK1 and pICln alter substrate specificity [132,135]. However, in the context of prostate cancer, pICln [136] but not MEP50 [137] mediates PRMT5 activity towards histones at the promoters of PRMT5 target genes.

Recently, my group demonstrated that PRMT5 and pICln bind to the promoters of multiple DNA damage response genes to symmetrically dimethylate histone H4R3, and this recruitment of PRMT5/pICln and histone methylation is enhanced upon DNA damage [136]. Mechanistically,

while overall expression of pICln and MEP50 did not change upon DNA damage, subcellular distribution of pICln and MEP50 changed oppositely: pICln accumulated in the nucleus while MEP50 localized in the cytoplasm.

As pICln and MEP50 can both enhance PRMT5 activity and H4R3 methylation is involved in both activation and repression of target gene expression [114,120,126,136], the composition of its interacting proteins may likely determine the activation or repression of PRMT5 target gene expression. Indeed, MEP50, pICln, and PRMT5 all bound to the promoter of PRMT5-repressed gene involucrin [138] and mediated repression of involucrin transcription. Thus, it is likely that MEP50 participates in transcriptional repression of PRMT5 target genes, whereas pICln participates in transcriptional activation of PRMT5 target genes.

1.5 PRMT5-driven regulation of AR signaling in prostate cancer

Androgen/AR signaling is the major driver of the normal prostate function and prostate cancer growth and progression [139]. Due to the critical role of AR signaling in prostate cancer, AR remains the primary therapeutic focus for this disease. Indeed, androgen deprivation therapy (ADT) suppresses the production of androgens or inhibition of AR itself and is the standard of care for metastatic prostate cancer [140]. However, AR signaling plasticity leads to the emergence of the therapeutic resistance and the development of castration-resistant prostate cancer (CRPC) via multiple mechanisms of AR reactivation, including emergence of gain-of-function mutations, *AR* gene amplification, and expression of ligand-independent splice variants [141]. Thus, understanding the regulatory mechanisms of AR expression and activity is necessary to develop novel approaches for the prostate cancer treatment.

1.5.1 Epigenetic regulation of *AR* transcription.

Epigenetic mechanisms mediate both positive and negative regulation of *AR* transcription [142]. As early as 2000, it was demonstrated that the level of *AR* promoter DNA methylation negatively correlates with AR expression [143]. Since then, multiple mechanisms such as histone methylation and expression of non-coding RNAs were identified to contribute to *AR* transcription [142]. The first report indicating the potential implication of histone methylation on *AR* transcription was published in 2012 [144]. In this study, treatment of LNCaP cells with the

inhibitor of multiple methyltransferases adenosine dialdehyde caused downregulation of AR expression, decrease of H3K9 methylation, and inhibition of cell growth. However, that study did not address the effect of general methyltransferases inhibition on the other methylation marks.

In 2017, it was shown that PRMT5 binds to the *AR* promoter and symmetrically dimethylates H4R3 at the *AR* promoter in hormone-naïve prostate cancer cell line LNCaP [137] (Figure 1.1). Targeting PRMT5 via either pharmacological inhibition or short hairpin RNA (shRNA)-mediated knockdown caused decrease of AR mRNA and protein expression accompanied by the decrease of cell proliferation in both cell culture and in LNCaP xenograft model. It was demonstrated that transcription factor Sp1 recruits PRMT5 to the *AR* promoter as PRMT5 does not have a DNA binding domain. However, since expression of AR splice variants and mutants is a major driver of prostate cancer progression, it will be necessary to investigate whether PRMT5 also epigenetically regulates AR expression in CRPC. As PRMT5-driven methylation of histones can also promote deposition of transcription activation marks such as H3K4me3 [127,129,145], it will also be interesting to investigate the potential interplay between arginine methylation and other chromatin modification marks in the context of AR transcription regulation.

1.5.2 Regulation of transcription factor-mediated *AR* transcription

In addition to direct regulation of *AR* transcription by methylation of histones at the proximal AR promoter, PRMT5 may also control *AR* transcription indirectly via modulation of AR-regulating transcription factors (Figure 1.1). For example, Sp1 is a major transcription factor to activate expression of AR [146]. In acute myeloid leukemia, PRMT5 downregulation causes downregulation of Sp1 expression likely via de-repression of miRNA miR-29b [128]. Interestingly, Sp1 recruits PRMT5 to the *AR* proximal promoter region to activate *AR* transcription in prostate cancer cells [137]. Given that expression of miR-29b is significantly lower in prostate cancer compared to normal tissues [147], it is likely that this positive feedback loop plays an essential role in regulation of AR expression in prostate cancer cells.

Like Sp1, c-Myc is another positive regulator of *AR* transcription and a prominent oncogene in prostate cancer [110]. c-Myc can also recruit PRMT5 to its target genes in glioblastoma [148]. Interestingly, c-Myc has been shown to upregulate PRMT5 transcription [149], and, vice versa, PRMT5 has been shown to upregulate c-Myc expression [150] in

lymphoma, suggesting another potential positive feedback loop mechanism. N-Myc, another transcription factor of Myc family, was implicated in progression of prostate adenocarcinoma to neuroendocrine prostate cancer (NEPC) [151]. Importantly, N-Myc simultaneously interacts with AR and EZH2 to promote transcriptional repression of AR target genes during prostate cancer neuroendocrine differentiation [111]. In neuroblastoma, PRMT5 functions as a key regulator of N-Myc protein stability [152]. With the prominent role of N-Myc in NEPC, it will be interesting to investigate if PRMT5 also regulates N-Myc stability in prostate cancer and if targeting PRMT5 can suppress the growth of NEPC via down-regulation of N-Myc expression.

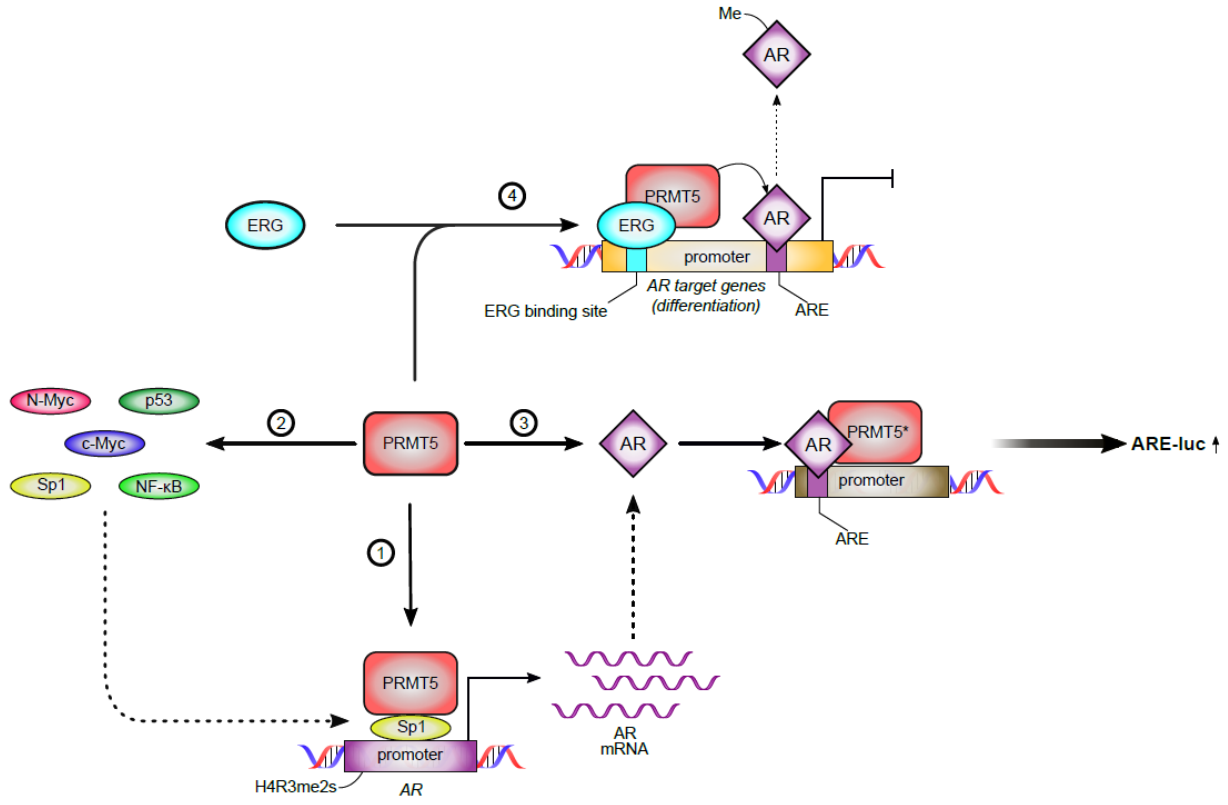

Figure 1.1. Mechanisms of PRMT5-driven regulation of AR signaling in prostate cancer.

PRMT5 is implicated in the regulation of AR signaling at multiple steps: (1) PRMT5 is recruited to the *AR* promoter by Sp1 to symmetrically dimethylate H4R3 thus promoting *AR* transcription. (2) PRMT5 can modulate activity of transcriptions factors that regulate AR expression. (3) PRMT5 can function as an AR co-activator independently of its methyltransferase activity to enhance activation of AR target gene expression. (4) PRMT5 can methylate AR in an ERG-dependent manner leading to a decreased recruitment of AR to the AR target gene promoters of differentiation-promoting genes leading to the increased cell proliferation. *mechanism (3) is independent of PRMT5 enzymatic activity.

Another transcription factor implicated in regulation of AR transcription in prostate cancer is NF-κB. NF-κB was shown to be capable of both transcriptional activation and repression of AR, indicating the context-dependent role of this protein [153,154]. In several models, NF-κB is activated by PRMT5 methylation enhancing NF-κB binding to target genes [155,156]. Thus, it is likely that in prostate cancer with PRMT5 overexpression [137], PRMT5 promotes AR expression via NF-κB activation. Interestingly, p53 is implicated in regulation of AR expression as transcriptional repressor [157], while PRMT5-mediated methylation inactivates p53 in lymphoma model [158]. In summary, PRMT5 is involved in regulation of AR expression at several levels, including direct transcription activation via association with *AR* promoter and modulation of AR-regulating transcription factors.

1.5.3 Regulation of AR transcriptional activity and target gene expression

Apart from regulating AR expression, PRMT5 can regulate AR activity directly by interacting with AR protein and modulating AR function as a transcription factor (Figure 1.1). The study by Hosohata et al. [159] suggested that PRMT5 may function as an AR co-activator independently of PRMT5 methyltransferase activity. Overexpression of either wild-type PRMT5 or the catalytically inactive PRMT5(R368A) mutant in PC3 cells enhanced luciferase activity of an androgen-responsive element (ARE)-containing luciferase reporter.

However, later report by Mounir et al. [160] indicated that in VCaP cells, PRMT5-mediated methylation of AR attenuated AR binding to a subset of AR target genes. This methylation led to the repression of genes associated with prostatic epithelium differentiation and promoted VCaP cell proliferation. The interaction of PRMT5 and AR was mediated by ERG and only occurred in TMPRSS2-ERG-positive cell lines such as VCaP but not TMRSS2-ERG-negative cell lines such as 22Rv1. However, PRMT5 may also interact with AR in TMRSS2-ERG-negative PC3 via the PRMT5-interacting protein MEP50, which was also reported to act as AR co-activator [161,162]. Taken together, these studies demonstrate that PRMT5 can regulate AR activity via non-epigenetic mechanisms in a context-dependent manner.

1.6 Interplay of PRMT5 with epigenetic regulators in prostate cancer cells

1.6.1 PRMT5 and other arginine methyltransferases

Arginine methylation is a ubiquitous posttranslational modification across species [116]. Eleven arginine methyltransferases have been described to date, and their function has been reviewed elsewhere [163,164]. However, PRMT5 is the most widely studied type II enzyme and PRMT9 is the only other type II enzyme. Out of these eleven enzymes, four were shown to monomethylate and asymmetrically dimethylate the same histone residues as PRMT5: H2AR3 by PRMT7, H3R2 by PRMT6, H3R8 by PRMT2, H4R3 by PRMT1, PRMT6, and PRMT7.

While PRMT1 and PRMT5 depose different types of methylation marks (asymmetrical vs symmetrical dimethylation) and possibly act in the opposite ways [165,166], inhibition of both PRMT5 and PRMT1 had synergistic effect in lung and pancreatic cells [167]. However, their potential competition was not explored in the context of prostate cancer. It remains to be established if both enzymes inhibition is a better therapeutic approach, especially in methylthioadenosine phosphorylase (MTAP)-deficient prostate cancer [168]. There is no direct evidence suggesting interplay between PRMT2 and PRMT5, and their relationship remains to be investigated. PRMT6 was suggested to be an oncogene in prostate cancer via activation of PI3K/Akt pathway, possibly by increasing asymmetrical dimethylation of H3R2 on the target gene promoters [169]. Interestingly, PRMT6 knockdown increased AR expression in prostate cancer cells, though whether PRMT6 directly regulates AR transcription via asymmetrical dimethylation of H3R2 or H4R3 remains to be determined [137]. However, PRMT5-driven symmetrical dimethylation of H3R2 enhanced the binding of H3R2 by the epigenetic reader WDR5 [145,170], while asymmetrical dimethylation of H3R2 (mark that is catalyzed by PRMT6) prevented the binding of WDR5 in biochemical assay [171]. These observations suggest that PRMT5 and PRMT6 may play opposite roles via regulation of target gene expression by depositing different types of arginine methylation, at least on H3R2 in prostate cancer cells.

Role of PRMT7 was not explored in the context of prostate cancer. However, PRMT7 expression is detected in prostate cancer (Protein Atlas), and PRMT7-mediated H4R17 monomethylation can allosterically promote PRMT5-mediated H4R3 dimethylation [172]. Additionally, multiple evidences suggest at least partial overlap of PRMT7 function with PRMT5 function [145] while maintaining unique substrates for both enzymes [173]. Future research

elucidating genome-wide differential binding of PRMT5 and PRMT7 and their substrates in prostate cancer cells may establish whether co-targeting PRMT5 and PRMT7 is a better approach than targeting single enzyme.

Apart from functional overlap in the epigenetic regulation, other arginine methyltransferases might interact with PRMT5 via post-translational modification of non-histone substrates. PRMT4 (also known as co-activator-associated arginine methyltransferase 1, CARM1) is an established co-activator of androgen receptor [174]. A 2006 study demonstrated that in hormone-naïve LNCaP cells, PRMT4 binding increased AR transcriptional activity and promoted cell proliferation and survival. Since PRMT5 may also function as AR co-activator, as discussed above [159], it will be beneficial to explore the possible combinational effect of PRMT4 and PRMT5 targeting on AR signaling.

1.6.2 PRMT5 and lysine methylation

Histone lysine methylation is a histone post-translational modification that has been linked to a variety of cellular processes such as transcription regulation, DNA replication, and DNA repair [175]. In prostate cancer, polycomb repressive complex 2 (PRC2) and its enzymatic component EZH2 is an established oncogene [176]. While direct PRMT5/PRC2 interaction was not investigated in prostate cancer, in leukemia model, PRMT5 colocalized with PRC2 at the promoters of tumor suppressors RBL2 and ST7, and PRMT5/PRC2 interaction was mediated by BRD7. This interaction was associated with transcriptional repression of RBL2 and ST7 [177]. Additionally, in lymphoma cells PRMT5 promotes expression of PRC2 through epigenetic repression of RBL2 [178], which possibly can lead to even further suppression of genes co-regulated by PRMT5 and PRC2. Based on in vitro evidence, it was suggested that SUZ12 directly interacts with MEP50 to recruit PRMT5 to histone H2A substrate [179].

However, contrary to the evidence that PRMT5 cooperates with PRC2 to repress gene transcription, observation in AML cells demonstrated that PRMT5-driven histone H3R8 symmetric dimethylation prevented methylation of H3K27 by PRC2 and activated multiple gene expression [180]. Taken together, these observations suggest that interaction of PRMT5 and PRC2, and transcriptional outcome of this interaction is highly context-dependent. Given the importance of PRC2 and EZH2 in prostate cancer, it is imperative to investigate this interaction in detail. EZH2

also functions as an AR co-activator outside of PRC2 [181], thus exploring the effect of co-targeting PRMT5 and EZH2 on AR signaling is warranted.

In addition to research on PRC2/PRMT5 axis, significant research effort was devoted to investigating the interplay of WDR5 and PRMT5. WDR5 recruits H3K4 methyltransferase complexes MLL1-4 to chromatin and functions as an oncogene in prostate cancer to promote AR recruitment to its target genes [182]. Despite well-characterized functional interaction of PRMT5 and WDR5, this interaction has not been investigated in prostate cancer. It was demonstrated that PRMT5-driven methylation of H3R2 in vitro [171], in lymphoma [145], lung cancer [129], and ovarian cancer [183] cells enhances binding of WDR5 to promote H3K4 trimethylation and activation of target gene transcription. On the contrary, in erythroleukemia cells and bone marrow, PRMT5-driven recruitment of WDR5 lead to transcriptional repression of γ-globin gene expression [170] again suggesting context-dependent outcome of PRMT5-driven histone methylation. Elucidation of composition of PRMT5-containing protein complexes at the regulatory elements of target genes may shed light on this discrepancy.

1.6.3 PRMT5 and lysine acetylation

The connection between histone acetylation and gene expression modulation was discovered as early as 1964, and since then, a variety of histone acetyltransferases and histone deacetylases was described [184]. p300/CBP is a well-known co-activator of AR transcriptional activity and was shown to be a potential driver of prostate cancer progression [185]. In prostate cancer cells, PRMT5 was present in the same complex with p300/CBP and nucleolin, and this interaction was facilitated by p300/CBP-interacting transactivator with E/D-rich carboxy-terminal domain-2 (CITED2) [186]. The formation of the complex promoted methylation and acetylation of nucleolin by PRMT5 and p300/CBP, respectively, and subsequent nucleolin nuclear export to promote AKT-mediated EMT and prostate cancer metastasis via increased translation of AKT mRNA. Interestingly, PRMT5- and p300/CBP-containing complex also included both RIOK1 and MEP50, though their functional involvement remains to be determined.

Another lysine acetyltransferase demonstrated to interact with and be regulated by PRMT5 is TIP60. Notably, both TIP60 and p300/CBP acetylate H4K5. In vitro, acetylation of H4K5 enhances methylation of H4R3 by PRMT5/MEP50 complex [187]. However, another study suggested that non-acetylated histone H4 was methylated by purified PRMT5 in complex with

Brg1 or hBrm more efficiently than H4K5-acetylated H4 [188]. The same study also found that PRMT5 was present in a complex containing c-Myc, histone deacetylase (HDAC) 2, and Brg1 on the two Myc target gene promoters to repress gene transcription, demonstrating the interplay between PRMT5-mediated histone methylation, histone acetylation/deacetylation, and chromatin remodeling. As Brg1 and PRMT5 bind to the AR promoter and catalyze H4R3 dimethylation to activate AR transcription [137], it will be interesting to examine status of H4K5 acetylation on the AR promoter.

Support for the interplay between histone methylation and acetylation also comes from a recent study demonstrating that in lymphoma, PRMT5-mediated H3R8 symmetric dimethylation is coupled with HDAC2- or 3-mediated deacetylation at H2BK12, H3K9, H3K14, and H4K8 on the promoter regions of three target miRNAs [150], which regulate expression of cyclin D1 and c-Myc. Interestingly, methylation of H4R3 by PRMT5/MEP50 may also impact the acetylation of H4K5 by TIP60, at least in vitro [189]. In short, interplay between PRMT5-mediated methylation and other marks has been explored extensively; future research will likely provide more insight into complex epigenetic regulation. However, biochemical evidence from in vitro studies must be cautiously taken as epigenetic regulation is heavily dependent on chromatic status and protein complex composition in cells.

1.6.4 PRMT5 and DNA methylation

DNA methylation, mediated by DNA methyltransferases (DNMTs), is essential for the maintenance of various cellular processes such as DNA repair, recombination, replication, and gene expression [190]. It was historically the first discovered epigenetic regulation mechanism [191]. In cancer, including prostate cancer, alterations of DNA methylation often lead to promoter hypo- and hypermethylation at oncogenes and tumor suppressor genes, respectively [190]. Although changes of DNA methylation status were well described in prostate cancer, and accumulating evidence suggests connection between PRMT5 activity and such alterations, this relationship has not been explored in prostate cancer specifically.

The direct relationship between PRMT5-driven histone methylation and DNA methylation was first observed in erythroid cells [192]. In this study, H4R3 methylation by PRMT5 at the γ-globin promoter caused recruitment of DNMT3a to the same region via interaction of H4R3me2s with DNMT3a. Methylation of CpG islands in this region was PRMT5-dependent, a phenomenon

also observed in gastric cancer [193]. However, it was not elucidated whether DNMT3a interacted with methylated histones or directly with PRMT5. In addition to potentially recruiting DNA methylases to its target regions, PRMT5 can also be recruited to already methylated DNA regions. In breast cancer cells, PRMT5/MEP50 was recruited to methylated DNA via interaction with methyl CpG binding domain 2 (MBD2) protein and coincided with increased methylation of histone H4R3 [194]. If both mechanisms are active in prostate cancer, it suggests a possible DNA methylation – histone H4R3 methylation positive feedback loop. Future research needs to investigate the relationship between other histone methylation marks mediated by PRMT5 and DNA methylation status.

1.7 Targeting PRMT5 for prostate cancer therapy

Although prostate cancer is a relatively well managed disease with 5-year overall survival of about 99%, it remains a second-leading cause of cancer-related deaths in males in US. Metastasis is the major cause prostate cancer death, and 30-50% of high-risk localized prostate cancer cases relapse and progress to metastatic stage. Thus, improving outcomes of radiation therapy and ADT to overcome radiation resistance and castration resistance will have a significant positive impact on therapy results and patients' lives.

1.7.1 Targeting PRMT5 to overcome AR reactivation

AR reactivation limits the therapeutic effect of ADT and ASI therapy [60,195]. Thus, targeting AR protein expression through either enhanced degradation of AR or reducing AR transcription or translation will be able to overcome AR reactivation. As it became evident, several AR degraders were tested in pre-clinical models [66,67], and one of the AR degraders utilizing PROTAC technology is in a Phase I clinical trial [68].

Quantification of the expression level of PRMT5 using tissue microarray (32 BPH tissues and 40 prostate cancer tissues (20 with Gleason score 6 and 20 with Gleason score$\geqslant$7)) indicated an equal increase of PRMT5 expression in both cytoplasm and nucleus in higher-grade tumors, and PRMT5 expression positively significantly correlated with AR expression in HNPC tumors [137]. Given that PRMT5 may regulate AR expression and activity via multiple mechanisms as both epigenetic activator and AR protein co-factor, exploring targeting PRMT5 for CRPC therapy

may provide a novel therapeutic approach. If PRMT5 indeed activates AR transcription in CRPC, targeting PRMT5 alone or in combination with ADT could possibly eliminate or at least significantly reduce expression of AR, AR splice variants and gain-of-function AR mutants in tumor cells, thus overcoming virtually all mechanisms of AR reactivation.

1.7.2 Targeting PRMT5 for radiosensitization

ADT is commonly used with radiation therapy to sensitize tumor cells to the ionizing radiation, and it was demonstrated that radiation therapy combined with ADT had better outcomes compared to radiation therapy or ADT alone [196], possibly through downregulation of AR signaling which in turn suppressed AR-activated DNA damage response genes [197–199].

Thus, as PRMT5 regulates AR expression in HNPC, and HNPC is treated with radiation therapy, targeting PRMT5 can be used as radiosensitization approach. In fact, in 2019 Owens et al. demonstrated that targeting PRMT5 either through knockdown or enzymatic inhibition sensitized prostate cancer cells to radiation independently of AR status [136]. It was shown that PRMT5 in complex with pICln functions as epigenetic activator for a subset of DNA damage response genes. With pending evaluation of PRMT5 targeting in pre-clinical models for radiation therapy, targeting PRMT5 could be explored for prostate cancer radiosensitization.

1.7.3 Possible approaches to target PRMT5

As PRMT5 is an enzyme, one possible approach to target PRMT5 can be inhibition of its' enzymatic activity. Five PRMT5 inhibitors are currently being evaluated in clinical phase I trials in the US: GSK3326595, JNJ-64619178, PF-06939999, PRT543, and PRT811 (clinicaltrials.gov). GSK3326595 and JNJ-6461917 are catalytic inhibitors of PRMT5, with GSK3326595 competing with peptide substrates in the substrate binding pocket and JNJ-64619178 binding competitively with both the SAM and substrate binding pockets (mechanisms of action of PF-06939999, PRT543, and PRT811 were not disclosed).

Additionally, PROTAC-based approaches to degrade PRMT5 protein can be explored. PROTAC PRMT5 degraders were reported and patented recently [200,201], however, these degraders were not evaluated clinically yet.

Finally, as PRMT5 activity strongly depends on its interacting proteins, targeting specific protein-protein interactions will likely achieve higher specificity and cause fewer adverse effects. For example, targeting PRMT5/pICln may be explored as a promising radiosensitization approach.

1.8 Conclusions and the scope of this dissertation

Prostate cancer affects one out of seven men in United States and remains the second leading cause of cancer death in men. The major cause of prostate cancer mortality is the development of metastatic disease. Currently, ADT in a form of either surgical castration or medical castration is the first-line treatment for the metastatic prostate cancer and the only radiosensitizer for radiation therapy. ADT decreases levels of circulating androgens, and since prostate cancer growth is dependent on androgens, tumors cease growth and shrink. In spite of initial success in most patients, ADT eventually fails, and almost all patients develop castration-resistant prostate cancer (CRPC).

AR reactivation through multiple mechanisms (such as *AR* gene amplification, increased rate of AR transcription, increased stability of the AR protein, expression of ligand independent splice variants or activating mutations of AR) is believed to be the main driving force of the tumor progression. Recently it was demonstrated in my group that PRMT5 epigenetically activates AR transcription in HNPC, however, whether CRPC cells utilize similar mechanism of AR expression regulation was not elucidated yet.

NEPC is the most lethal type of prostate cancer and a significant clinical challenge. NEPC typically arises from prostate adenocarcinoma during neuroendocrine differentiation (NED). NED can be induced by the majority of prostate cancer treatments including ADT and ASI. Cells that undergo NED are resistant to apoptosis and often lack AR expression. As such, NEPC is highly resistant to virtually any therapy and is not detected by the PSA screening. It is estimated that ~30% of patients with metastatic prostate cancer develop NEPC, and there are no curative treatments for this lethal disease. Thus, identification of novel therapeutic targets to prevent NED in PC is in urgent need.

In this dissertation, I aimed to explore whether PRMT5 is required for the cell growth of AR-dependent CRPC due to the PRMT5-dependent activation of AR expression. If that is true, targeting AR expression at the level of transcription through its potential regulator PRMT5 may

provide a novel approach for CRPC therapy by eliminating virtually all possible mechanisms of AR reactivation.

Interestingly, preliminary data from my group suggested that both PRMT5 and its cofactor MEP50 are required for ADT- and ASI-induced NED *in vitro*. Co-overexpression of these proteins together is sufficient to induce NED in HNPC cells. These exciting preliminary findings lead me to explore a possibility that PRMT5/MEP50 complex functions as a regulator of NED in prostate cancer and can participate in the NED induction.

CHAPTER 2. PRMT5 ACTIVATES TRANSCRIPTION OF AR IN CRPC

The following chapter was reproduced and modified with permission from:
Beketova E. et al. Protein arginine methyltransferase 5 promotes pICln-dependent androgen receptor transcription in castration-resistant prostate cancer. Cancer Research, 2020 (published online first) doi: 10.1158/0008-5472.CAN-20-1228 [202].

2.1 Summary

The majority of advanced prostate cancer therapies aim to inhibit androgen receptor (AR) signaling. However, AR reactivation inevitably drives disease progression to castration-resistant prostate cancer (CRPC). Previously, my group identified protein arginine methyltransferase 5 (PRMT5) as an activator of AR expression in hormone-naïve prostate cancer. In this study I demonstrate that PRMT5 functions as an epigenetic activator of *AR* transcription in CRPC. *In vitro* and in xenograft tumors in mice, targeting PRMT5 suppressed growth of CRPC cells. My results suggest that targeting PRMT5 may be explored as a novel therapy for CRPC treatment by suppressing expression of AR and AR splice variants to circumvent AR reactivation.

2.2 Introduction

Prostate cancer remains the second leading cause of cancer death in American men [203]. The primary cause of prostate cancer mortality is the development of metastasis [204]. Currently, androgen deprivation therapy (ADT), in combination with either docetaxel or abiraterone acetate, is the first-line treatment for metastatic prostate cancer [205]. Because the growth of prostate cancer cells is dependent on androgen receptor (AR) signaling, suppressing AR signaling via ADT inhibits tumor growth. Despite initial positive response in the majority of patients, ADT eventually fails, leading to the development of castration-resistant prostate cancer (CRPC) [206].

AR reactivation drives CRPC progression and occurs via multiple mechanisms (AR gene amplification, expression of ligand-independent splice variants, or mutations of AR, and others) [206]. For example, AR splice variant 7 (AR-V7) presents in 18-28% of CRPC tissues [60]. AR-V7 expression correlates with poor patients' prognosis [60]. Because AR-V7 lacks the ligand-binding domain, it is constitutively active and can regulate transcription of AR target genes despite

castrate levels of androgens [195]. Inhibitors that target AR signaling, such as enzalutamide, demonstrate poor outcome towards CRPC that express AR-V7. Moreover, targeting full-length AR (AR-FL) can increase AR-V7 expression, exacerbating the condition [195]. Thus, there is an urgent need to develop therapeutic approaches to overcoming AR reactivation. Because my group had recently shown that protein arginine methyltransferase 5 (PRMT5) activates *AR* transcription in hormone-naïve prostate cancer (HNPC) [137], I investigated whether PRMT5 also regulates the transcription of AR and AR variants in CRPC.

PRMT5 is a methyltransferase that catalyzes symmetrical dimethylation of arginine residues in histones (H4R3, H3R8, H3R2, and H2AR3) to regulate the transcription of various target genes [114,120,126,163]. While PRMT5 is generally considered an epigenetic repressor [114,120,126,163], PRMT5 also functions as an epigenetic activator [136,137,180]. Here I provide the evidence that PRMT5 promotes the growth of CRPC cells via epigenetic activation of transcription of both AR-FL and AR-V7. Results from the *in vitro* and *in vivo* studies suggest that targeting PRMT5 may present a promising approach for CRPC treatment.

2.3 Results

2.3.1 PRMT5 promotes growth of CRPC cells via epigenetic activation of AR expression

To determine the role of PRMT5 in CRPC, I analyzed effect of PRMT5 inhibition on the growth of CRPC cell line 22Rv1, which expresses both full-length AR (AR-FL) and AR-V7. Treatment of 22Rv1 cells with the PRMT5 inhibitor BLL3.3, also called CMP5 [137,207], reduced cell proliferation compared to DMSO control (Figure 2.1A) and downregulated AR-FL and AR-V7 at protein and mRNA levels in 22Rv1 (Figure 2.1B-D). I also evaluated the effect of another PRMT5 inhibitor JNJ-64619178 (JNJ) which is currently in Phase I clinical trial for Non-Hodgkin lymphoma and solid tumors [208]. Similarly, JNJ treatment significantly reduced cell growth and downregulated AR-FL and AR-V7 expression (Figure 2.1E-H). To corroborate these findings, I used lentivirus-based shRNA constructs (two separate shRNA constructs per gene) to establish doxycycline (Dox)-inducible PRMT5 knockdown cell lines in 22Rv1 (22Rv1-shPRMT5 and 22Rv1-shPRMT5#2). PRMT5 knockdown inhibited cell growth (Figure 2.1I, Figure S2.1A) and decreased expression of both AR-FL and AR-V7 (Figure 2.1J-L, Figure S2.1B-D) while expression of scramble control (22Rv1-shSC) did not affect cell growth or protein expression

(Figure 2.1M-P). Moreover, expression of several AR target genes [62] was suppressed upon PRMT5 knockdown (Figure S2.1E), consistent with the decreased AR expression. These results suggest that PRMT5 regulates cell growth, AR expression, and AR signaling in 22Rv1.

Because AR reactivation occurs via several mechanisms, I next determined whether PRMT5 regulates AR expression in other CRPC models. My group reported previously that PRMT5 targeting downregulates AR expression and inhibits growth in C4-2 cells, which model CRPC via AR overexpression [137]. I further evaluated the effect of PRMT5 inhibition in VCaP cells which bear *AR* gene amplification [209] and LN95 cells which express AR splice variants [210] and observed that both PRMT5 inhibitors BLL3.3 and JNJ suppressed cell growth and downregulated AR expression (Figure S2.1F-M). Cell cycle analysis confirmed that PRMT5 knockdown caused G_1 arrest in 22Rv1 (Figure 2.1Q), consistent with previous observations [211,212]. No significant induction of cell death was observed (Figure S2.1N). Collectively, these results suggest that PRMT5 promotes cell growth via activation of AR transcription in CRPC cells with AR overexpression, AR gene amplification, or expression of AR splice variants.

To investigate whether PRMT5 regulates AR expression via histone methylation at the *AR* promoter, I performed chromatin immunoprecipitation (ChIP)-assays in 22Rv1 using PRMT5-specific antibody. PRMT5 bound to the proximal region of the promoter (−493 to −226 bp from transcription start site (TSS)) but not to the distal region (-4481 to -4308 bp from TSS) (Figure 2.1R). ChIP-qPCR analysis of H2AR3me2s, H3R2me2s, H3R8me2s, and H4R3me2s revealed that H4R3me2s and H3R2me2s were highly enriched at the *AR* proximal promoter (Figure 1S). Further, PRMT5 knockdown decreased these enrichments and PRMT5 binding, confirming that PRMT5 methylates H4R3 and H3R2 at the *AR* promoter (Figure S2.1O). As observed in LNCaP cells [137], Brg1 and Sp1 also bound to the same region (Figure S2.1P). Taken together, these findings demonstrate that PRMT5 activates *AR* transcription in CRPC cells by binding to the proximal region of the *AR* promoter to methylate histones H4R3 and H3R2 in a similar manner as in HNPC cells [137].

As I established that PRMT5 epigenetically regulates *AR* transcription and is required for CRPC cell proliferation, I next aimed to check whether the anti-proliferative effect of PRMT5 knockdown is mediated through the regulation of AR expression. For this purpose, I performed AR rescue assays. I transfected 22Rv1-shPRMT5 and 22Rv1-shSC cells with the plasmid encoding FLAG-AR expression or the empty vector control. Remarkably, exogenously expressed

AR completely restored cell proliferation in 22Rv1-shPRMT5 cells but did not affect cell proliferation in 22Rv1-shSC (Figure 2.2) as observed previously in LNCaP-shPRMT5 cells [137]. This observation suggests that the inhibition of 22Rv1 cell proliferation upon PRMT5 knockdown is primarily mediated through the downregulation of AR expression.

Figure 2.1. PRMT5 promotes growth of CRPC cells via epigenetic activation of AR expression.

A, Growth curve (MTT assay) of 22Rv1 cells incubated with 10 μM PRMT5 inhibitor (BLL3.3) or equal volume of vehicle (DMSO) for 6 days. B-C, Representative western blot images (B) and quantification (C) of protein expression in cell lysates from Day 6 of A. D, qPCR analysis of gene expression in cells from Day 6 of A. E, Growth curve (MTT assay) of 22Rv1 cells incubated with 10 μM PRMT5 inhibitor (JNJ-64619178, referred to as JNJ) or equal volume of vehicle (DMSO) for 6 days. F-G, Representative western blot images (F) and quantification (G) of protein expression in cell lysates from Day 6 of E. H, qPCR analysis of gene expression in cells from Day 6 of E. I, Growth curve (MTT assay) of 22Rv1 cells with doxycycline-inducible PRMT5 knockdown (22Rv1-shPRMT5) incubated in the presence (Dox (+)) or absence (Dox (-)) of doxycycline for 6 days. J-K, Representative western blot images (J) and quantification (K) of protein expression in cell lysates from Day 6 of I. L, qPCR analysis of gene expression in cells from Day 6 of I. M, Growth curve (MTT assay) of 22Rv1 cells with doxycycline-inducible scramble control expression (22Rv1-shSC) incubated in the presence (Dox (+)) or absence (Dox (-)) of doxycycline for 6 days. N-O, Representative western blot images (N) and quantification (O) of protein expression in cell lysates from Day 6 of M. P, qPCR analysis of gene expression in cells from Day 6 of M. Q, Flow cytometry analysis of cells following PI staining at Day 6 of I (sub-G_1 cells were gated out). R, ChIP-qPCR for PRMT5 binding to the proximal or distal AR promoter. S, ChIP-qPCR for the enrichment of the indicated histone methylations on the proximal promote region of AR. For MTT, western blotting, cell cycle, and qPCR analysis, statistical significance of group difference was determined for 'DMSO vs BLL3.3', 'DMSO vs JNJ', or 'Dox (-) vs Dox (+)'. For ChIP-qPCR, values were normalized to the corresponding IgG control, and indicated statistical significance of group difference was determined for 'specific IP vs IgG IP'. For all experiments, results are mean ± SD from 3 independent experiments. For western blotting of AR, the AR N-20 antibody (sc-816, Santa Cruz) was used. Student *t*-test with Welch's correction was performed to determine statistical significance of group difference. *ns* $P > 0.05$, * $P < 0.05$, ** $P < 0.01$, *** $P < 0.001$.

Figure 2.1 continued

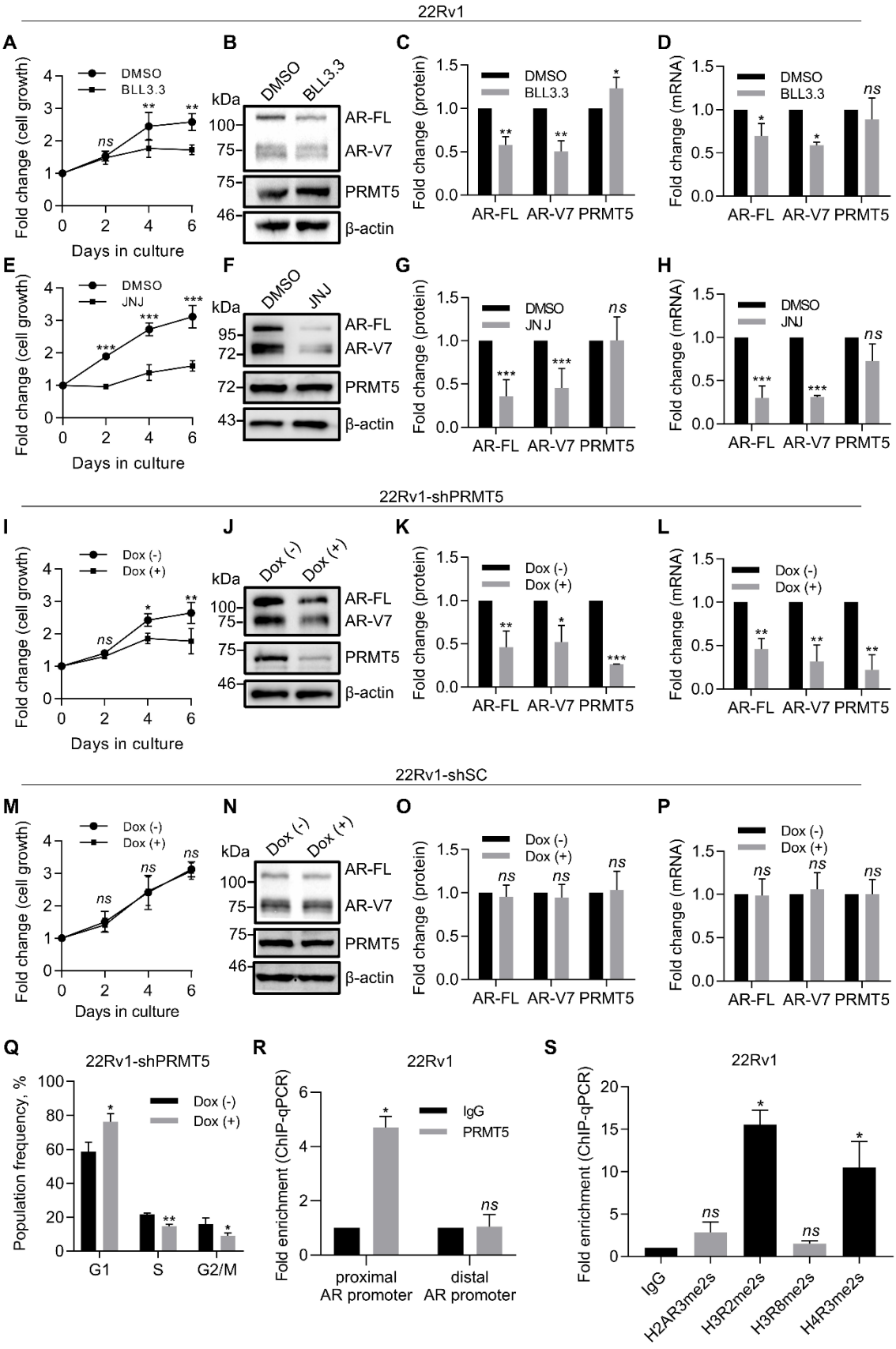

2.3.2 Nuclear-localized PRMT5 promotes cell proliferation and AR expression in prostate cancer cells

Results of the study by Gu et al. [213] suggested distinct roles of PRMT5 in the cytosol and nucleus. To investigate this further, I examined whether nuclear-localized PRMT5 promotes cell proliferation. Antonysamy et al. reported that PRMT5 protein tended to aggregate in the absence of its cofactors [119]. Thus, I reasoned that overexpression of PRMT5 alone may promote aggregate formation and decrease the cellular amount of active PRMT5 leading to reduced cell proliferation which was previously observed in LNCaP cells by Gu et al. [213]. In line with this, I performed overexpression of mutant shRNA-resistant PRMT5 fused with nuclear localization signal (NLS) or nuclear export signal (NES) or without signals in LNCaP or 22Rv1 cells on the background of PRMT5 knockdown. Consistent with previous report by Gu et al., NLS-PRMT5 decreased while NES-PRMT5 promoted cell proliferation in WT cells (Figure 2.3A, D). Conversely, NLS-PRMT5 promoted while NES-PRMT5 decreased cell proliferation in LNCaP-shPRMT5 and 22Rv1-shPRMT5 (Figure 2.3A, D). In cells with PRMT5 knockdown, NLS-PRMT5 promoted AR expression at both protein (Figure 2.3B, E) and mRNA level (Figure 2.3C, F). These observations further confirm that nuclear-localized PRMT5 promotes cell proliferation and AR expression in prostate cancer cells.

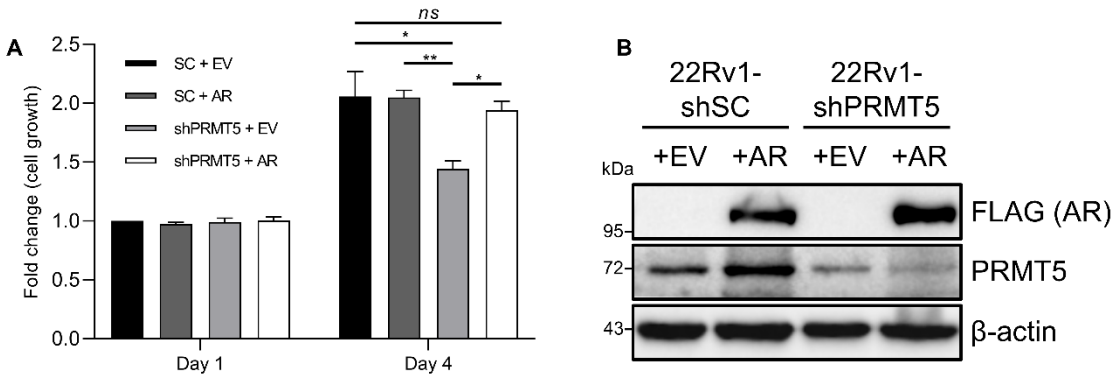

Figure 2.2. AR re-expression restores cell proliferation after PRMT5 knockdown in 22Rv1.

A, 22Rv1 cells with Dox-inducible expression of scramble control (22Rv1-shSC) or PRMT5 shRNA (22Rv1-shPRMT5) were treated with Dox and transfected with either empty vector (+EV) or plasmid for FLAG-AR expression (+AR). MTT assay was performed at Day 1 and Day 4 of treatment. B, Western blot analysis of protein expression in cell lysates at Day 4 of A. Statistical analysis for A was performed using Brown-Forsythe and Welch ANOVA followed by Dunnett's T3 multiple comparisons test. *ns* $P > 0.05$, * $P < 0.05$, ** $P < 0.01$.

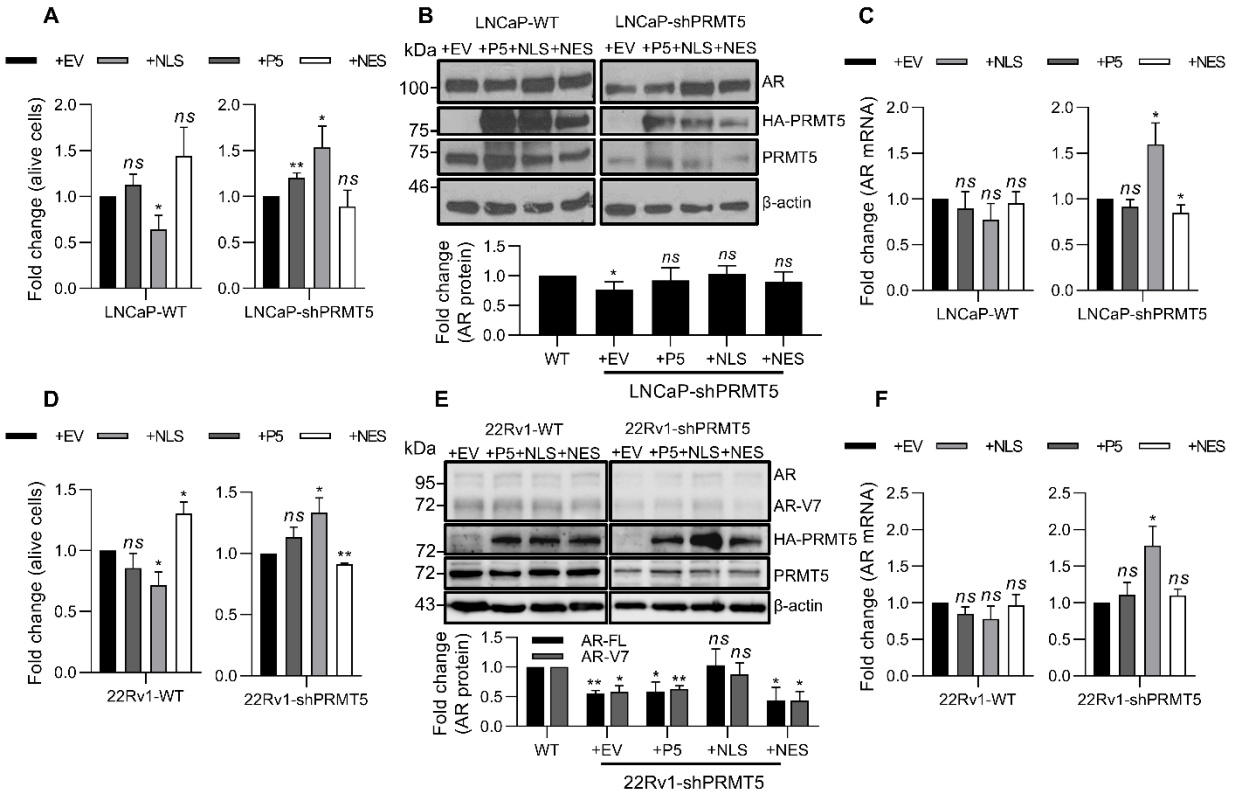

Figure 2.3. Nuclear-localized PRMT5 promotes cell proliferation and AR expression in LNCaP and 22Rv1.

A-C, Wild-type LNCaP (LNCaP-WT) or LNCaP with Dox-inducible knockdown of PRMT5 (LNCaP-shPRMT5) were transfected with empty vector (+EV), or constructs for overexpression of PRMT5 (+P5), nuclear-localized PRMT5 (+NLS), or cytoplasmic PRMT5 (+NES). A, Alive cell number was analyzed using Trypan Blue staining after 4 days of transfection. B, Representative western blot and quantification of protein expression in cell lysates from A. C, qPCR analysis of AR expression in cells from A. D, Wild-type 22Rv1 (22Rv1-WT) or 22Rv1 with Dox-inducible knockdown of PRMT5 (22Rv1-shPRMT5) cells were similarly transfected with the plasmids indicated in A. Alive cell number was analyzed using Trypan Blue staining after 4 days of transfection. E, Representative western blot and quantification of protein expression in cell lysates from D. F, qPCR analysis of AR expression in cells from D. For western blot, statistical significance of group difference was determined for comparison with 'WT' group. For Trypan Blue staining and qPCR, statistical significance of group difference was determined for comparison with '+EV' group. For all experiments, results are mean ± SD from at least 3 independent experiments. For western blotting of AR, the AR N-20 antibody (sc-816, Santa Cruz) was used. Brown-Forsythe and Welch ANOVA was performed to determine statistical significance of group difference. *ns* $P > 0.05$, * $P < 0.05$, ** $P < 0.01$.

2.3.3 Knockdown of PRMT5 suppresses CRPC tumor growth in mice

To determine whether targeting PRMT5 can suppress the growth of CRPC tumors *in vivo*, I implanted 22Rv1-shPRMT5 and 22Rv1-shSC cells subcutaneously into male, pre-castrated NRG mice. When the average tumor volumes reached 100 mm^3, shRNA expression was induced by Dox treatment, and tumor growth was monitored. PRMT5 knockdown significantly suppressed tumor growth (Figure 2.4A), consistent with the suppression of AR expression in xenograft tumors (Figure 2.4B). Analysis of cleaved caspase-3 staining suggested no induction of apoptosis by PRMT5 knockdown (Figure 2.4C), confirming *in vitro* findings. Ki-67 analysis showed that tumors with PRMT5 knockdown had significantly lower proliferative index compared to scramble control tumors (Figure 2.4D). Taken together, these results suggest that PRMT5 also regulates AR expression and the growth of CRPC tumors *in vivo*.

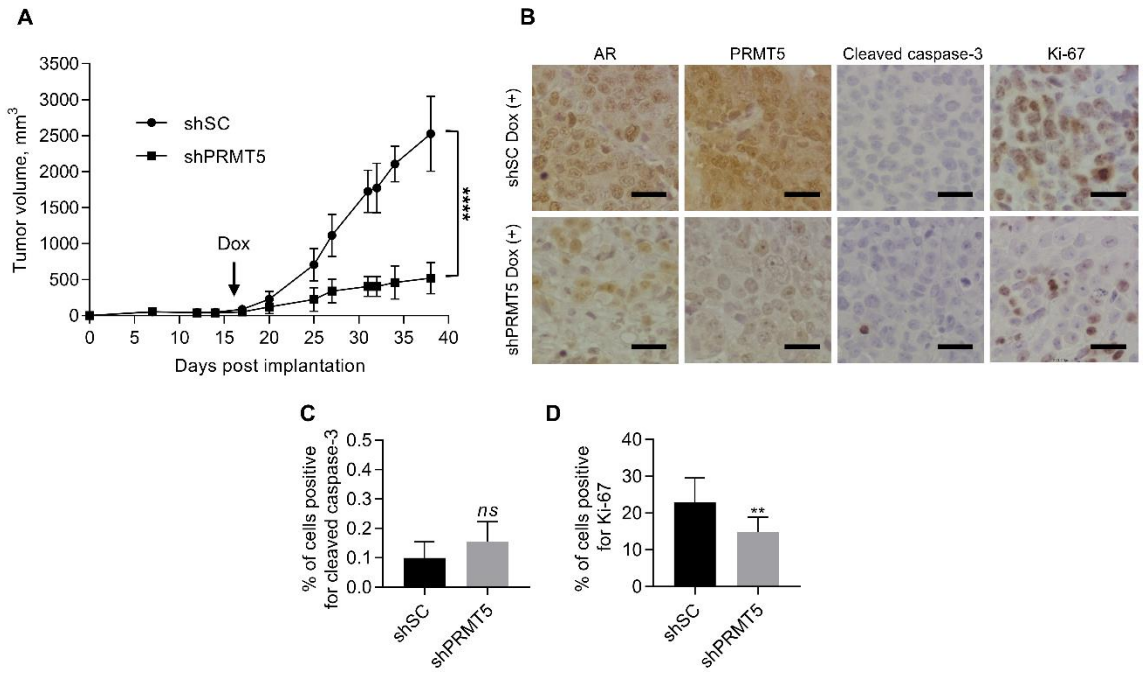

Figure 2.4. Knockdown of PRMT5 or pICln suppresses CRPC tumor growth in mice.

22Rv1 cells with Dox-inducible knockdown of PRMT5 (shPRMT5) or scramble control (shSC) were injected subcutaneously into the right flanks of surgically castrated male NRG mice. Tumor-bearing mice were treated with doxycycline in drinking water once tumors reached ~100 mm^3. A, Tumor growth curves were determined and compared between treatment groups (ANOVA; ****, $P < 0.0001$). B-D, At the end of treatment, tumors were resected and probed for AR, PRMT5, cleaved caspase-3 and Ki-67 using IHC. Presented are representative images (B) and the quantification of the percentage of positively stained cells out of the total number of cells (C and D). Scale bar indicates 40 μm. Results are mean ± standard deviation (n = 10 per group). C and D, Student *t*-test was performed to determine statistical significance. *ns* $P > 0.05$, ** $P < 0.01$.

2.3.4 Targeting PRMT5 overcomes resistance to ASI treatment in CRPC cells and tumors

As androgen signaling inhibitor (ASI) treatment is a mainstay of CRPC treatment, I examined whether targeting PRMT5 is an effective approach to overcome the resistance to ASI. Since intracellular androgen synthesis by prostate cancer cells is one of the AR reactivation mechanisms in CRPC, and 22Rv1 produces CYP17A1 [214], I also treated 22Rv1 cells with the CYP17A1 inhibitor abiraterone. First, I performed MTT assay with 22Rv1 cells treated with either PRMT5 enzymatic inhibitors (BLL3.3 or JNJ-64619178) or ASI (abiraterone or enzalutamide) alone, in combination, or vehicle (DMSO). Notably, the combinational treatment decreased cell growth more effectively than either of drugs alone (Figure 2.5A). However, using the Chou-

Talalay method and software CompuSyn (http://www.combosyn.com/) to analyze the drug interaction, the combinational indexes for BLL3.3/abiraterone and BLL3.3/enzalutamide pair were 0.91 and 0.92, and for JNJ-64619178/abiraterone and JNJ-64619178/enzalutamide were 0.94 and 0.91 (Figure 2.6), respectively, indicating that PRMT5 inhibition in combination with ASI can achieve additive effect.

Figure 2.5. Targeting PRMT5 overcomes resistance to ASI treatment in CRPC cells and tumors. A, Growth curve (MTT assay) of 22Rv1 cells incubated with 10 μM PRMT5 inhibitor (BLL3.3 or JNJ-64619178, referred to as JNJ) or 10 μM of either abiraterone acetate (Abi) or enzalutamide (Enz), or equal volume of vehicle (DMSO) for 6 days. Cell proliferation assays were performed at the indicated time points, and OD550 values were normalized to values from Day 0 for each cell line. ANOVA test with Welch's correction was performed to determine statistical significance. Stars represent significant difference with DMSO group, squares represent significant difference of "Abi" vs "Abi + BLL3.3", "Abi vs Abi + JNJ", "Enz" vs "Enz + BLL3.3", or "Enz vs Enz + JNJ" groups. Results are mean ± SD from 3 independent experiments. B, 22Rv1 cells with Dox-inducible knockdown of PRMT5 were injected subcutaneously into right flanks of surgically castrated male NRG mice. Once tumors reached ~100 mm^3, tumor-bearing mice were treated with doxycycline in drinking water, or abiraterone acetate per oral 200 mg/kg/day, or enzalutamide 25 mg/kg/day, or combination. Tumor growth curves were determined and compared between groups (ANOVA; *, $P < 0.05$). C, Survival of tumor–bearing mice is represented as Kaplan–Meier plot. D-F, At the end of treatment, tumors were resected and probed for cleaved caspase-3 and Ki-67 using IHC. Shown are representative images of IHC staining (D) and the quantified percentage of positively stained cells out of the total number of cells counted (E, F). Results are mean ± standard deviation (n = 10 per group). Student *t*-test was performed to determine statistical significance of difference vs "Control" group. *ns* $P > 0.05$, *** $P < 0.001$, **** $P < 0.0001$.

Figure 2.5 continued

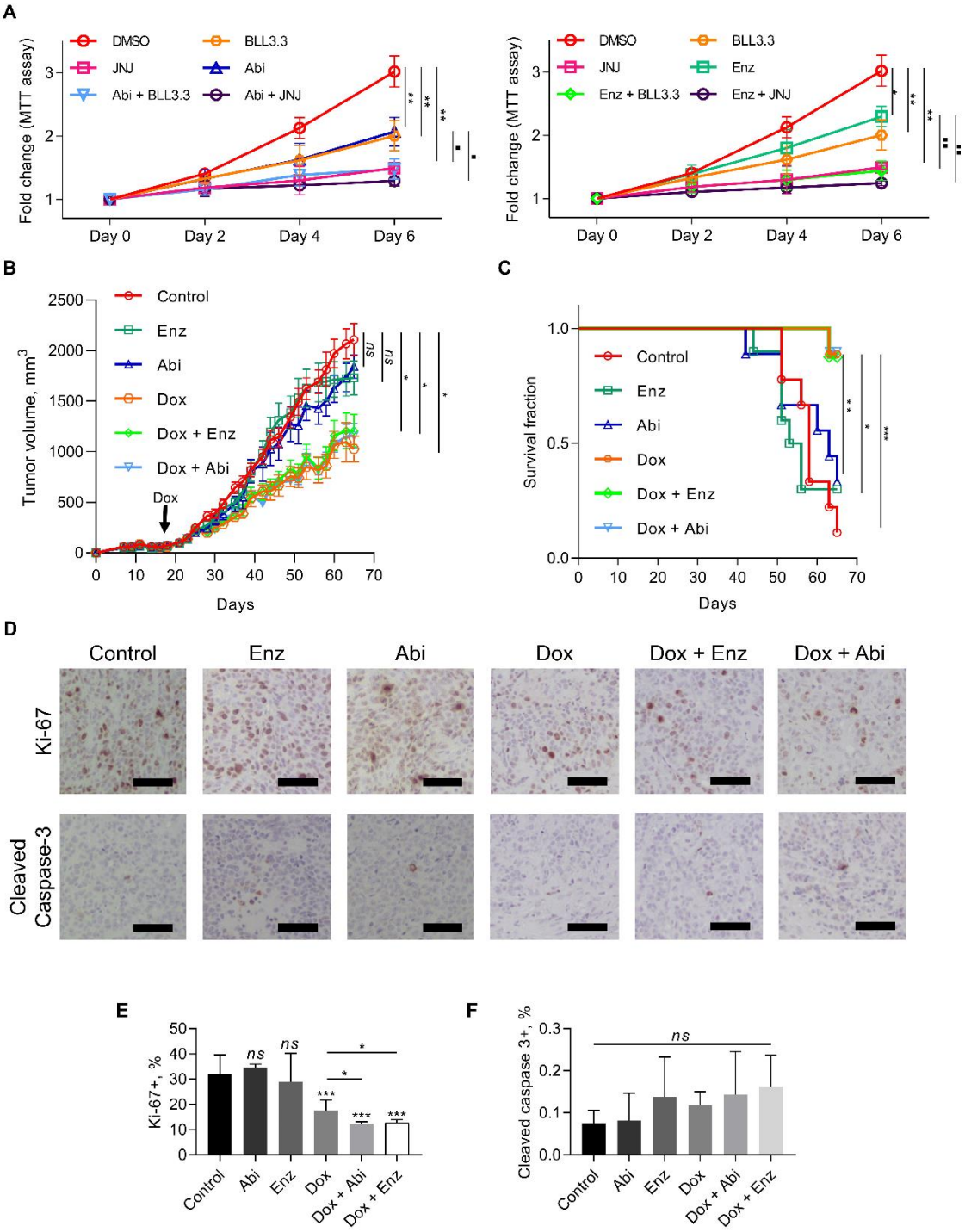

Next, I implanted 22Rv1-shPRMT5 cells in the castrated male mouse as described in Chapter 2.3.3 to evaluate the observed *in vitro* effect. After average tumor volumes reached 100 mm^3, PRMT5 knockdown was initiated (Dox), or treatment with ASI (abiraterone acetate or enzalutamide) started. Consistent with previous findings that 22Rv1 xenografts tumors in mice are resistant to ASI [215,216], treatment of mice with either drug alone did not affect tumor growth (Figure 2.5B and C). However, PRMT5 knockdown significantly suppressed tumor growth and showed better survival.

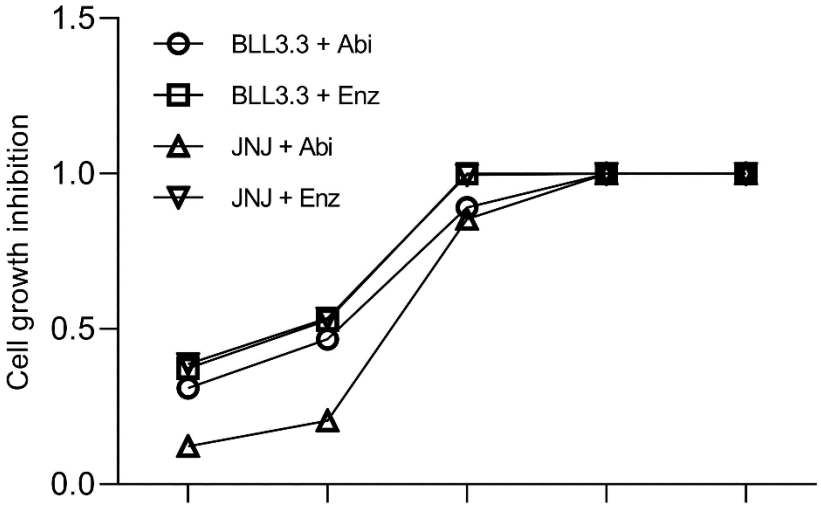

BLL3.3 (μM)	4.25	8.5	17	34	68
JNJ-64619178 (μM)	5.5	11	22	44	88
Abiraterone (μM)	4	8	16	32	64
Enzalutamide (μM)	10	20	40	80	160

Figure 2.6. PRMT5 targeting and ASI have some additive effect in 22Rv1.

MTT assay of 22Rv1 cells incubated with indicated concentrations of PRMT5 inhibitor (BLL3.3 or JNJ-64619178, referred to as JNJ) or either abiraterone acetate (Abi) or enzalutamide (Enz) for 72 hours.

Although combinational treatment was not more effective than PRMT5 knockdown alone in terms of tumor growth suppression (Figure 2.5B), Ki-67 analysis suggested that combination of PRMT5 knockdown with ASI showed a better inhibition of tumor cell proliferation (Figure 2.5D and E). Thus, PRMT5 targeting alone is effective to overcome the resistance of CRPC tumors to

ASI in mice. The lack of additive effect of PRMT5 knockdown and ASI on tumor growth in the xenograft model is likely due to the fact that PRMT5 knockdown and ASI both act on the same AR signaling pathway. Alternatively, incomplete knockdown of PRMT5 in xenograft tumors may be an attributing factor (Figure 2.7).

Analysis of cleaved caspase-3 staining suggested no significant induction of apoptosis by ASI treatment or PRMT5 knockdown (Figure 2.5F), confirming the *in vitro* findings. Taken together, these results suggest that PRMT5 targeting is an effective treatment approach for ASI-resistant CRPC.

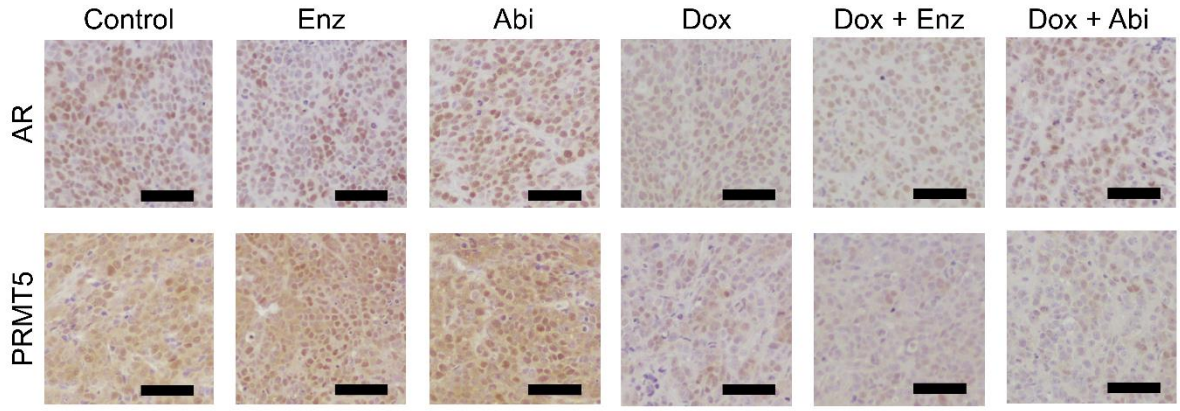

Figure 2.7. Expression of AR and PRMT5 in 22Rv1 xenografts.

22Rv1 cells with Dox-inducible knockdown of PRMT5 were injected subcutaneously in right flanks of surgically castrated male nude mice. Once tumors reached ~100 mm^3, tumor-bearing mice were treated with doxycycline in drinking water, or abiraterone acetate per oral 200 mg/kg/day, or enzalutamide 25 mg/kg/day, or combination. At the end of treatment tumors were resected and probed for AR and PRMT5. Representative IHC images are shown. Scale bar indicates 100 μm.

2.4 Discussion

2.4.1 PRMT5 may regulate AR signaling through multiple mechanisms

PRMT5 has emerged as a putative oncogene in multiple human cancers [120]. Although earlier studies suggested that PRMT5 promotes proliferation of cancer cells via epigenetic repression of tumor suppressors [114,120,126,163], recent study by my group suggested that

PRMT5 epigenetically activates *AR* transcription in HNPC [137]. Because AR drives prostate cancer development and progression, I investigated whether PRMT5 also regulates AR expression in CRPC. I present the evidence demonstrating that PRMT5 activates transcription of AR and AR-V7 in multiple CRPC cell lines. First, knockdown or pharmacological inhibition of PRMT5 in several CRPC cell lines (22Rv1, VCaP, C4-2 and LN95) reduced the expression of AR and AR-V7 at both mRNA and protein levels. Second, PRMT5 bound to the proximal promoter of *AR* and methylated H4R3 and H3R2. Third, transcriptomic analysis confirmed that PRMT5 regulated AR signaling in CRPC cells. Finally, PRMT5 expression positively correlates with the expression of AR and AR-V7 in CRPC tissues. Collectively, PRMT5 is overexpressed in prostate cancer tissues, and PRMT5-driven regulation of AR transcription is conserved in HNPC and CRPC cells.

PRMT5 may also regulate AR signaling through a non-epigenetic mechanism [159,160]. TMPRSS2-ERG fusion is present in ~50% of prostate cancer cases, and AR-driven expression of this fusion promotes prostate cancer growth [217]. In TMPRSS2-ERG-positive VCaP cells, mass spectrometry identified PRMT5 as an interacting protein of ERG [160]. Mechanistically, ERG mediated both the methylation of arginine 761 on AR by PRMT5 and the recruitment of PRMT5 to the AR target gene promoters. PRMT5-catalyzed methylation of AR attenuated AR binding to a subset of AR target genes, resulting in transcriptional repression of genes associated with prostatic epithelium differentiation. Thus, PRMT5 promoted cell proliferation in TMPRSS2-ERG-positive cells. However, PRMT5 knockdown did not inhibit growth of TMPRSS2-ERG-negative 22Rv1 cells. This contrasts with the observations that both pharmacological inhibition and knockdown of PRMT5 significantly decreased proliferation of several CRPC cell lines, including TMPRSS2-ERG-negative 22Rv1 and C4-2. This discrepancy could be due to the use of heterogeneous pool of shRNA-expressing cells in their study whereas here single-cell-derived stable clones that express shRNAs targeting different regions of PRMT5 were used.

In another study, ectopic overexpression of either PRMT5 or catalytically inactive PRMT5(R368A) mutant in TMPRSS2-ERG-negative PC3 cells enhanced luciferase activity of an androgen-responsive element-containing luciferase reporter [159], suggesting that PRMT5 might also function as a co-activator of AR independent of its methyltransferase activity. As PRMT5 may regulate prostate cancer cell growth via direct regulation of AR signaling and indirect modulation of other AR regulators, future investigation of these additional mechanisms will provide a full picture of PRMT5-driven regulation of prostate cancer cell growth. Further, genetic

analysis for the role of PRMT5 in prostate cancer development and progression in mouse models will provide evidence to validate PRMT5 as a therapeutic target for CRPC.

2.4.2 Cellular localization can determine the biological effect of PRMT5

PRMT5 has a variety of interacting partners and substrates that can be located both in the nucleus (for example, histones within the chromatin) and in the cytoplasm (for example, Sm proteins). Moreover, it appears that PRMT5 sub-cellular localization and translocation is critical during early embryonic phases [218]. Additionally, multiple groups discovered that localization of PRMT5 correlates with cancer stage and prognosis in several types of cancer [219–222] with contradicting results suggesting either nuclear or cytoplasmic PRMT5 can be associated with worse cancer prognosis, although, overall, high nuclear PRMT5 expression was detected in more aggressive tumors. Further, Gu et al. [213] suggested distinct roles of PRMT5 in the cytosol and nucleus in prostate cancer cells.

To investigate the cellular effect of PRMT5 localization, I performed overexpression of PRMT5 with different localization signals on the background of PRMT5 knockdown in HNPC and CRPC cells. My results indicate that nuclear-localized PRMT5 promotes both cell proliferation and AR expression (Figure 2.3). Furthermore, my group has previously shown that nuclear expression of PRMT5 is higher in HNPC tumors with higher Gleason score [137]. Overall, these results suggest that nuclear PRMT5 promotes cancer cells proliferation and survival.

However, it is still not clear how PRMT5 is translocated to the nucleus and why this translocation can be higher in prostate cancer cells, especially given that PRMT5 itself does not have any strong nuclear-localization signals [213]. Several proteins were suggested to function as shuttling partners of PRMT5 in different models, including BLIMP-1 in mouse primordial germ cells [223], AJUBA in osteosarcoma cells [224], and nucleolin in prostate cancer cells [225].

Interestingly, Owens et al. has recently shown that upon DNA damage, PRMT5 is upregulated and nuclear translocation of pICln, an interacting protein of PRMT5, is enhanced, leading to the epigenetic activation of several DNA-damage response genes. Thus, it would be interesting to investigate the correlation of PRMT5-interacting proteins and PRMT5 expression in nucleus and cytoplasm of prostate cancer cells in connection with AR expression. I will present these results in Chapter 4 of this dissertation.

2.4.3 Targeting PRMT5 as a novel approach for prostate cancer treatment

Although targeting AR signaling remains a mainstay of CRPC treatment [206], the inevitable emergence of resistance via AR reactivation limits the therapeutic effect of ASI [60,195]. Targeting AR protein expression instead may provide an alternative approach for the CRPC treatment and potentially overcome multiple AR reactivation mechanisms. In fact, targeting AR expression by promoting AR degradation effectively suppressed prostate cancer cell growth in several pre-clinical studies [66,67]. One of the AR degraders utilizing PROTAC technology is in a Phase I clinical trial [68].

Given that epigenetic landscapes of CRPC and HNPC are largely distinct [226], the conserved role of PRMT5 in epigenetic activation of AR transcription in HNPC and CRPC is interesting and significant [137]. As the vast majority of HNPC and CRPC demonstrate dependency on the AR signaling, targeting PRMT5 may offer an alternative or even more effective treatment for both HNPC and CRPC. In fact, PRMT5 targeting alone effectively suppressed CRPC growth. Additionally, since AR reactivation promotes resistance to the next generation ASI, I explored whether targeting PRMT5 can overcome this resistance. Indeed, PRMT5 inhibition in combination with ASI showed additive effect on the proliferation of CRPC cells *in vitro*. Interestingly, PRMT5 knockdown alone showed suppression of 22Rv1 xenograft tumor growth in mice as well as combination treatments, indicating that targeting PRMT5 might be an effective approach to overcoming resistance to ASI.

Five PRMT5 inhibitors are currently in clinical trials for leukemia and solid tumors (clinicaltrials.gov). As PRMT5 is an essential gene in normal organism processes, such as hematopoiesis and keratinocyte differentiation [227,228], targeting PRMT5 may cause adverse effects. If so, targeted prostate-specific membrane antigen-based delivery of PRMT5 inhibitors will likely provide an alternative to suppress AR expression in prostate cancer specifically [229]. Alternatively, targeting PRMT5/pICln interaction may provide another promising approach for both HNPC and CRPC by suppressing or even eliminating AR expression.

2.5 Materials and Methods

2.5.1 Cell lines and reagents

LNCaP, 22Rv1, VCaP, COS-1, and 293T cells were purchased from ATCC (Manassas, VA, US). LN95 cells were a kind gift from Dr. Jun Luo of Johns Hopkins University. Frozen cultures were recovered and expanded in complete media (LNCaP and 22Rv1 in RPMI1640 (Corning, NY, US), LN95 in RPMI1640 without phenol red (Corning, NY, US), 293T, COS-1, and VCaP in DMEM (Corning, NY, US)) supplemented with 10% FBS (Atlanta Biologicals, Lawrenceville, GA, US) or for LN95 charcoal-stripped FBS (Corning, NY, US), 2 mM L-glutamine (Corning, NY, US), and 100 units/mL penicillin and 100 μg/mL streptomycin (Gibco, Gaithersburg, MD, US)). Cells were not passaged more than 30 times. Long-term storage, cell authentication and mycoplasma contamination check were described previously [136]. Methocel A4M was purchased from Sigma (St. Louis, MO, US), abiraterone acetate and enzalutamide were purchased from MedChemExpress (Monmouth Junction, NJ, US).

2.5.2 Plasmid construction

Plasmids for the doxycycline (Dox)-inducible knockdown of genes of interest were generated by cloning short hairpin RNA (shRNA) targeting the gene of interest mRNA into EcoRI/AgeI sites of the pLKO-tet-ON vector (Addgene #21915). The full list of used shRNA sequences, including the scramble control (SC) sequence, is in Appendix B. For overexpression of AR, AR cDNA was cloned into the pCMV vector containing FLAG tag.

2.5.3 Stable cell line generation

Lentiviral transduction was used for the generation of cell lines with Dox-inducible expression of shRNA that targets PRMT5 mRNA or scramble control (SC). Two shRNA sequences that target different regions of the mRNA were used. The full list of used shRNA sequences, including the SC sequence, is in Appendix B. Briefly, 293T cells were co-transfected with corresponding pLKO-tet-ON-shRNA plasmids (described above) and envelope and packaging plasmids (pHR'-CMV-8.2ΔVPR, Addgene #8455, and pHR'-CMV-VSV-G, Addgene #8454) using FuGENE HD reagent (Promega, Madison, WI, US) according to the manufacturer's

protocol. Viral particles were harvested 48 h later and used to infect 22Rv1 cells in the presence of 0.01 mg/mL polybrene, and 48 h later selection of infected cells was initiated by applying 2 μg/mL puromycin. After selection, single-cell derived stable cell lines were generated using limiting dilution cloning by diluting cell suspension to 2 cells per mL and plating 250 μL cell suspension per well of 96-well plate [230]. The knockdown was confirmed via western blot for the PRMT5 and qPCR with PRMT5-specific primers.

2.5.4 Western blotting

For protein level analysis, cells were trypsin-dissociated and lysed in RIPA buffer (10 mM Tris-HCl, pH 8.0, 5 mM EDTA, 1% Triton X-100, 0.1% sodium deoxycholate, 0.1% sodium dodecyl sulfate (SDS), 140 mM NaCl, 5 μg/mL of each chymostatin, leupeptin, pepstatin A, and antipan, and 1 mM PMSF) for 30 min on ice. The insoluble fraction was separated by centrifugation at 12000 x g for 10 min at 4°C. Total protein concentration was measured using the Bradford method. Twenty μg of total cell lysate was loaded on 10% or 15% SDS-polyacrylamide gel, separated, and then transferred to nitrocellulose membrane. Antibodies against AR (1:2000 dilution, Santa Cruz Biotechnology), PRMT5 (1:1000, Millipore), β-actin (1:1000, Sigma-Aldrich), and secondary sheep anti-mouse IgG ECL antibody HRP conjugated (1:1000, GE Healthcare) and secondary donkey anti-rabbit IgG ECL antibody HRP Conjugated (1:1000, GE Healthcare) were used for western blotting probing. Membranes were visualized with Bio-Rad ChemiDoc Touch Imaging System (Bio-Rad, Hercules, CA, US). The intensity of bands was determined with Image Lab software (Bio-Rad, Hercules, CA, US) and normalized to corresponding loading controls. All used antibodies, catalog numbers, and RRID are listed in Appendix A.

2.5.5 Cell proliferation assay

The cell proliferation assay was performed using MTT reagent (Sigma, St Louis, MO, US). Cell medium was removed, and 70 μL of MTT solution (0.5 mg/mL) was added into each well and incubated at 37°C for 4 h. At the end of incubation, the MTT solution was removed, then 130 μL of DMSO was added into each well and incubated at 37°C for another 15 min. The absorbance

value was then read at 550 nm using the BioTek Synergy™ 4 Microplate Reader (BioTek Instruments, Winooski, VT, US).

2.5.6 Cell cycle analysis

Approximately 10^6 cells were trypsinized, filtered through a 70 μm mesh to remove aggregates, and fixed in 1000 μL 70% v/v ethanol overnight at 4ºC. After that, cells were washed in PBS and incubated in 300 μL of staining solution (20 μg/mL propidium iodide and 20 μg/mL RNase A in PBS) overnight at 4ºC. Cells were analyzed with Guava EasyCyte Flow Cytometer (Guava Technologies, Hayward, CA, US), and at least 20000 live cells were counted per sample. Data were subsequently analyzed using FlowJo software. Sub-G_1 cells were gated out, and proportions of cells in different stages of the cell cycle were determined using Dean-Jett-Fox modeling [231].

2.5.7 RNA isolation, reverse transcription, and quantitative real-time PCR

For analysis of gene expression at the mRNA level, total cell RNA was isolated using TRIzol Reagent (Ambion, Carlsbad, CA, US). At least 1 μg of total RNA was used for the reverse transcription (RT) using the High Capacity cDNA Reverse Transcription Kit (Promega, Madison, WI, US) and random primers according to manufacturer's instruction. qPCR was conducted using FastStart Universal SYBR Green Master Mix (Thermo Fisher Scientific, Waltham, MA, US) in a QuantStudio 6 system (Applied Biosystems, Foster City, CA). Expression levels of genes were normalized to glyceraldehyde-3-phosphate dehydrogenase (GAPDH) level and were calculated using the $2^{-\Delta\Delta CT}$ method [232]. All RT-qPCR primers are listed in Appendix B.

2.5.8 Chromatin immunoprecipitation (ChIP)

First, cross-linking was performed by adding 270 μL of 37% formaldehyde per 10 mL media directly into cell culture media and incubating plates at room temperature for 10 min. Then, 1.12 mL of 1.25 M glycine was added per 10 mL media to stop the cross-linking, and plates were incubated at room temperatures for additional 5 min. All next steps were performed on ice. Cells were scraped off the plates, washed twice in cold PBS, and resuspended in the immunoprecipitation (IP) buffer with protease and phosphatase inhibitors: 50 mM Tris-HCl pH

7.4, 150 mM NaCl, 5 mM EDTA, 1% Triton X-100, 0.5% NP-40, 0.5 mM DTT, 5 μg/mL of each chymostatin, leupeptin, pepstatin A, and antipan, 0.5 mM PMSF, 30 mM PNPP, 10 mM NaF, 0.1 mM Na_3VO_4, 0.1 mM Na_3MoO_4, 10 mM β-glycerophosphate. Cells were sonicated using Branson Model 250 Sonifier at Output 4, 90% duty cycle to generate ~500 base pairs chromatin fragments. Chromatin fragments size was verified using agarose/ethidium bromide gel.

Two micrograms of each of antibodies against PRMT5 (Millipore), H2AR3me2s (Abcam), H3R2me2s (EpiGentek), H3R8me2s (Abcam), H4R3me2s (Abcam) were used to immunoprecipitate protein-DNA complexes for the subsequent isolation of DNA using Chelex [233]. DNA immunoprecipitated with naïve rabbit or mouse IgG served as a control. The co-immunoprecipitated DNA was quantified by qPCR using gene-specific primers. All used antibodies are listed in the Appendix A, and ChIP-qPCR primers are listed in the Appendix B.

qPCR was conducted using FastStart Universal SYBR Green Master Mix (Thermo Fisher Scientific, Waltham, MA, US) in a QuantStudio 6 system (Applied Biosystems, Foster City, CA, US).

2.5.9 Xenograft tumor growth

Animal experiments were performed in the Biological Evaluation Facility of the Purdue University Center for Cancer Research and approved by the Purdue University Animal Care and Use Committee. Six to eight weeks old male non-obese diabetic-Rag1(null)-γ chain(null) (NRG) mice were castrated, and 14 days later 2 x 10^5 cells of 22Rv1-shPRMT5 or -shSC in 100 μL of RPMI-1640 media were mixed with 100 μL of Matrigel (200 μL total) and injected subcutaneously into the right lower flank (10 mice/group). After tumor volumes reached ~100 mm^3, mice were treated with Dox (1 mg/mL in drinking water) to induce the expression of shRNA or treated 5 days/week with ASI in 0.5% Methocel orally (abiraterone acetate 200 mg/kg/day, enzalutamide 25 mg/kg/day), or in combination. Control group mice were similarly treated with vehicle. Tumor growth was measured every 2-3 days, and tumor volume was calculated using ½ × L × W × H without blinding method. When control tumors reached ~2000 mm^3, tumors were resected for immunohistochemistry (IHC) analysis.

2.5.10 Immunohistochemistry analysis of xenograft tumors

Paraffin embedment and slide preparation of tumor samples were performed at the Purdue Histology Research Laboratory.

Samples were deparaffinized and rehydrated by incubating slides overnight at 37°C, and then for 2 h at 65°C, followed by incubation in Xylenes solution and a range of ethanol concentration from 100% to 30%, and finally in Millie-Q water at room temperature. Endogenous peroxides were inactivated by incubation of slides in 3% H_2O_2 for 10 min at room temperature. Antigen retrieval was performed by incubating slides soaked in 10 mM Tris pH 10 on boiling water bath for 30 min. Slides were then blocked with 5% non-fat milk solution in PBS for 1 h at room temperature with shaking. Antibodies against AR (1:100, Santa Cruz Biotechnology), PRMT5 (1:100, Millipore), Ki-67 (1:500, BD Biosciences), or cleaved caspase-3 (1:500, Cell Signaling Technology) were applied on sections overnight in 5% non-fat milk in PBS. After 3 washes in PBS, sections were probed with corresponding secondary HRP-conjugated antibodies diluted (1:100) in 5% non-fat milk in PBS for 1 h at room temperature. Following another triple washing of slides with PBS, the chromogenic reaction was performed with DAB peroxidase kit (Vector Laboratories, Inc., Burlingame, CA, US), and then slides were counter-stained with hematoxylin-eosin (HE) solution (Vector Laboratories, Inc.). The slides were subsequently dehydrated and mounted using VectaMount™ permanent mounting medium (Vector Laboratories, Inc.). Image analysis and quantification were performed using ImmunoRatio online software [234].

2.5.11 Statistical analysis

Unless stated otherwise, results are presented as mean ± SD. Analysis of low-throughput data was performed using GraphPad Prism 8.00 (GraphPad Software, La Jolla California US, www.graphpad.com). For qPCR experiments, the analysis was performed on C_T values of genes normalized to the C_T value of GAPDH loading control. For ChIP-qPCR experiments, the analysis was performed on C_T values of specific IP normalized to the C_T value of non-specific IgG control. For western blotting experiments, the analysis was performed on protein band intensity normalized to β-actin loading control band intensity. MTT assay was performed at indicated time points, and OD550 values were normalized to values from Day 0 for each cell line. For the comparison of two sample groups, unpaired two-tailed *t*-test with Welch's correction was used. A *p* value less than

0.05 was considered significant and marked by asterisk in the figures (*, $p < 0.05$; **, $p < 0.01$; and ***, $p < 0.001$) while ns represents insignificant p-value ($p > 0.05$).

For animal studies, the group size was calculated based on pilot experimental data using G*Power software [235]. Based on preliminary data, a 2-fold decrease of growth upon the PRMT5 knockdown with SD of 0.25 was expected (where 1 is no knockdown group growth). To detect 0.25-fold change at the power level 80%, alpha level 0.05, and sample effect 0.5, the sample size of a group should be 10 mice.

2.6 Supplemental Figure S2.1. PRMT5 promotes growth of CRPC cells via epigenetic activation of AR expression.

A, Growth curve (MTT assay) of 22Rv1 cells with doxycycline-inducible PRMT5 knockdown (22Rv1-shPRMT5#2) incubated in the presence (Dox (+)) or absence (Dox (-)) of doxycycline for 6 days. B-C, Representative western blot analysis (B) and quantification (C) of protein expression in cell lysates from Day 6 of A. D, qPCR analysis of gene expression in cells from Day 6 of A. E, qPCR of AR target genes in 22Rv1-shPRMT5 cell line after 6 days of PRMT5 knockdown. F, Growth curve (MTT assay) of VCaP cells incubated with 10 μM PRMT5 inhibitor (BLL3.3) or equal volume of vehicle (DMSO) for 9 days. G-H, Representative western blot analysis (G) and quantification (H) of protein expression in cell lysates from Day 9 of F. I, qPCR analysis of gene expression in cells from Day 9 of F. J, Growth curve (MTT assay) of LN95 cells incubated with 10 μM PRMT5 inhibitor (BLL3.3 or JNJ) or equal volume of vehicle (DMSO) for 6 days. K-L, Representative western blot analysis (K) and quantification (L) of protein expression in cell lysates from Day 6 of J. M, qPCR analysis of gene expression in cells from Day 6 of J. N, Trypan blue cell viability analysis in 22Rv1-shPRMT5 cells after 6 days of PRMT5 knockdown. O, ChIP-qPCR analysis of histone methylation and PRMT5 binding at the proximal AR promoter at Day 6 of PRMT5 knockdown was performed with indicated antibodies. P, ChIP-qPCR analysis with antibodies of indicated specificity was performed using 22Rv1 cells lysates. Specific primers for the proximal region of AR promoter was used. For MTT, western blotting, cell cycle, and qPCR analysis, statistical significance of group difference was determined for 'DMSO vs BLL3.3' or 'Dox (-) vs Dox (+)'. For ChIP-qPCR, values were normalized to the corresponding IgG control. For O, statistical significance of group difference was determined for 'Dox (-) vs Dox (+)'. For P, indicated statistical significance of group difference was determined for 'specific IP vs IgG IP'. For all experiments, results are mean ± SD from 3 independent experiments. For western blotting of AR, the AR N-20 antibody (sc-816, Santa Cruz) was used. Student *t*-test with Welch's correction was performed to determine statistical significance of group difference. *ns* $P > 0.05$, * $P < 0.05$, ** $P < 0.01$, *** $P < 0.001$.

Figure S 2.1 continued

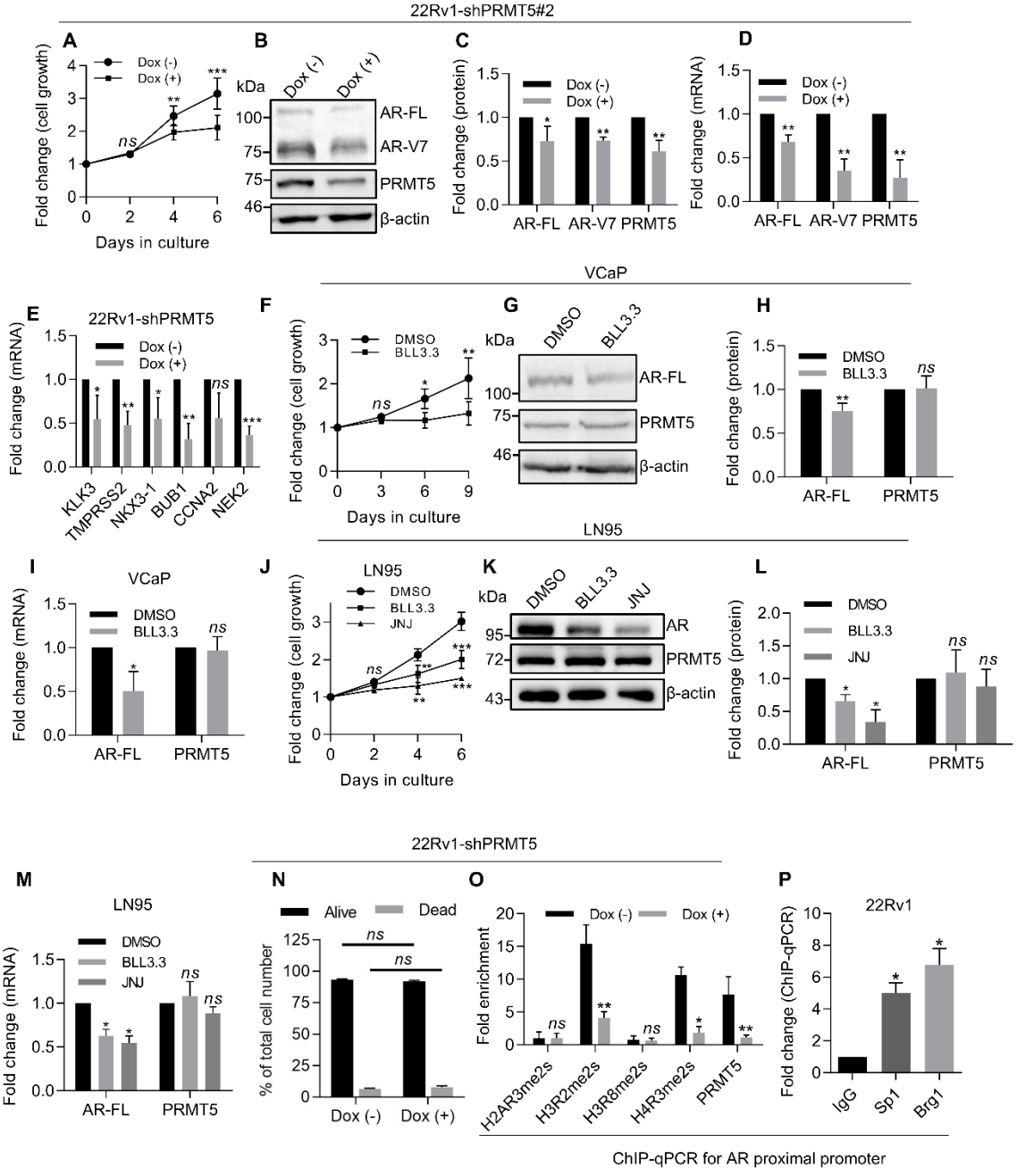

CHAPTER 3. PICLN PROMOTES PRMT5-MEDIATED ACTIVATION OF AR TRANSCRIPTION

The following chapter was reproduced and modified with permission from:
Beketova E. et al. Protein arginine methyltransferase 5 promotes pICln-dependent androgen receptor transcription in castration-resistant prostate cancer. Cancer Research, 2020 (published online first) doi: 10.1158/0008-5472.CAN-20-1228 [202].

3.1 Summary

PRMT5 is an emerging epigenetic enzyme that regulates multiple targets in normal organism and cancer. Activity of PRMT5 is highly dependent on the presence of its interacting proteins. Here, I present the evidence that pICln, and not MEP50, is the interacting protein of PRMT5 to activate *AR* transcription. pICln binding was detected at the *AR* promoter, and pICln was required for the PRMT5-mediated methylation of histone H4R3. Knockdown of pICln decreased prostate cancer cell proliferation *in vitro* and in xenograft, and decreased AR signaling similarly to PRMT5 knockdown. Expression of pICln highly correlated with PRMT5 and AR expression in prostate cancer patients' samples at the protein and mRNA level, and pICln mRNA expression negatively correlated with patient's survival. Taken together, these results suggest that targeting PRMT5/pICln may be explored for CRPC treatment.

3.2 Introduction

PRMT5 is a methyltransferase that can symmetrically dimethylate arginine residues in histones (H4R3, H3R8, H3R2, and H2AR3) to regulate transcription of target genes [114,120,126,163]. While PRMT5 is generally considered an epigenetic repressor, PRMT5 also functions as an epigenetic activator [136,137,180]. Although *in vitro* studies suggest that PRMT5 interacting proteins methylosome protein 50 (MEP50) and methylosome subunit pICln enhance PRMT5 enzymatic activity [130,236], how these proteins cooperate with PRMT5 to regulate gene transcription and substrate selection *in vivo* remains unknown.

MEP50 functions as a PRMT5 cofactor facilitating substrate recognition and positioning via interaction with the N-terminal region of PRMT5 to form a heterooctameric complex [119,130]. Since both pICln and MEP50 can enhance PRMT5 activity towards SmD3 protein *in vitro*

[135,237], pICln may interact with PRMT5 similarly as MEP50 does to activate PRMT5 methyltransferase activity or alter substrate specificity. Indeed, my group has recently demonstrated that pICln, but not MEP50, cooperates with PRMT5 to activate transcription of DNA damage response genes [136]. Here I provide the evidence that PRMT5 promotes the growth of CRPC cells via epigenetic activation of transcription of both AR-FL and AR-V7 in a pICln-dependent, but MEP50-independent, manner. Results from the *in vitro* and *in vivo* studies suggest that targeting PRMT5 may present a promising approach for CRPC treatment.

3.3 Results

3.3.1 MEP50 is not required for PRMT5-mediated activation of AR transcription in CRPC cells

MEP50 is considered a canonical cofactor of PRMT5 [114,120,126,163]. To evaluate the role of MEP50 in PRMT5-driven activation of *AR* transcription, I established Dox-inducible MEP50 knockdown stable cell lines in 22Rv1 (22Rv1-shMEP50 and 22Rv1-shMEP50#2). Unexpectedly, MEP50 knockdown affected neither AR-FL/AR-V7 expression (Figure 3.1A-C, Figure. S3.1A-C) nor the expression of AR target genes (Figure S3.1D). However, MEP50 knockdown de-repressed expression of involucrin (*IVL*) mRNA (Figure 3.1C), confirming that PRMT5/MEP50 represses *IVL* transcription [238].

To determine whether this lack of MEP50 role in regulating AR expression is unique for CRPC cells, I then examined the effect of MEP50 knockdown in LNCaP. Again, MEP50 knockdown did not impact AR expression (Figure 3.1D-F), and MEP50 did not bind to the *AR* promoter (Figure 3.1G-H), though MEP50 antibody efficiently immunoprecipitated MEP50 (Figure S3.1E) and MEP50 bound to the *IVL* promoter (Figure 3.1G-H). Additionally, MEP50 knockdown in 22Rv1 did not significantly change H4R3me2s and H3R2me2s levels at *AR* proximal promoter (Figure S3.1F). Notably, MEP50 knockdown decreased the total cellular level of H3R2me2s but did not significantly affect the total level of H4R3me2s (Figure S3.1G). Contrary to the lack of cell death following PRMT5 knockdown (Figure S2.1I), MEP50 knockdown induced both cell death (Figure 3.1I) and G_1-cell cycle arrest (Figure 3.1J) in 22Rv1 cells, indicating that PRMT5 and MEP50 might have distinct roles in cell proliferation. Taken together, MEP50 does not appear to participate in the regulation of AR transcription by PRMT5.

Figure 3.1. MEP50 is not required for PRMT5-mediated activation of *AR* transcription in CRPC cells.

A-B, Representative western blot images (A) and quantification (B) of protein expression in cell lysates of 22Rv1 cells with doxycycline-inducible MEP50 knockdown (22Rv1-shMEP50) incubated in the presence (Dox (+)) or absence (Dox (-)) of doxycycline for 6 days. C, qPCR analysis of gene expression in cells from A. D-E, Representative western blot images (D) and quantification (E) of protein expression in cell lysates of LNCaP cells with doxycycline-inducible MEP50 knockdown (LNCaP-shMEP50) incubated in the presence (Dox (+)) or absence (Dox (-)) of doxycycline for 6 days. F, qPCR analysis of gene expression in cells from D. G-H, ChIP-qPCR assay of MEP50 binding to the proximal *AR* promoter or control gene *IVL* promoter was performed with non-specific IgG binding as a control in 22Rv1 (G) and LNCaP (H) cells. I, Trypan blue cell viability analysis in 22Rv1-shMEP50 cells after 6 days of MEP50 knockdown. J, Flow cytometry analysis of cells following PI staining at Day 6 of MEP50 knockdown in 22Rv1-shMEP50 (sub-G_1 cells were gated out). For western blotting, cell cycle, cell viability, and qPCR analysis, statistical significance of group difference was determined for 'Dox (-) vs Dox (+)'. For ChIP-qPCR, values were normalized to the corresponding IgG control, and indicated statistical significance of group difference was determined for 'specific IP vs IgG IP'. Results are mean ± SD from 3 independent experiments. For western blotting of AR, the AR N-20 antibody (sc-816, Santa Cruz) was used. Student *t*-test with Welch's correction was performed to determine statistical significance. *ns* $P > 0.05$, * $P < 0.05$, ** $P < 0.01$, *** $P < 0.001$.

Figure 3.1 continued

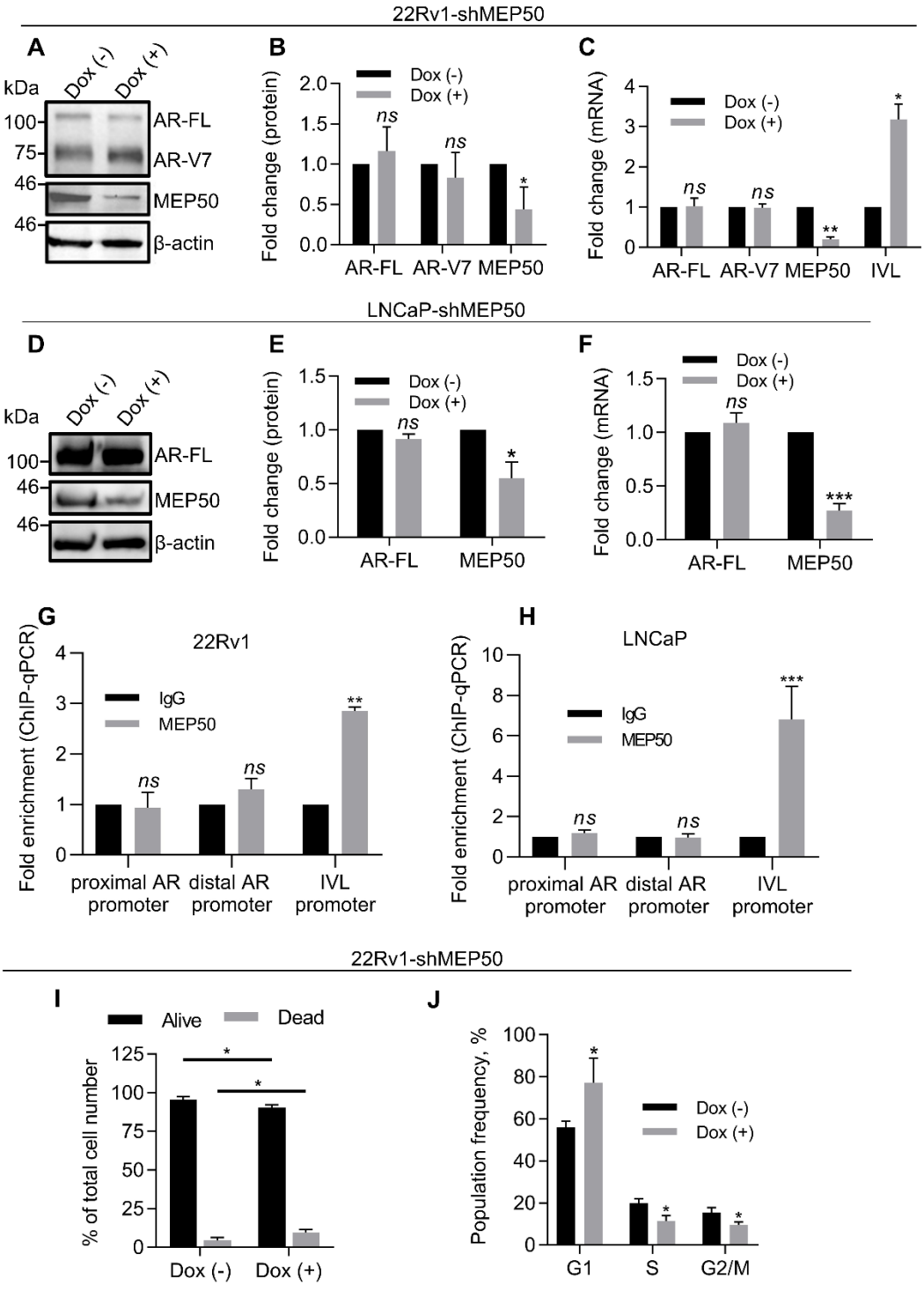

3.3.2 pICln participates in epigenetic activation of AR transcription

The surprising finding that MEP50 was not involved in AR transcription regulation in HNPC and CRPC cells prompted me to search for PRMT5-interacting proteins (pICln, RIOK1, and COPR5) that might cooperate with PRMT5 to regulate AR transcription [132,134,135].

Using ChIP-qPCR with protein-specific antibodies and primers specific to the *AR* proximal promoter region, I found that only pICln, but not RIOK1 and COPR5, bound to the same *AR* proximal promoter region as PRMT5 did (Figure 3.2A).

Next, I established Dox-inducible pICln knockdown cell lines in 22Rv1 and LNCaP cells (22Rv1-shpICln and LNCaP-shpICln) to further interrogate a role of pICln in AR regulation. Indeed, pICln knockdown significantly decreased cell proliferation (Figure 3.2B and C) and AR expression at both protein and mRNA levels in 22Rv1 (Figure 3.2D-F) and LNCaP (Figure 3.2G-I). Consistent with its effect on AR expression, pICln knockdown decreased pICln binding and the H4R3me2s level at the *AR* promoter (Figure 3.2J). However, pICln knockdown did not affect PRMT5 binding nor the H3R2me2s level (Figure 3.2J). Consistently, at the total cellular level, pICln knockdown decreased H4R3me2s but did not affect H3R2me2s (Figure S3.2). In contrast, PRMT5 knockdown decreased pICln binding to the *AR* promoter (Figure 3.2K). These results suggest that PRMT5 recruits pICln to the *AR* promoter, and PRMT5/pICln interaction is required for H4R3 methylation in this region.

Figure 3.2. pICln participates in epigenetic activation of *AR* transcription.

A, ChIP-qPCR assay for binding of PRMT5-interacting proteins to the proximal *AR* promoter in 22Rv1 cells. Values were normalized to IgG control. B-C, Growth curve (MTT assay) of 22Rv1 (B) or LNCaP (C) cells with Dox-inducible pICln knockdown (shpICln). D-E, Representative western blot images (D) and quantification (E) of protein expression in 22Rv1 after 6 days of pICln knockdown. F, qPCR analysis of gene expression in 22Rv1 after 6 days of pICln knockdown. G-H, Representative western blot images (G) and quantification (H) of protein expression in LNCaP after 5 days of pICln knockdown. I, qPCR analysis of gene expression in LNCaP after 5 days of pICln knockdown. J, ChIP-qPCR assay for pICln and H4R3me2s presence at the proximal *AR* promoter in 22Rv1 upon pICln knockdown. K, ChIP-qPCR assay for pICln presence at the proximal *AR* promoter upon PRMT5 knockdown. L, Trypan blue cell viability analysis in 22Rv1-shpICln cells after 6 days of pICln knockdown. M, Flow cytometry analysis of fixed and stained with propidium iodide 22Rv1-shpICln cells after 6 days of pICln knockdown. For MTT, western blotting, cell cycle, and qPCR analysis statistical significance of group difference was determined for 'Dox (-) vs Dox (+)'. For ChIP-qPCR, values were normalized to the corresponding IgG control, and indicated statistical significance of group difference was determined for 'specific IP vs IgG IP' (A) or 'Dox (-) vs Dox (+)' (J, K). For all experiments, results are mean ± SD from 3 independent experiments. For western blotting of AR, the AR N-20 antibody (sc-816, Santa Cruz) was used. Student *t*-test with Welch's correction was performed to determine statistical significance. *ns* $P > 0.05$, * $P < 0.05$, ** $P < 0.01$, *** $P < 0.001$.

Figure 3.2 continued

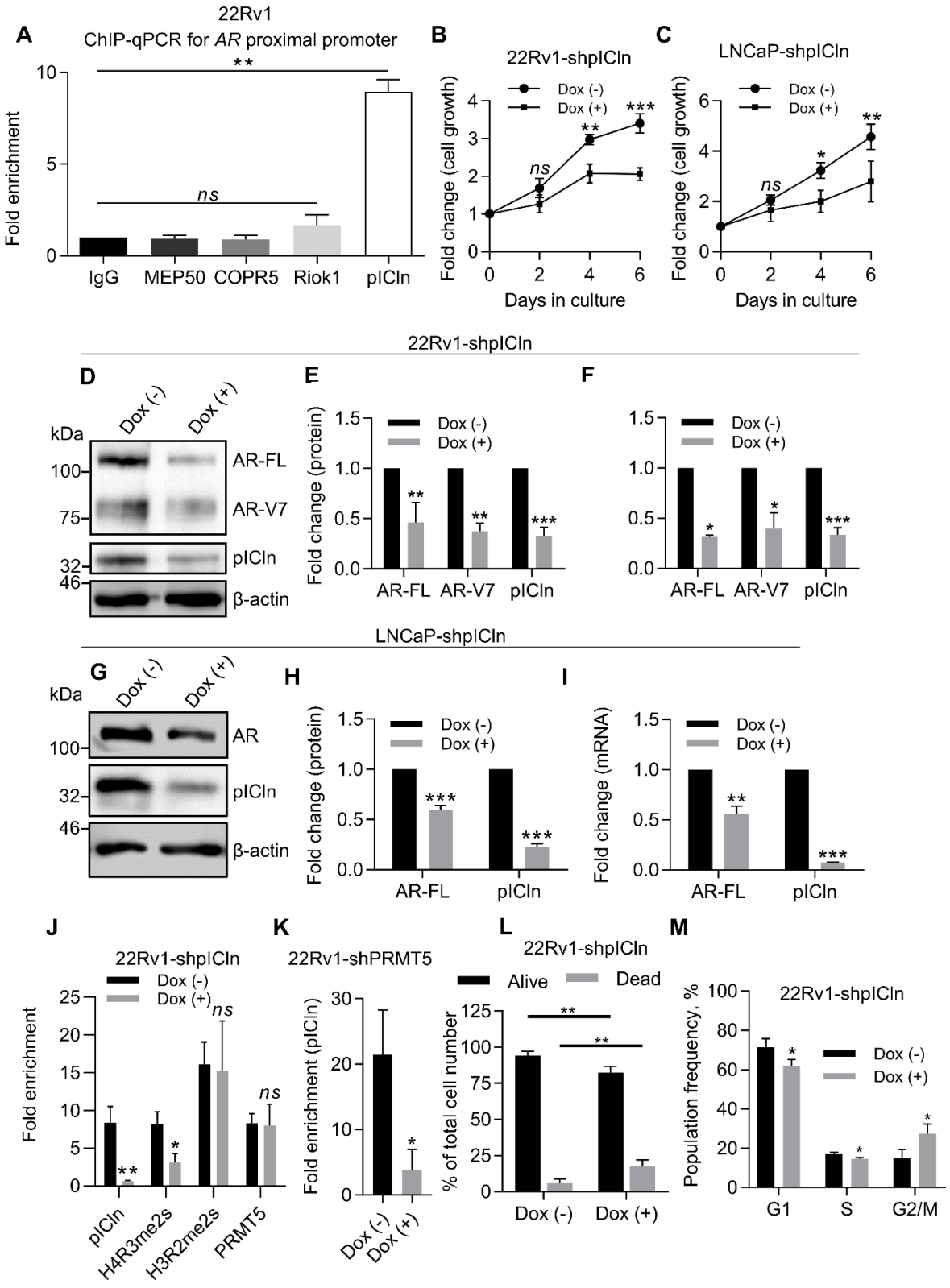

Contrary to PRMT5 knockdown that caused G_1 cell cycle arrest and did not cause cell death, pICln knockdown induced cell death (Figure 3.2L) and G_2 cell cycle arrest in 22Rv1 cells (Figure 3.2M). Thus, pICln has additional roles in cell proliferation and survival independently of PRMT5. Nonetheless, these results demonstrate that pICln is required for PRMT5-mediated H4R3 methylation to activate AR transcription.

As I established that PRMT5/pICln epigenetically regulate AR transcription and are both required for CRPC cell proliferation, I next aimed to check whether the anti-proliferative effect of pICln knockdown is mediated through the regulation of AR expression. For this purpose, I performed AR rescue assays similarly as described in Chapter 2. I transfected 22Rv1-shpICln and 22Rv1-shSC cells with the plasmid encoding FLAG-AR expression or the empty vector control. Remarkably, exogenously expressed AR completely restored cell proliferation in 22Rv1-shpICln cells but did not affect cell proliferation in 22Rv1-shSC (Figure 3.3A for proliferation data and B for western blot confirmation of protein expression). This observation suggests that the inhibition of 22Rv1 cell proliferation upon pICln knockdown is primarily mediated through downregulation of AR expression.

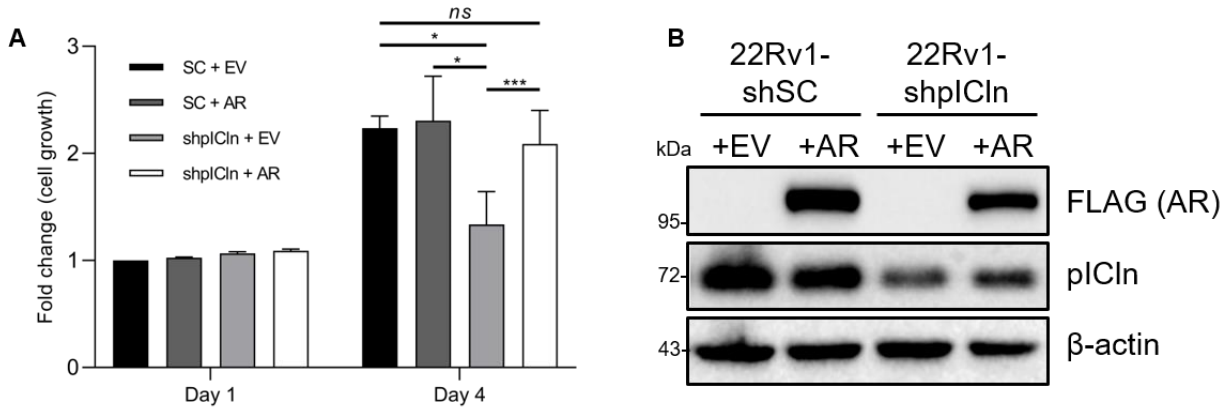

Figure 3.3. AR re-expression restores cell proliferation after pICln knockdown in 22Rv1.

A, 22Rv1 cells with Dox-inducible expression of scramble control (22Rv1-shSC) or pICln shRNA (22Rv1-shpICln) were treated with Dox and transfected with either empty vector (+EV) or plasmid for Flag-AR expression (+AR). MTT assay was performed at Day 1 and Day 4 of treatment. B, Western blot analysis of protein expression in cell lysates at Day 4 of A.

3.3.3 pICln may compete with MEP50 for PRMT5 binding

To investigate whether pICln binds to the N-terminal region of PRMT5 as MEP50 does [119,130], I utilized the bimolecular fluorescence complementation (BiFC) assay [239]. Co-expression of PRMT5(NT292)-VN155 and VC155-pICln in COS-1 cells resulted in YFP fluorescence, indicating that pICln interacted with N-terminal fragment of PRMT5 (Figure 3.4A). To determine whether pICln might bind to a similar site in PRMT5 as MEP50 does, I used the BiFC competition assay, in which VN155-PRMT5 and VC155-MEP50 were co-expressed with MEP50 or pICln. Indeed, overexpression of MEP50 or pICln similarly decreased BiFC efficiency of the PRMT5-MEP50 BiFC interaction (Figure 3.4B-D), suggesting that pICln may indeed function as a cofactor by binding to the N-terminus of PRMT5 like MEP50 [119].

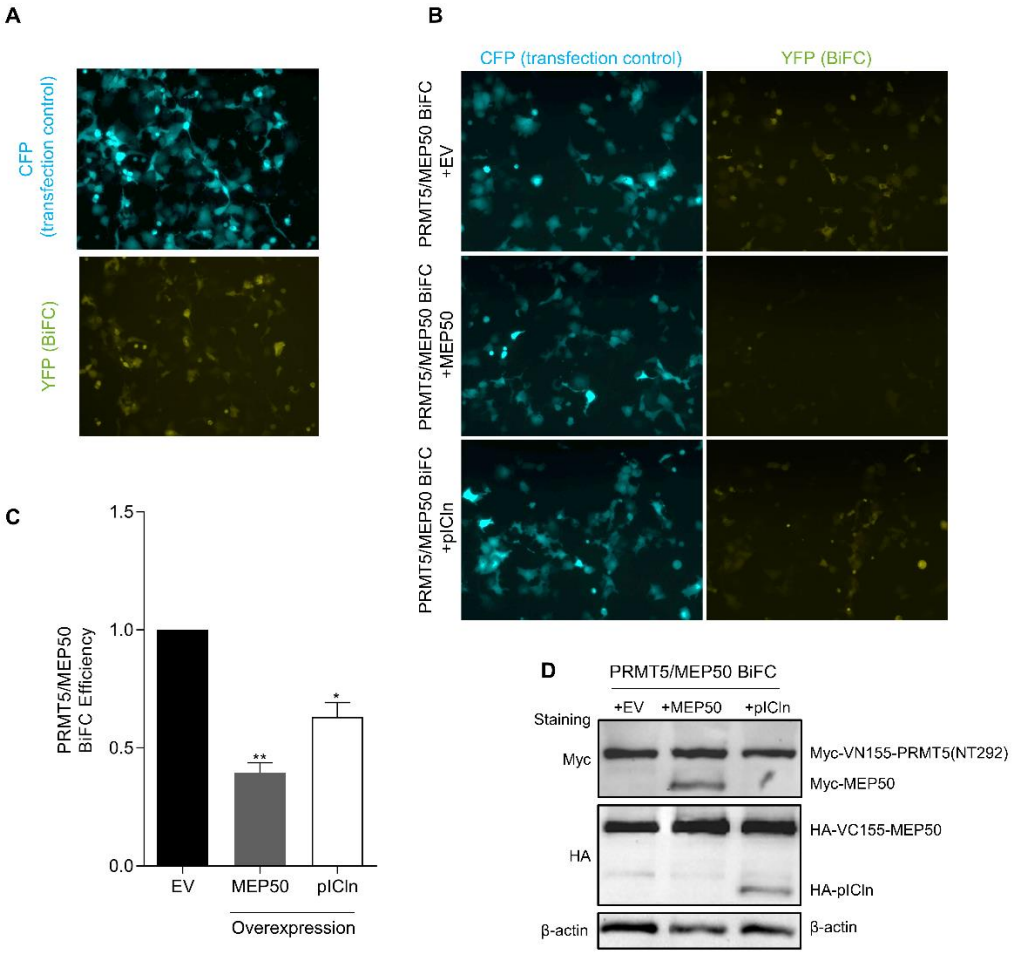

Figure 3.4. pICln may compete with MEP50 for PRMT5 binding.

A, COS-1 cells were co-transfected with BiFC plasmids to co-express VC155-pICln and VN155-PRMT5(NT292) along with the plasmid expressing CFP as a transfection control. Images were taken 48 h post-transfection. YFP fluorescence indicates reconstituted Venus as a result of PRMT5/pICln interaction. 20x magnification. B-D, COS-1 cells were co-transfected with BiFC plasmids to co-express VC155-MEP50 and VN155-PRMT5(NT292) and the plasmid expressing MEP50 (+MEP50) or pICln (+pICln) as well as the plasmid expressing CFP as a transfection control. B, Representative images were taken 48 h post-transfection. C, Quantification of PRMT5/MEP50 BiFC efficiency (ratio of Venus/CFP fluorescence intensities) from B. D, Western blot analysis of protein expression in lysates of cells from B. Probing is indicated on the left, and detected proteins are indicated on the right. Results are mean ± SD from 3 independent experiments. Student *t*-test with Welch's correction was performed to determine statistical significance between groups. *ns* $P > 0.05$, * $P < 0.05$, ** $P < 0.01$.

3.3.4 PRMT5 and pICln regulate the AR signaling independently of MEP50

The above results suggest distinct regulatory roles of PRMT5, MEP50, and pICln in cell proliferation, cell cycle progression, and cell death. To further understand the roles of these proteins in genome-wide gene regulation, RNA-seq of 22Rv1 cells with and without knockdown of PRMT5, MEP50, or pICln was performed. Differentially expressed transcript (DET) analysis identified 6,730 out of 23,334 genes which had at least one DET upon PRMT5 knockdown, including 3,426 genes with upregulated transcripts and 3,304 genes with downregulated ones (Figure 3.5A). Following MEP50 knockdown, 447 upregulated and 626 downregulated differentially expressed genes (DEGs) overlapped with the PRMT5-knockdown DEGs (Figure 3.5A). Notably, pICln knockdown led to more overlapped genes with the PRMT5-knockdown DEGs, including 1,033 upregulated and 1,361 downregulated genes (Figure 3.5A).

To confirm the regulation of the AR signaling by PRMT5 and pICln, the enrichment of different sets of DEGs involved in AR signaling pathway, Gene Ontology GO:0030521, was identified. Consistently, genes of this pathway were significantly over-represented among PRMT5- and pICln-knockdown DEGs but not among MEP50-knockdown DEGs (Figure 3.5B). Compared to fold changes (in log scale with base 2) of selected AR signaling pathway DEGs identified by mRNA-seq (left panel in Figure 3.5C), qPCR analysis confirmed that PRMT5 and pICln, but not MEP50, similarly regulate the expression of AR signaling pathway genes (right panel in Figure 3.5C). These results suggest that PRMT5 and pICln co-regulate AR signaling in a MEP50-independent way.

The GO enrichment analysis explored many GO terms and KEGG pathways significantly enriched in DEGs downregulated after the knockdown of PRMT5 or pICln or MEP50 (Figure 3.5D). For example, GO:0051301 “cell division”, GO:0007049 “cell cycle”, and GO:0000086 “G_2/M transition of mitotic cell cycle” were shared by repressed genes after PRMT5/pICln/MEP50 knockdown. GO functions associated with G_1/S phase regulation were notably over-represented in DEGs downregulated by PRMT5- or MEP50-knockdown, but not in the pICln-knockdown group, for instance, GO:0000082 “G_1/S transition of mitotic cell cycle”, GO:0000083 “regulation of transcription involved in G_1/S transition of mitotic cell cycle”, and GO:0006270 “DNA replication” among others. This was consistent with the cell cycle analysis results (Figure 2.2Q, 3.1J, 3.2M).

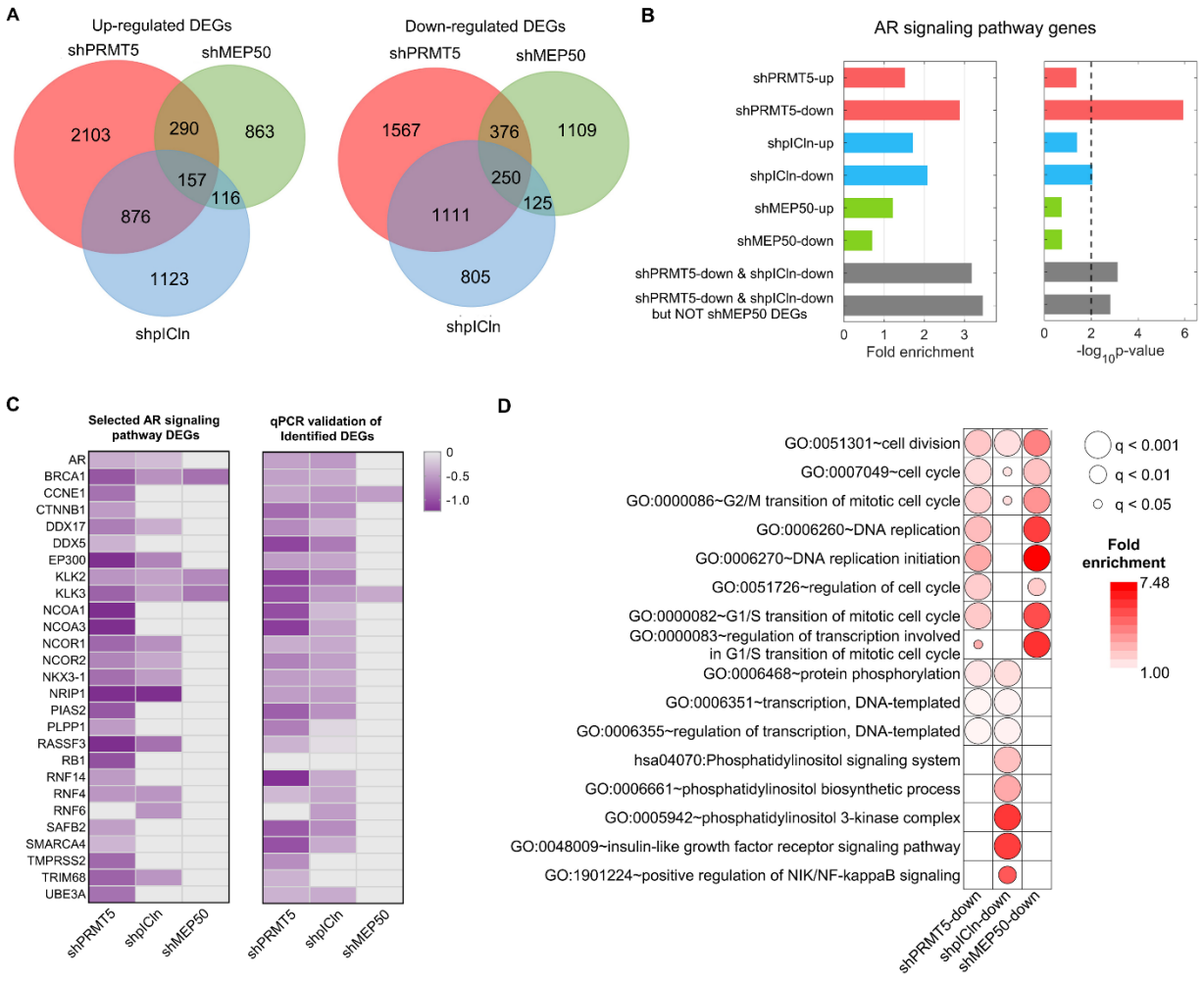

Figure 3.5. PRMT5 and pICln regulate the AR signaling independently of MEP50.

A, RNA-seq analysis of 22Rv1 cells upon 6 days of shRNA-mediated knockdown of PRMT5 (shPRMT5), MEP50 (shMEP50), or pICln (shpICln). Venn diagrams indicate overlap of upregulated and downregulated DEGs among three experiments. B, Presence of AR signaling pathway (GO:0030521) among identified up- and downregulated DEGs. C, Heatmap indicating expression fold change (FC, $\log_2$) of individual AR signaling pathway genes down-regulated upon knockdown of PRMT5 (shPRMT5), MEP50 (shMEP50), and pICln (shpICln) from RNA-seq analysis (left panel) and qPCR validations (right panel). D, Gene ontology (GO) analysis of DEGs that were downregulated upon knockdown of PRMT5 (shPRMT5-down), pICln (shpICln-down), and MEP50 (shMEP50-down). Presented are selected GO terms significantly enriched in the DEG sets related to cell-cycle regulation, DNA replication, transcription, and phosphorylation. The color of each dot indicates the fold enrichment for the GO term, whereas the size of the dot indicates q-value (FDR-corrected p-value) of statistical significance of the enrichment.

Noticeably, PRMT5- or MEP50-knockdown DEGs could be different, even though they were associated with the same GOs or KEGG pathways. But PRMT5 and pICln tended to mediate the same DEGs involved in some GOs and KEGG pathways, e.g. GO:0006351 “transcription, DNA-templated” and GO:0006355 “regulation of transcription, DNA-templated” (Figure 3.5D). Interestingly, pICln appears to have additional roles in regulating phosphatidylinositol signaling and NF-κB signaling in prostate cancer independently of PRMT5 (Figure 3.5D). Taken together, this genome-wide gene expression analysis confirms the role of PRMT5/pICln in AR signaling in prostate cancer and reveals distinct regulatory roles of PRMT5, MEP50, and pICln in various cellular processes such as cell cycle progression.

3.3.5 PRMT5 and pICln expression positively correlates with AR in CPRC patients

To investigate the clinical relevance of described above findings, I examined the expression of AR, PRMT5, pICln, and MEP50 in HNPC and CRPC tissues. Nuclear PRMT5 and pICln expression was the highest in CRPC tissues with elevated AR expression (Figure 3.6A), and nuclear PRMT5, pICln, and MEP50 expression correlates positively with AR expression (Figure 3.6B). In general, correlation with AR expression was higher for PRMT5 and pICln compared to MEP50 (Figure 3.6B, Figure 3.7A-D). Notably, when samples were stratified by top and bottom 50% of AR staining (AR^{high} and AR^{low}), the nuclear PRMT5/pICln expression was lower in AR^{low} tissues compared to AR^{high} (Figure 3.7E and F). However, PRMT5/MEP50 correlation was similar between AR^{low} and AR^{high} groups (Figure 3.7G-I). Consistent with the nuclear PRMT5/AR expression correlation in HNPC tissues [137], nuclear pICln expression also positively correlated with both nuclear PRMT5 and AR expression in these tissues (Figure 3.7J and K). These results further suggest that PRMT5 and pICln are strongly associated with higher AR expression.

Next, 34 datasets from GEO and cBioportal including a total of 3425 HNPC and 1199 CRPC cases with mRNA expression profiles were retrieved. PRMT5/AR and pICln/AR correlations were significantly higher than MEP50/AR correlation, confirming the role of PRMT5/pICln in AR signaling (Figure 3.6C). Interestingly, comparable PRMT5/pICln and PRMT5/MEP50 correlations were observed, consistent with their distinct cellular roles. These results further support the finding that PRMT5 cooperates with pICln to activate transcription of AR in HNPC and CRPC tissues.

I further investigated the relationship of PRMT5 and pICln mRNA expression with patients' survival in CRPC [86]. Notably, patients with high expression of either PRMT5 or pICln had lower survival (Figure 3.6D). These findings support that expression levels of PRMT5 and pICln may affect patient outcomes or potential responses to therapy, indicating their role in prostate cancer progression.

Figure 3.6. PRMT5 and pICln expression positively correlates with AR in CPRC patients.

A-B, AR, AR-V7, PRMT5, pICln, and MEP50 protein expressions were analyzed by IHC in metastatic CRPC samples. A, Representative IHC images of AR, AR-V7, PRMT5, pICln, and MEP50 expression. Scale bar indicates 100 μm. B, Spearman correlations of protein-level expression of AR, AR-V7, PRMT5, pICln, and MEP50 in CRPC tissues. C, Spearman correlations of mRNA expression levels between AR, PRMT5, pICln, and MEP50. The mRNA expression data for 4624 patient samples were obtained from 34 published datasets. Each dot denotes one dataset, representing the gene expression correlation between the pair of selected mRNAs. The dot color indicates the sample size of corresponding dataset. D, Kaplan-Meier curves comparing influences of mRNA expression levels of PRMT5 and pICln, respectively, on patients' survival. Red curves represent patients with high (top 50%) expression of PRMT5 and pICln, whereas blue ones are groups with low (bottom 50%) expression. The mRNA expression and patient survival data were downloaded from the cBioportal SU2C-PCF dataset.

Figure 3.6 continued

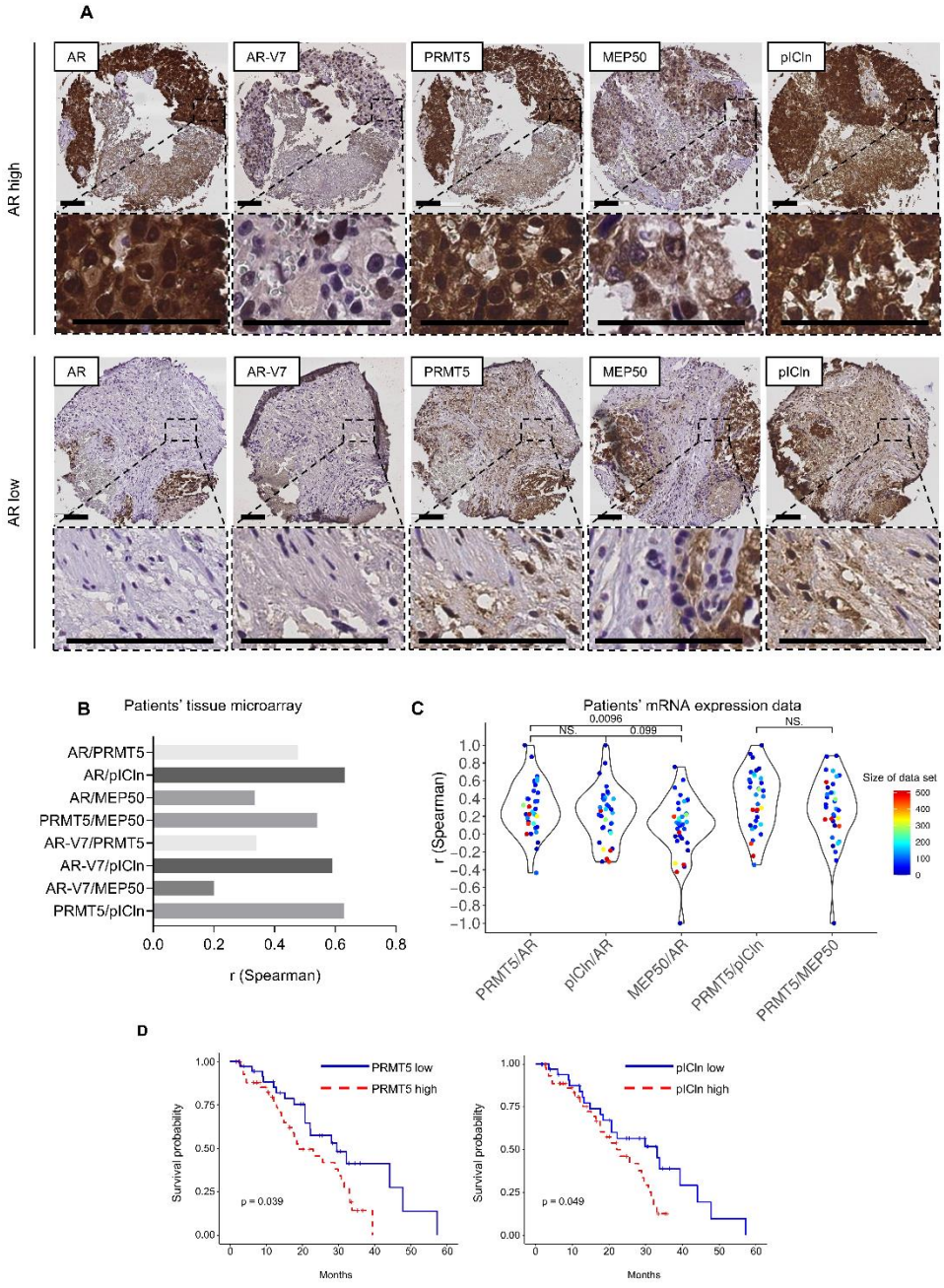

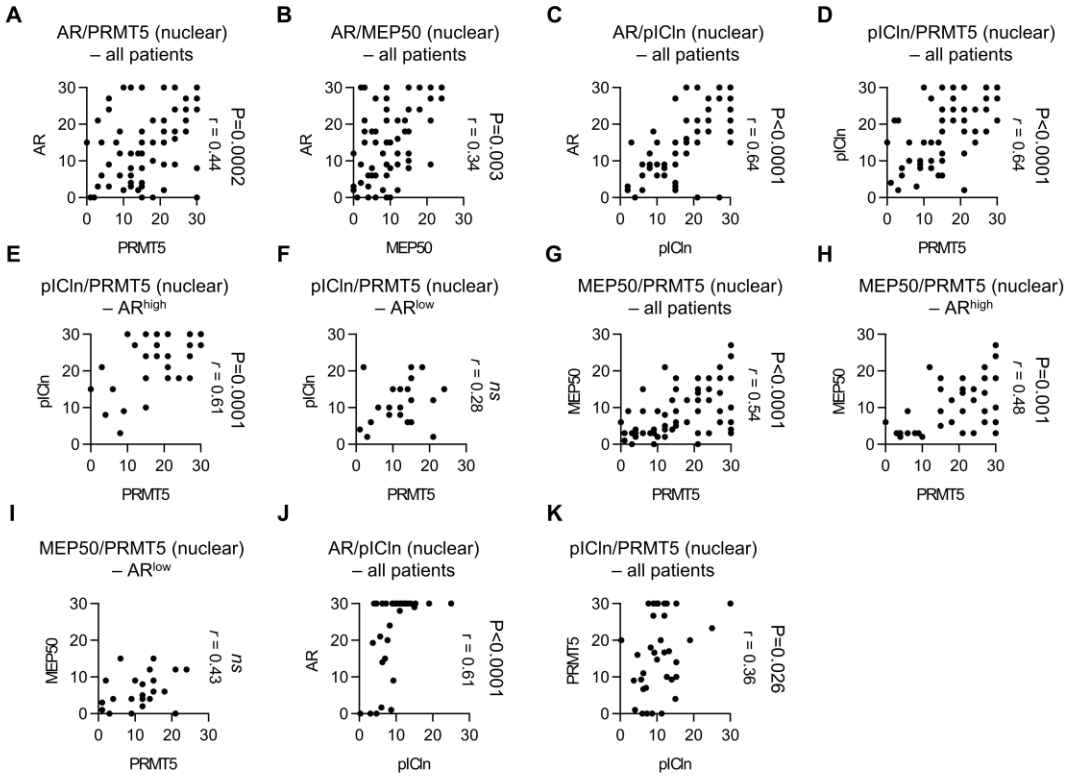

Figure 3.7. PRMT5 and pICln nuclear expression positively correlates with nuclear expression of AR in CRPC and HNPC tissues.

A-K, Correlation analysis (Spearman) of corresponding protein pairs in CRPC and HNPC tissue microarrays (A-I, CRPC tissue microarray; J and K, HNPC tissue microarray). For E-F, H-I same analysis was performed for data stratified based on AR expression. ns $P > 0.05$.

3.3.6 Knockdown of pICln suppresses CRPC tumor growth in mice

To determine whether targeting PRMT5 cofactor pICln can suppress the growth of CRPC tumors *in vivo*, I implanted 22Rv1-shpICln, and 22Rv1-shSC cells subcutaneously into male, pre-castrated NRG mice. When the average tumor volumes reached 100 mm^3, shRNA expression was induced by Dox treatment, and tumor growth was monitored. pICln knockdown significantly suppressed tumor growth (Figure 3.8A), consistent with the suppression of AR expression in xenograft tumors (Figure 3.8B). Analysis of cleaved caspase-3 staining suggested slight induction of apoptosis by pICln knockdown (Figure 3.8C), confirming *in vitro* findings. Ki-67 analysis showed that tumors with pICln knockdown had significantly lower proliferative index compared to scramble control (Figure 3.8D). Taken together, these results demonstrate that PRMT5 and pICln also regulate AR expression and the growth of CRPC tumors *in vivo*.

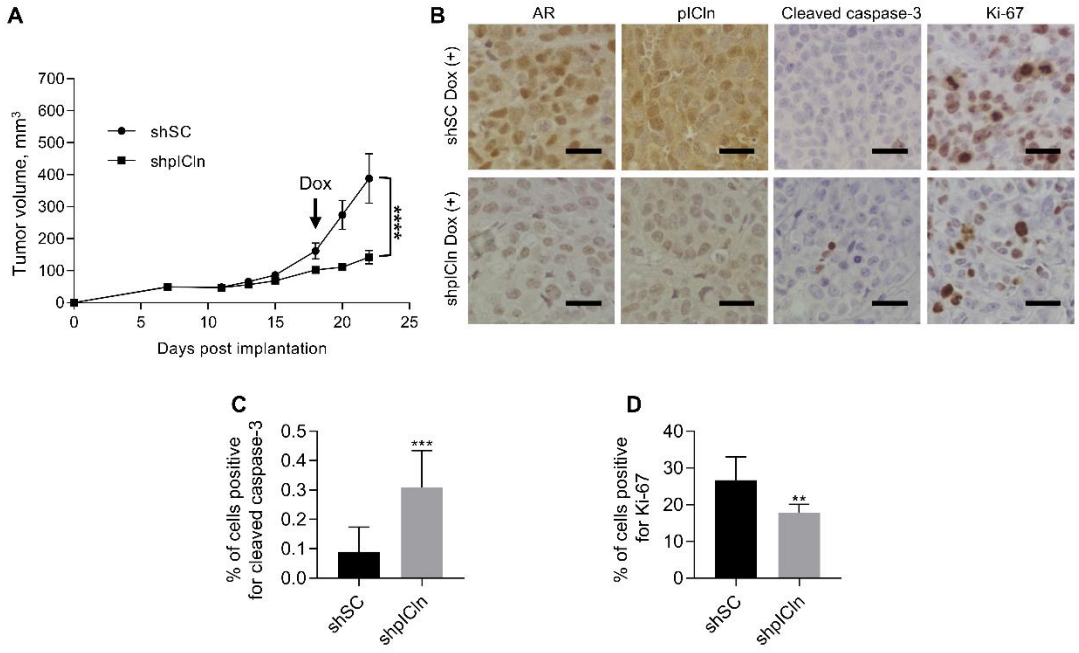

Figure 3.8. Knockdown of pICln suppresses CRPC tumor growth in mice.

22Rv1 cells with Dox-inducible knockdown of pICln (shpICln) or scramble control (shSC) were injected subcutaneously into right flanks of surgically castrated male NRG mice. Tumor-bearing mice were treated with doxycycline in drinking water once tumors reached ~100 mm^3. A, Tumor growth curve was determined and compared between treatment groups (ANOVA; ****, $P <$ 0.0001). B-D, At the end of treatment, tumors were resected and probed for cleaved caspase-3 and Ki-67 using IHC. Presented are representative images (B) and the quantification of the percentage of positively stained cells out of the total number of cells (C, D). Scale bar indicates 40 μm. Results are mean ± standard deviation (n = 10 per group). C, D, Student *t*-test was performed to determine statistical significance. *ns* $P > 0.05$, ** $P < 0.01$, *** $P < 0.001$.

3.4 Discussion

3.4.1 PRMT5 interacts with pICln to epigenetically activate AR transcription independently of MEP50

The finding that PRMT5 epigenetically activates AR transcription prompted me to examine whether MEP50, a canonical cofactor of PRMT5 [120], participates in the activation of AR transcription by PRMT5. Surprisingly, MEP50 was not present at the *AR* promoter, and MEP50 knockdown did not affect AR expression in LNCaP and 22Rv1 cells. This led to the discovery of pICln as a potential cofactor of PRMT5 to activate *AR* transcription. Transcriptomic analysis of PRMT5, pICln and MEP50 target genes further confirmed that pICln, but not MEP50, cooperates

with PRMT5 to regulate AR signaling in CRPC tissues (Figure 3.5). Interestingly, pICln also cooperates with PRMT5 to activate transcription of multiple DNA damage response genes upon ionizing radiation (IR) independent of MEP50 [136]. Thus, pICln rather than MEP50 might be required for the activation of PRMT5 target genes. In contrast, MEP50 might form a complex with PRMT5 and pICln to repress gene transcription. For example, *IVL* promoter was co-occupied by PRMT5, MEP50, and pICln, and knockdown of either MEP50 or pICln increased IVL expression (Figure 3.1C) [136]. Future studies may examine whether the co-occupancy of target gene promoters by PRMT5 and PRMT5-interacting proteins, e.g. MEP50, pICln, RIOK1, and COPR5, determines the transcriptional activation versus repression.

Several studies also demonstrated that PRMT5 may activate transcription of individual genes in a variety of tissues and conditions [136,159,160,216,217,240]. Consistent with recent transcriptomic analysis in LNCaP cells showing that majority of identified DEGs (1136 out of 2035) was downregulated upon PRMT5 knockdown [136], similar number of upregulated and downregulated DEGs was identified in this study upon PRMT5 knockdown in 22Rv1 cells. Thus, PRMT5 likely functions as an epigenetic activator or repressor for different target genes. This notion is also supported by two recent transcriptomic studies in lung cancer cells A549 [241] and leukemia cells MOLM-13 [180]. Because PRMT5 interacts with many chromatin remodelers [114], future studies focusing on the interplay between PRMT5 and PRMT5-interacting proteins including cofactors and other chromatin remodelers will likely shed new light on the epigenetic mechanism of PRMT5-mediated transcriptional regulation of target gene expression.

3.4.2 Competing PRMT5-interacting proteins may alter PRMT5 activity

Results from my group indicate that the binding of pICln may decrease the binding of MEP50 to PRMT5(Chapter 3.3.3). Additionally, it was shown in my group that RIOK1, another interacting protein of PRMT5, can also decrease binding of MEP50 to PRMT5 in competition BiFC assay similar to pICln as shown in the Figure 3.4 (RIOK1 data not shown). On the contrary, Guderian et al. demonstrated that RIOK1 competes with pICln but not MEP50 [132], although this data was generated using recombinant proteins *in vitro*. Furthermore, structural modeling data from Stopa et al. study [120] indicates that RIOK1 and Menin (PRMT5-interacting protein that recruits PRMT5 into MLL complex) can replace MEP50 in PRMT5:MEP50 complex. These observations raise an interesting possibility that balance of expression level and cellular

distribution of PRMT5-interacting proteins, likely in addition to expression and localization of PRMT5 itself, may regulate PRMT5 activity to drive methylation of specific epigenetic and non-epigenetic factors. Here, I observed strong nuclear expression of pICln and PRMT5 that were significantly correlated with AR expression (Figure 3.6 and 3.7). Importantly, Owens et al. observed that distribution of pICln changes upon radiation treatment in LNCaP cells to promote pICln nuclear localization by that promoting H4R3 methylation at the promoters of DNA damage response genes [136]. However, the mechanism of pICln nuclear translocation upon DNA damage is not established.

In non-transformed cells pICln is predominantly cytoplasmic and functions as chaperone for Sm protein assembly to assist formation of small nuclear ribonucleoproteins (snRNPs) [242]. At the same time pICln can be present in the nucleus as well, but nuclear pICln is not a part of snRNPs and does not get shuttled into cytoplasm together with Sm proteins [242]. On the contrary, in cancer cells pICln can be predominantly nuclear-localized [132]. Thus, further elucidation of mechanism of pICln function and translocation in the nucleus as well as structural studies of PRMT5-pICln and PRMT5-MEP50-pICln interaction is required.

On the other hand, RIOK1 appears strongly cytoplasmic in cancer cells [132]. Notably, RIOK1 is not expressed in prostate cancer (https://www.proteinatlas.org/ENSG00000124784-RIOK1/pathology) and is rather associated with RAS-driven cancers such as colorectal, gastric, and lung tumors [243,244]. Given the important cytoplasmic role of PRMT5 in post-translational regulation of signaling molecules, it will be important to investigate the role of RIOK1 role in regulation of PRMT5 activity, particularly in the context of prostate cancer progression to the neuroendocrine phenotype.

3.4.3 Targeting interaction of PRMT5 with specific binding partners may provide a better approach for the cancer therapy

Although targeting PRMT5 enzymatic activity or protein expression can be explored as therapeutic approach for prostate and other cancers treatment (in fact, five PRMT5 enzymatic inhibitors are in clinical trials for cancer treatment right now), it is possible that targeting all PRMT5 activity can have significant side effects in the body. Targeted delivery, for example, PSMA-based approaches, could overcome this obstacle. Alternatively, targeting specific protein-protein interactions (PPIs) will allow to achieve higher precision and efficiency of therapy. For

example, targeting PRMT5-pICln interaction can decrease AR signaling for HNPC and CRPC therapy without significantly interrupting other PRMT5 functions. Elucidation of the function of specific interacting partners of PRMT5, as well as the structure of the complex will allow to develop this specific targeting approach. As PRMT5 functions within larger epigenetic complexes, further elucidation of PRMT5 interactome will significantly advance drug development for PRMT5 targeting.

3.5 Methods

3.5.1 Cell lines and reagents

LNCaP, 22Rv1, COS-1, and 293T cells were purchased from ATCC (Manassas, VA, US). Frozen cultures were recovered and expanded in complete media (RPMI1640 (Corning, NY, US), supplemented with 10% FBS (Atlanta Biologicals, Lawrenceville, GA, US), 2 mM L-glutamine (Corning, NY, US), and 100 units/mL penicillin and 100 µg/mL streptomycin (Gibco, Gaithersburg, MD, US)). Cells were not passaged more than 30 times. For long-term storage, cells were frozen in freezing media (80% fresh complete media, 10% conditioned complete media, 10% DMSO v/v). Cell authentication and mycoplasma contamination check were performed as described previously [136].

3.5.2 Plasmid construction

Plasmids for the doxycycline (Dox)-inducible knockdown of genes of interest were generated by cloning short hairpin RNA (shRNA) targeting the gene of interest mRNA into EcoRI/AgeI sites of the pLKO-tet-ON vector (Addgene #21915). The full list of used shRNA sequences and scramble control (SC) sequence is in the Appendix B. Plasmids for BiFC analysis of the PRMT5:pICln interaction were generated by cloning the N-terminal 1-292 fragment of PRMT5 fused with the N-terminal 1-155 fragment of Venus fluorescent protein into the pCMV vector containing the Myc-tag (pCMV-Myc-PRMT5(NT292)-VN155) and the complementary C-terminal fragment of Venus fused with pICln into the pCMV vector containing the HA-tag (pCMV-HA-VC155-pICln). Plasmids for BiFC analysis of the PRMT5:MEP50 interaction were generated by cloning the N-terminal 1-155 fragment of Venus fused with the N-terminal 1-292 fragment of PRMT5 into the pCMV vector containing the Myc-tag (pCMV-Myc-VN155-

PRMT5(NT292)) and the complementary C-terminal fragment of YFP fused with MEP50 into the pCMV vector containing the HA-tag (pCMV-HA-VC155-MEP50). For overexpression of pICln, pICln cDNA was cloned into the pCMV vector containing HA-tag (pCMV-HA-pICln).

3.5.3 Stable cell line generation

Lentiviral transduction was used for the generation of cell lines with Dox-inducible expression of shRNA that target genes of interest. For each gene, two shRNA sequences that target different regions of the mRNA were used. The full list of shRNA sequences and scramble control sequence is in the Appendix B. Briefly, 293T cells were co-transfected with corresponding pLKO-tet-ON-shRNA plasmids (described above) and envelope and packaging plasmids (pHR'-CMV-8.2ΔVPR, Addgene #8455, and pHR'-CMV-VSV-G, Addgene #8454) using FuGENE HD reagent (Promega, Madison, WI, US) according to the manufacturer's protocol. Viral particles were harvested 48 h later and used to infect 22Rv1 or LNCaP cells in the presence of 0.01 mg/mL polybrene, and 48 h later selection of infected cells was initiated by applying 2 μg/mL puromycin. After selection, single-cell derived stable cell lines were generated using limiting dilution cloning by diluting cell suspension to 2 cells per mL and plating 250 μL cell suspension per well of 96-well plate [230]. The knockdown was confirmed via western blot for the protein of interest and qPCR with gene-specific primers.

3.5.4 Western blotting

For protein level analysis, cells were trypsin-dissociated and lysed in RIPA buffer (10 mM Tris-HCl, pH 8.0, 5 mM EDTA, 1% Triton X-100, 0.1% sodium deoxycholate, 0.1% sodium dodecyl sulfate (SDS), 140 mM NaCl, 5 μg/mL of each chymostatin, leupeptin, pepstatin A, and antipan, and 1 mM PMSF) for 30 min on ice. The insoluble fraction was separated by centrifugation at 12000 x g for 10 min at 4^{o}C. Total protein concentration was measured using the Bradford method. Twenty μg of total cell lysate was loaded on 10% or 15% SDS-polyacrylamide gel, separated, and then transferred to nitrocellulose membrane. Antibodies against AR (1:2000 dilution, Santa Cruz Biotechnology), PRMT5 (1:1000, Millipore), β-actin (1:1000, Sigma-Aldrich), pICln (1:2000, Abcam), MEP50 (1:500, Cell Signaling Technology), and secondary sheep anti-mouse IgG ECL antibody HRP conjugated (1:1000, GE Healthcare) and secondary

donkey anti-rabbit IgG ECL antibody HRP Conjugated (1:1000, GE Healthcare) were used for western blotting probing. Membranes were visualized with Bio-Rad ChemiDoc Touch Imaging System (Bio-Rad, Hercules, CA, US). The intensity of bands was determined with Image Lab software (Bio-Rad, Hercules, CA, US) and normalized to corresponding loading controls. All used antibodies, catalog numbers, and RRID are listed in Appendix A.

3.5.5 Cell proliferation assay

The cell proliferation assay was performed using MTT reagent (Sigma, St Louis, MO, US). Cell medium was removed, and 70 μL of MTT solution (0.5 mg/mL) was added into each well and incubated at 37°C for 4 h. At the end of incubation, the MTT solution was removed, then 130 μL of DMSO was added into each well and incubated at 37°C for another 15 min. The absorbance value was then read at 550 nm using the BioTek Synergy™ 4 Microplate Reader (BioTek Instruments, Winooski, VT, US).

3.5.6 Cell cycle analysis

Approximately 10^6 cells were trypsinized, filtered through a 70 μm mesh to remove aggregates, and fixed in 1000 μL 70% v/v ethanol overnight at 4°C. After that, cells were washed in PBS and incubated in 300 μL of staining solution (20 μg/mL propidium iodide and 20 μg/mL RNase A in PBS) overnight at 4°C. Cells were analyzed with Guava EasyCyte Flow Cytometer (Guava Technologies, Hayward, CA, US), and at least 20000 live cells were counted per sample. Data were subsequently analyzed using FlowJo software. Sub-G_1 cells were gated out, and proportions of cells in different stages of the cell cycle were determined using Dean-Jett-Fox modeling [231].

3.5.7 RNA isolation, reverse transcription, and quantitative real-time PCR

For analysis of gene expression at the mRNA level, total cell RNA was isolated using TRIzol Reagent (Ambion, Carlsbad, CA, US). At least 1 μg of total RNA was used for the reverse transcription (RT) using the High Capacity cDNA Reverse Transcription Kit (Promega, Madison, WI, US) and random primers according to manufacturer's instruction. qPCR was conducted using FastStart Universal SYBR Green Master Mix (Thermo Fisher Scientific, Waltham, MA, US) in a

QuantStudio 6 system (Applied Biosystems, Foster City, CA). Expression levels of genes were normalized to glyceraldehyde-3-phosphate dehydrogenase (GAPDH) level and were calculated using the $2^{-\Delta\Delta CT}$ method [232]. All RT-qPCR primers are listed in Appendix B.

3.5.8 Chromatin immunoprecipitation (ChIP)

First, cross-linking was performed by adding 270 μL of 37% formaldehyde per 10 mL media directly into cell culture media and incubating plates at room temperature for 10 min. Then, 1.12 mL of 1.25 M glycine was added per 10 mL media to stop the cross-linking, and plates were incubated at room temperatures for additional 5 min. All next steps were performed on ice. Cells were scraped off the plates, washed twice in cold PBS, and resuspended in the immunoprecipitation (IP) buffer with protease and phosphatase inhibitors: 50 mM Tris-HCl pH 7.4, 150 mM NaCl, 5 mM EDTA, 1% Triton X-100, 0.5% NP-40, 0.5 mM DTT, 5 μg/mL of each chymostatin, leupeptin, pepstatin A, and antipan, 0.5 mM PMSF, 30 mM PNPP, 10 mM NaF, 0.1 mM Na_3VO_4, 0.1 mM Na_3MoO_4, 10 mM β-glycerophosphate. Cells were sonicated using Branson Model 250 Sonifier at Output 4, 90% duty cycle to generate ~500 bp chromatin fragments. Chromatin fragments size was verified using agarose/ethidium bromide gel.

Two micrograms of each of antibodies against PRMT5 (Millipore), MEP50 (Cell Signaling Technology), RIOK1 (Bethyl), COPR5 (Novus Biological), pICln (Abcam), H2AR3me2s (Abcam), H3R2me2s (EpiGentek), H3R8me2s (Abcam), or H3R3me2s (Abcam) were used to immunoprecipitate protein-DNA complexes for the subsequent isolation of DNA using Chelex [233]. DNA immunoprecipitated with naïve rabbit or mouse IgG served as a control. The co-immunoprecipitated DNA was quantified by qPCR using gene-specific primers. All used antibodies are listed in the Appendix A, and ChIP-qPCR primers are listed in the Appendix B.

qPCR was conducted using FastStart Universal SYBR Green Master Mix (Thermo Fisher Scientific, Waltham, MA, US) in a QuantStudio 6 system (Applied Biosystems, Foster City, CA, US).

3.5.9 Bimolecular fluorescence complementation (BiFC)

BiFC plasmids (250 ng each) encoding a protein of interest fused to the N- or C-terminal fragment of the Venus fluorescent protein (VN155 or VC155) and 100 ng of the plasmid encoding

the Cerulean fluorescent protein (CFP, as a positive control for transfection) were co-transfected into COS-1 cells and BiFC efficiency (YFP/CFP) was analyzed essentially as described previously [239]. For BiFC competition assay, 500 ng of the plasmid encoding a PRMT5 interacting protein (MEP50 or pICln) or empty vector control were co-transfected to analyze the inhibition of PRMT5:MEP50 interaction. Results are presented as median ± SD from three independent biological replicates.

3.5.10 Xenograft tumor growth

Animal experiments were performed in the Biological Evaluation Facility of the Purdue University Center for Cancer Research and approved by the Purdue University Animal Care and Use Committee. Six to eight weeks old male non-obese diabetic-Rag1(null)-γ chain(null) (NRG) mice were castrated, and 14 days later 2 x 10^5 cells of 22Rv1-shpICln or -shSC in 100 μL of RPMI-1640 media were mixed with 100 μL of Matrigel (200 μL total) and injected subcutaneously into the right lower flank (10 mice/group). After tumor volumes reached ~100 mm^3, mice were treated with Dox (1 mg/mL in drinking water) to induce the expression of shRNA. Tumor growth was measured every 2-3 days, and tumor volume was calculated using ½ × L × W × H without blinding method. When control tumors reached ~2000 mm^3, tumors were resected for IHC analysis.

3.5.11 Immunohistochemistry analysis of xenograft tumors

Paraffin embedment and slide preparation of tumor samples were performed at the Purdue Histology Research Laboratory.

Samples were deparaffinized and rehydrated by incubating slides overnight at 37°C, and then for 2 h at 65°C, followed by incubation in Xylenes solution and a range of ethanol concentration from 100% to 30%, and finally in Millie-Q water at room temperature. Endogenous peroxides were inactivated by incubation of slides in 3% H_2O_2 for 10 min at room temperature. Antigen retrieval was performed by incubating slides soaked in 10 mM Tris pH 10 on boiling water bath for 30 min. Slides were then blocked with 5% non-fat milk solution in PBS for 1 h at room temperature with shaking. Antibodies against AR (1:100, Santa Cruz Biotechnology), PRMT5 (1:100, Millipore), Ki-67 (1:500, BD Biosciences), or cleaved caspase-3 (1:500, Cell Signaling Technology) were applied on sections overnight in 5% non-fat milk in PBS. After 3

washes in PBS, sections were probed with corresponding secondary HRP-conjugated antibodies diluted (1:100) in 5% non-fat milk in PBS for 1 h at room temperature. Following another triple washing of slides with PBS, the chromogenic reaction was performed with DAB peroxidase kit (Vector Laboratories, Inc., Burlingame, CA, US), and then slides were counter-stained with hematoxylin-eosin (HE) solution (Vector Laboratories, Inc.). The slides were subsequently dehydrated and mounted using VectaMount^{TM} permanent mounting medium (Vector Laboratories, Inc.). Image analysis and quantification were performed using ImmunoRatio online software [234].

3.5.12 Immunohistochemistry analysis of HNPC and CRPC prostate cancer tissue microarrays

Antibodies against AR (Agilent), AR-V7 (RevMab Biosciences), PRMT5 (Millipore Sigma), MEP50 (Cell Signaling), and pICln (Abcam) were used for staining according to manufacturers' protocol. The tissue staining in the TMA was semi-quantified blindly (with tissues deidentified) as follows: the intensity of staining was scored from 0 (no staining) to 3 (high staining), and the proportion of cells showing expression was scored from 0 (no cells stained) to 10 (all cells stained). The staining score was derived by multiplying the intensity of staining by the proportion of cells with this staining level. The staining was scored separately in the nucleus and the cytoplasm. Spearman correlation analysis was used to determine the correlation of protein expression.

3.5.13 Clinical data analysis

Gene expression profiles of 34 prostate cancer data sets were obtained from Gene Expression Omnibus (GEO) [245], cBioportal [246,247], and Oncomine [248] (see Appendix C for datasets detail) with total of 4624 samples. Gene expression levels of datasets from GEO were $\log_2$ transformed and median centered. Gene expression profiles from cBioportal were downloaded with annotation of "mRNA_median_Zscores". If one gene had multiple gene expression files in the same dataset, the sum of all corresponding mRNA levels was used to represent the expression level of the gene. Spearman's rank correlation coefficients were calculated to evaluate the correlations of specific gene pairs. Wilcoxon Rank Sum test was used to compare the differences between groups of correlations for all 34 datasets.

The clinical information and gene expression data for prostate cancer [86] were downloaded from cBioPortal [246,247] for the survival analysis. Patients were divided into two groups based on the top and bottom 50% quantile of expression levels for selected genes. Survival probability was computed in R using the survfit function in the R package survival. Kaplan-Meier plots were generated using the ggsurvplot function of package survminer.

Construction of CRPC tissue microarray (TMA) containing samples from 20 patients and HNPC TMA containing samples from 72 HNPC patients (32 with BPH, 20 with prostate cancer Gleason score 6, and 20 with prostate cancer Gleason score⩾7) was described previously [137,249].

3.5.14 RNA-seq analysis

22Rv1 cells with Dox-inducible knockdown of PRMT5, MEP50, pICln (22Rv1-shPRMT5, -shMEP50, -shpICln) were grown in absence or presence of Dox (1 μg/mL) for 6 days. Dox was replenished every 48 h. At the end of treatment, cells were harvested, and TRIzol reagent (Ambion, Carlsbad, CA, US) was used for total RNA isolation. RNA integrity and purity were confirmed using agarose gel (no degradation or contamination) and Agilent 2100 (RNA integrity number ≥ 6.8). At least 1 μg of total RNA was used for DNA library preparation with NEB Next Ultra II kit (New England Biolabs, Ipswich, MA, US). The sequence reads were mapped to the UCSC human genome hg38 using RNA-seq aligner STAR (v2.5) [250] with the following parameter: "--outSAMmapqUnique 60". Then, uniquely mapped sequencing reads were assigned to transcripts using featureCounts (v1.6.2) [251] based on GENECODE GRCh38 release 25 annotation gtf file. The low expressed transcripts were filtered out from further analysis if their read count per million (CPM) > 0.5 in less than three samples. TMM (trimmed mean of M values) method was adopted to perform cross-sample normalization on transcript expressions. Finally, the differential expression analysis between WT and shRNA treated samples was performed by using edgeR (v3.20.8) [252,253]. Differentially expressed transcripts (DETs) were determined if their p-values were less than 0.01 after multiple test correction with false discovery rate (FDR) adjustment. The unique genes with differentially expressed transcripts were identified as differentially expressed genes (DEGs). In order to distinguish Gene Ontology (GO) functions and KEGG pathways significantly over-represented in DEGs, DAVID [254,255] was used to perform functional enrichment analysis on up- or down-regulated DEG sets, respectively.

Raw data is deposited in GEO, accession number GSE154951.

3.5.15 Statistical analysis

Unless stated otherwise, results are presented as mean ± SD. Analysis of high-throughput data is described above and analysis of low-throughput data was performed using GraphPad Prism 8.00 (GraphPad Software, La Jolla California US, www.graphpad.com). For qPCR experiments, the analysis was performed on C_T values of genes normalized to the C_T value of GAPDH loading control. For ChIP-qPCR experiments, the analysis was performed on C_T values of specific IP normalized to the C_T value of non-specific IgG control. For western blotting experiments, the analysis was performed on protein band intensity normalized to β-actin loading control band intensity. MTT assay was performed at indicated time points, and OD550 values were normalized to values from Day 0 for each cell line. For the comparison of two sample groups, unpaired two-tailed *t*-test with Welch's correction was used. A *p* value less than 0.05 was considered significant and marked by asterisk in the figures (*, $p < 0.05$; **, $p < 0.01$; and ***, $p < 0.001$) while ns represents insignificant *p*-value ($p > 0.05$).

For animal studies, the group size was calculated based on pilot experimental data using G*Power software [235]. Based on preliminary data, a 2-fold decrease of growth upon the PRMT5 knockdown with SD of 0.25 was expected (where 1 is no knockdown group growth). To detect 0.25-fold change at the power level 80%, alpha level 0.05, and sample effect 0.5, the sample size of a group should be 10 mice.

3.6 Supplemental figures

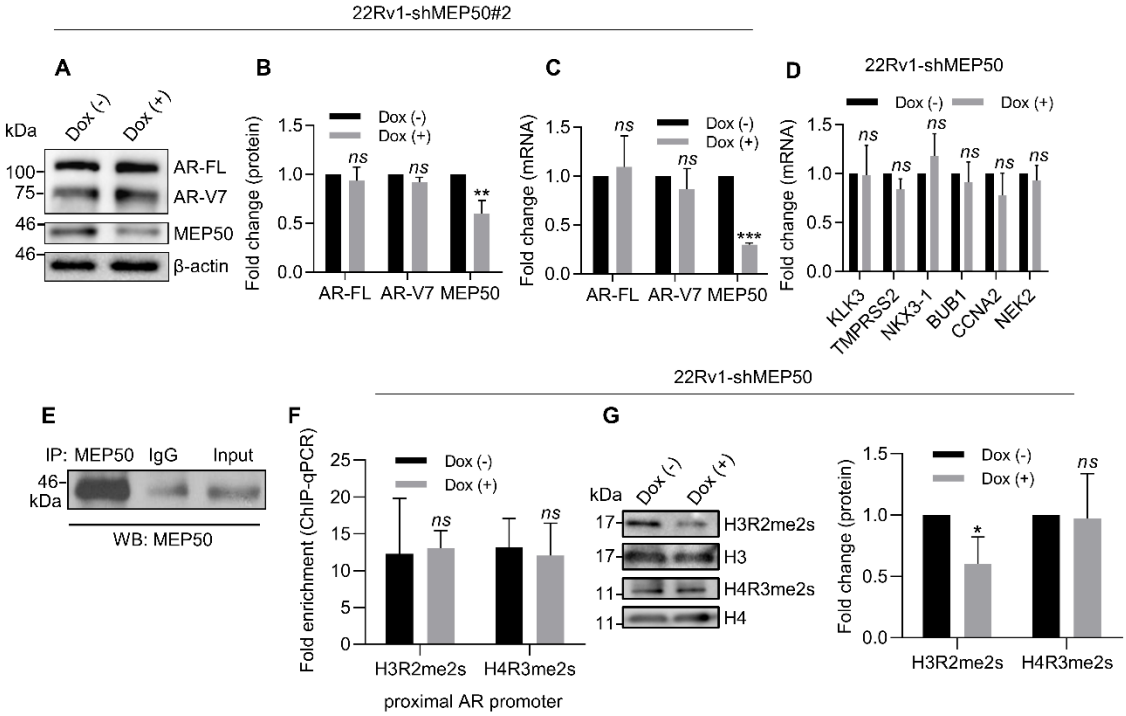

Figure S3.1. MEP50 is not required for PRMT5-mediated activation of AR transcription in CRPC cells.

A-B, Representative western blot analysis (A) and quantification (B) of protein expression in cell lysates of 22Rv1 cells with doxycycline-inducible MEP50 knockdown (22Rv1-shMEP50#2) incubated in the presence (Dox (+)) or absence (Dox (-)) of doxycycline for 6 days. C, qPCR analysis of gene expression in cells from A. D, qPCR of AR target genes in 22Rv1-shMEP50 cells after 5 days of MEP50 knockdown. E, western blot analysis of immunoprecipitates of MEP50 from LNCaP cell lysate. F, ChIP-qPCR analysis of histone methylation at the proximal AR promoter at Day 6 of MEP50 knockdown was performed with indicated antibodies. G, Representative western blot analysis and quantification of H4R3me2s and H3R2me2s in cell lysates of 22Rv1-shMEP50 incubated in the presence (Dox (+)) or absence (Dox (-)) of doxycycline for 6 days. For ChIP-qPCR, values were normalized to the corresponding IgG control. For western blotting, ChIP-qPCR, and qPCR analysis, statistical significance of group difference was determined for 'Dox (-) vs Dox (+)'. Results are mean ± SD from 3 independent experiments. For western blotting of AR, the AR N-20 antibody (sc-816, Santa Cruz) was used. Student *t*-test with Welch's correction was performed to determine statistical significance. *ns* $P > 0.05$, * $P < 0.05$, ** $P < 0.01$, *** $P < 0.001$.

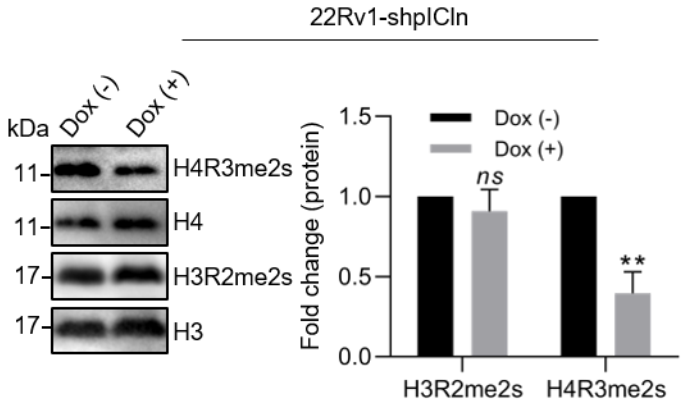

Figure S3.2. Representative western blot analysis and quantification of H4R3me2s and H3R2me2s in cell lysates of 22Rv1 cells with doxycycline-inducible pICln knockdown (22Rv1-shpICln) incubated in the presence (Dox (+)) or absence (Dox (-)) of doxycycline for 6 days.

CHAPTER 4. ROLE OF PRMT5/MEP50 IN PROSTATE NEUROENDOCRINE DIFFERENTIATION

Results presented in this Chapter were not published at the moment of the dissertation deposit.

4.1 Summary

Prostate cancer is one of the most frequently diagnosed non-skin cancers and a second-leading cause of cancer-related death in males in United States. Neuroendocrine prostate cancer (NEPC) is the most lethal subtype of prostate cancer: compared to prostate adenocarcinoma with the median survival of about ten years, the median survival length for NEPC patients is less than a year. There are no curative treatment options available for NEPC patients. The major cause of NEPC emergence is neuroendocrine differentiation (NED) of prostate cancer cells in response to the treatment. Preliminary results from my group indicate that PRMT5 and MEP50 together are necessary and sufficient to induce NED in prostate cancer cells *in vitro*. Here, I present evidence that co-overexpression of PRMT5 and MEP50 in mouse prostate induces NED in prostate cells *in vivo*. Co-overexpression of PRMT5/MEP50 increased proliferative index of prostate tissues. Furthermore, *in vitro*, during ADT-induced NED PRMT5 dissociates from AR promoter and does not function as an epigenetic activator of AR transcription.

4.2 Introduction

4.2.1 NEPC is often induced by prostate cancer therapy

Prostate cancer is estimated to cause 33,330 deaths in US in 2020 [21] in spite of significant progress made for prostate cancer treatment. The major cause of prostate cancer mortality is metastasis, which can be present at the time of diagnosis or develop as a result of localized prostate cancer recurrence after the local therapy (radiation or surgery). About 50% of high-risk localized prostate cancer cases recur within 5 years following therapy [256].

Androgen deprivation therapy (ADT) is a standard of care for patients with metastatic disease. Additionally, ADT is used as a radiosensitizer for radiation therapy of high-risk localized prostate cancer. ADT aims to decrease the serum level of circulating androgens and thus reduce

the activity of androgen receptor (AR) signaling in prostate cancer cells. Nearly 100% of patients receiving ADT will experience reduction of prostate cancer growth and associated symptoms. However, all cases of prostate cancer eventually become resistant to ADT.

One of the mechanisms of ADT resistance is neuroendocrine differentiation (NED). During NED, prostate cancer cells become independent of AR signaling and acquire neuroendocrine (NE)-like features such as expression of chromogranin A (CgA) and neuron-specific enolase (NSE). These NE-like cells are highly resistant to apoptosis and promote growth and apoptotic resistance in other prostate cancer cells via paracrine signaling [82]. NE-like cells share multiple genetic alterations with CRPC cells, at the same time the phenotype of cells of these two cancer types is vastly different, and the transdifferentiation process is reversible [257]. Because of these observations, it was suggested that epigenetic shift can be the driving force of NEPC progression.

As PRMT5 functions as an epigenetic activator of AR expression in CRPC in pICln-dependent and MEP50-independent manner, and NE-like cells are typically AR-negative, I sought to investigate the status of PRMT5, MEP50, pICln, and associated histone methylations at the AR promoter and control PRMT5/MEP50 repressed gene (IVL).

4.2.2 PRMT5 and MEP50 are necessary and sufficient for NED *in vitro*

Initially, my group identified PRMT5 as an interacting protein of CREB, a transcriptional regulator of radiation-induced NED [258]. Preliminary data from my group indicates that PRMT5 and the canonical cofactor of PRMT5 methylosome protein (MEP50) are upregulated in HNPC LNCaP cells upon ADT-induced NED (mimicked by the treatment of cells with charcoal-dextran-stripped FBS (CSS-FBS)-containing media) (Figure 4.1A).

Co-overexpression of PRMT5 and MEP50 in LNCaP cells induced NED in LNCaP cells (Figure 4.1B), while co-overexpression of catalytically inactive PRMT5 mutant with MEP50 or PRMT5 with interaction-deficient MEP50 mutant does not induce NED (Figure 4.1B). These observations indicate that PRMT5 and MEP50 are sufficient for NED induction, and their interaction is required for this process.

Moreover, doxycycline (Dox)-induced knockdown of either of these proteins prevents ADT-induced NED of LNCaP (Figure 4.1C and D) suggesting that PRMT5/MEP50 complex is necessary for NED in LNCaP cells.

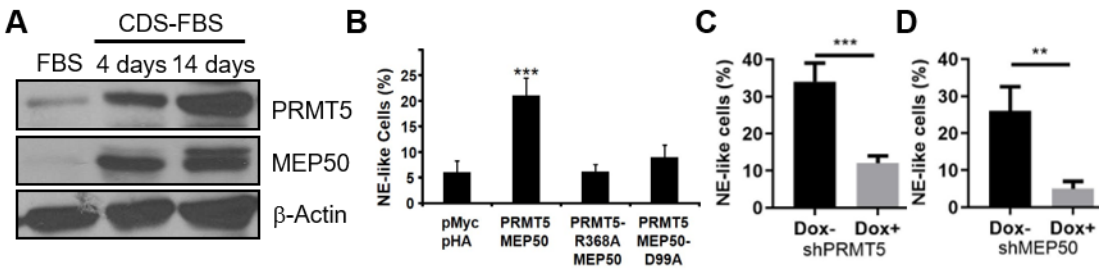

Figure 4.1. PRMT5/MEP50 complex is required for NED in LNCaP cells.

A, LNCaP cells were cultured in regular media (FBS) or in androgen-depleted media (CDS-FBS) for 4 or 14 days, and cell lysates were analyzed with western blot. **B**, LNCaP cells were transfected with the combination of empty vectors (pMyc pHA), vectors for myc-PRMT5 and HA-MEP50 expression, or in combination with catalytically inactive PRMT5 (PRMT5-R368A) and interaction deficient mutant MEP50 (MEP50-D99A). After 72 h, the percentage of NE-like cells was quantified. **C**, **D**, LNCaP cells with Dox-inducible PRMT5 (**C**) or MEP50 (D) knockdown were treated with CDS-FBS for 4 days with or without Dox (Dox+ and Dox-, correspondingly), and percentage of NE-like cells was quantified. NE-like cells were defined as cells with neurite-like extension at least twice longer than cell body diameter. ** $P < 0.01$, *** $P < 0.001$.

These results were generated by Xuehong Deng, unpublished.

4.2.3 Mouse models of NEPC

Animal models of NEPC are extremely important for fundamental understanding of molecular mechanisms of NED to develop novel therapeutic approaches for NEPC therapy. Multiple models of NEPC were developed in genetically engineered mice [259]. Overwhelming majority of these models rely on the expression of viral antigens, such as SV40 large and small T antigens to induce tumor formation [259]. In these models, viral antigens promote tumor progression by inhibiting function of RB1 and p53 [259]. Another GEM model involves conditional knockout of RB1 and p53 in mouse prostate epithelium [106]. Thus, the existing mouse models of NEPC rely on direct or indirect inactivation of RB1 and p53 which does not adequately represent clinical progression of treatment-induced NEPC [260].

Since co-overexpression of PRMT5 and MEP50 mediates treatment-induced NED *in vitro*, I sought to investigate the potential of combined prostate-specific overexpression of PRMT5 and MEP50 to induce NEPC in the mouse model to mimic treatment-induced NED.

4.3 Results

4.3.1 PRMT5 dissociates from AR promoter during NED in vitro

My group has established that PRMT5 function as an epigenetic activator of AR transcription in LNCaP cells via binding to the AR promoter and symmetrically dimethylating histone H4R3 [137]. As NE-like cells are typically AR-negative, I sought to investigate whether binding of PRMT5 to the AR promoter changes after NED. To this end, I utilized the model of NED in which LNCaP cells are treated with media containing charcoal-dextran-stripped FBS (CDS-FBS) [261]. Treatment of FBS with charcoal and dextran removes lipophilic molecules including steroid hormones and factors such as estradiol, prostaglandins, vitamin B, and androgens. Although CDS-FBS is depleted of multiple hormones and not only androgens and thus results of treatment of cells with such media would reflect more complicated effect rather than effect of only androgen depletion, supplementation of the CDS-FBS media with DHT at the moment of NED induction prevents NED in LNCaP cells [261]. Thus, CDS-FBS media treatment of LNCaP can be used as *in vitro* model for NED induction.

To investigate the binding of PRMT5 and its cofactors to the specific chromatin loci during NED, I used chromatin immunoprecipitation assay with following quantitative polymerase chain reaction (ChIP-qPCR) in LNCaP cells treated with CDS-FBS media for 7 days (NED-LNCaP) and LNCaP cultured in the regular media (WT-LNCaP). I also analyzed the presence of PRMT5-mediated methylation marks (H2AR3me2s, H3R2me2s, H3R8me2s, and H4R3me2s) as an indicator of PRMT5 enzymatic activity in the region of interest.

NED-LNCaP demonstrated reduced binding of PRMT5 to the proximal region of the AR promoter (−493 219 to −226 bp from transcription start site (TSS)) compared to the WT-LNCaP (Figure 4.2A). Consistently, methylation levels of H3R2 and H4R3 were decreased (Figure 4.2A). At the same time, binding of pICln (that is recruited to the proximal AR promoter by PRMT5 as described in Chapter 3 of this dissertation) was also decreased. Binding of MEP50 or presence of other PRMT5-catalyzed methylation marks were not affected (Figure 4.2A). Taken together, these results indicate that upon NED PRMT5 dissociates from AR promoter, and this dissociation is accompanied by a decrease of pICln binding and H4R3me2s and H3R2me2s level.

As a control for PRMT5 and associated methylation binding I used a distant region of AR promoter (-4481 to 220 -4308 bp from TSS). ChIP-qPCR assay for this region indicated no

significant change of PRMT5 or cofactors binding and PRMT5-mediated methylation (Figure 4.2B).

Since PRMT5 functions as both activator for AR and repressor for IVL (as discussed in Chapter 3), I next determined whether PRMT5 presence changes upon NED at the IVL promoter. Notably, PRMT5 and cofactors binding as well as PRMT5-driven methylation marks in NED-LNCaP were decreased compared to the WT-LNCaP (Figure 4.2C).

Taken together, these observations indicate that, upon NED, LNCaP cells undergo significant epigenetic shift, simultaneously, PRMT5 and cofactors binding to its target genes promoters AR and IVL drastically decreases.

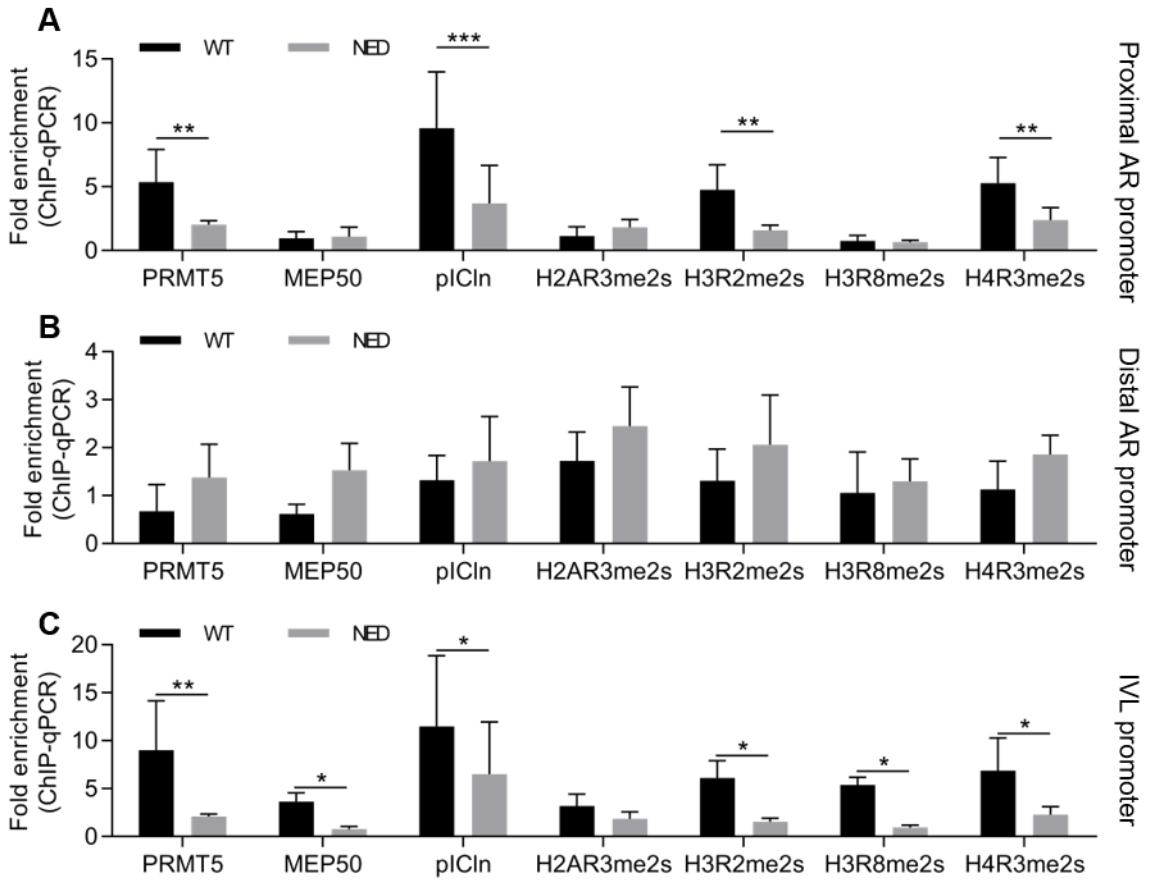

Figure 4.2. PRMT5 binding to its target genes promoters changes drastically upon NED.

LNCaP cells were cultured in CDS-FBS media for 7 days (NED) or normal media (WT) and harvested for ChIP-qPCR. IP for indicated proteins was performed, followed by qPCR for proximal AR promoter (**A**), distal AR promoter (**B**), and IVL promoter (**C**). Values were normalized using IgG control, and statistical significance of group difference was determined for 'WT vs NED'. ns $P > 0.05$, * $P < 0.05$, ** $P < 0.01$, *** $P < 0.001$.

4.3.2 Generation of PB-PRMT5; PB-MEP50 transgenic mice

Previously, my group observed that co-overexpression of PRMT5 and MEP50 in LNCaP cells induces NED. Because of that, I sought to investigate whether similar effect can be observed upon prostate-specific co-overexpression of PRMT5 and MEP50 *in vivo*. For this purpose, I developed transgenic mice with rat probasin (PB) promoter-driven expression of either PRMT5 and MEP50 (PB-PRMT5; PB-MEP50), or each transgene alone (PB-PRMT5 and PB-MEP50), or wild-type control without overexpression of recombinant protein (Figure 4.3A). PB promoter provides high expression of transgenes in prostate epithelial cells [262]. In my model, both

transgenic PRMT5 and MEP50 had myc-tag allowing to monitor both transgenes expression using simple chromogenic staining.

After generating mice with required genotypes (Figure 4.3B), first, I confirmed that transgenes are expressed in the prostate tissues using IHC staining with myc-specific antibody (Figure 4.3C). As expected, mice with PB-PRMT5; PB-MEP50 genotype had the strongest myc staining, while tissues with expression of single transgene demonstrated weaker staining compared to mice with double transgenic genotype. WT mice had virtually no staining.

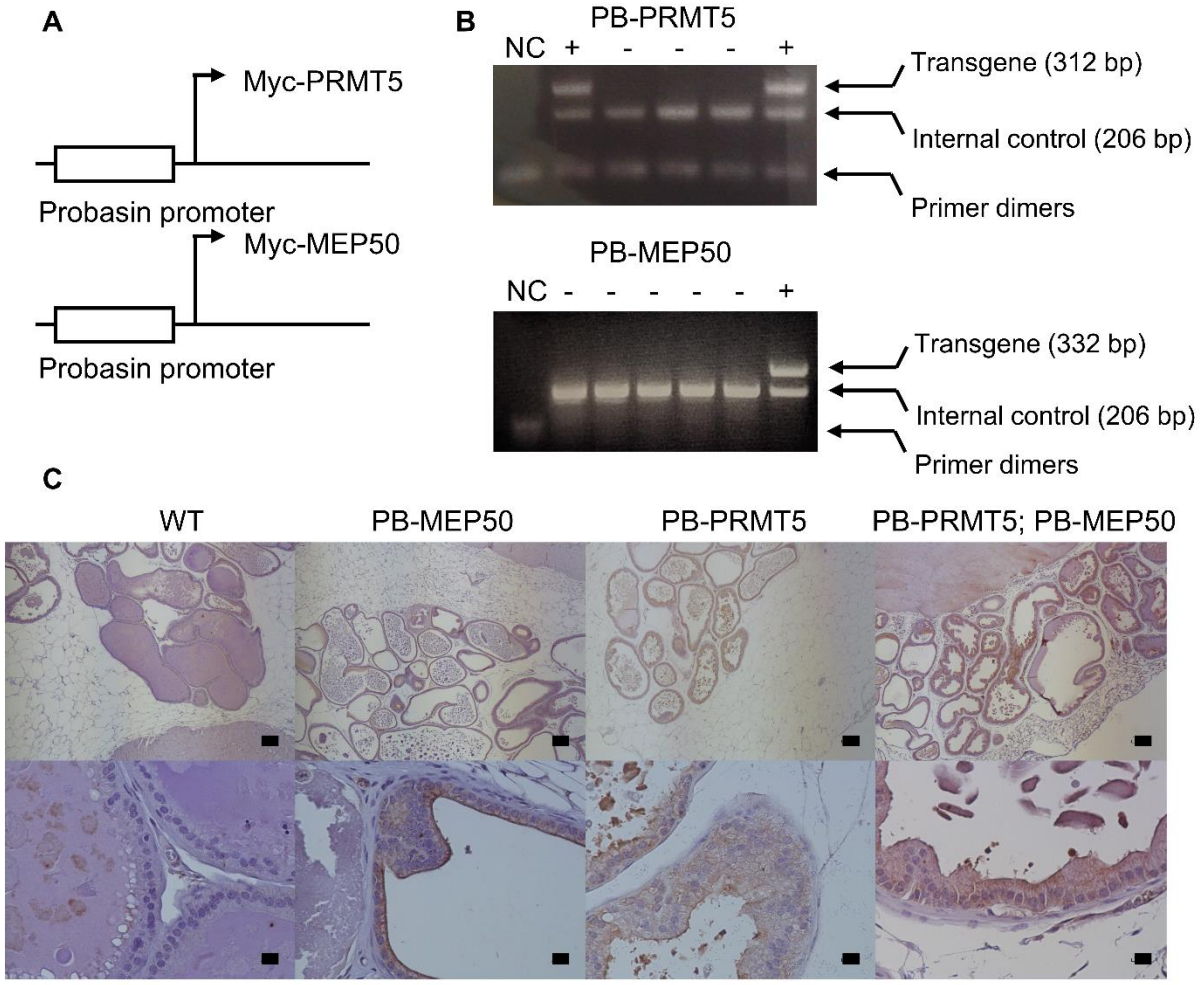

Figure 4.3. Generation of transgenic mice.

A, Schematic representation of probasin-driven transgene expression. B, Representative gel images of PCR genotyping. NC, negative (no template) control PCR, +, sample with transgene, -, wild-type. C, GU organs of 1-year old mice with indicated genotypes were harvested and probed for myc presence. Scale bar indicates 200 μm for the top row and 20 μm for the bottom row.

4.3.3 Co-overexpression of PRMT5 and MEP50 in mice prostate increases proliferation of epithelial cells

To examine whether co-overexpression of PRMT5 and MEP50 affects proliferation in mouse prostates, prostate tissues of transgenic mice were collected at different age and probed for the presence of proliferation marker Ki-67 [263] (Figure 4.4A for representative images and B for quantification as percentage of positively stained cells in the field in all prostate lobes). Ki-67 presence was also analyzed separately in the anterior (AP), ventral (VP), and dorso-lateral (DLP) lobes of prostates because expression levels of transgenes under the control of PB promoter is not equal between different lobes [262]. Among mice of 12 weeks, 6 months, and 1-year age most drastic difference was observed for 1-year old mice (Figure 4.4D). No difference of Ki-67 presence was detected in AP of prostates from mice from all ages analyzed (Figure 4.5B-D). At the same time, percentage of Ki-67-positive cells in VP and DLP of PB-PRMT5; PB-MEP50 mice (Double) was significantly higher compared to WT mice at 6 months and 1 year (Figure 4.5F-J). Taken together, this data indicates that co-overexpression of PRMT5 and MEP50 in mouse prostates increases proliferative index in prostate tissues.

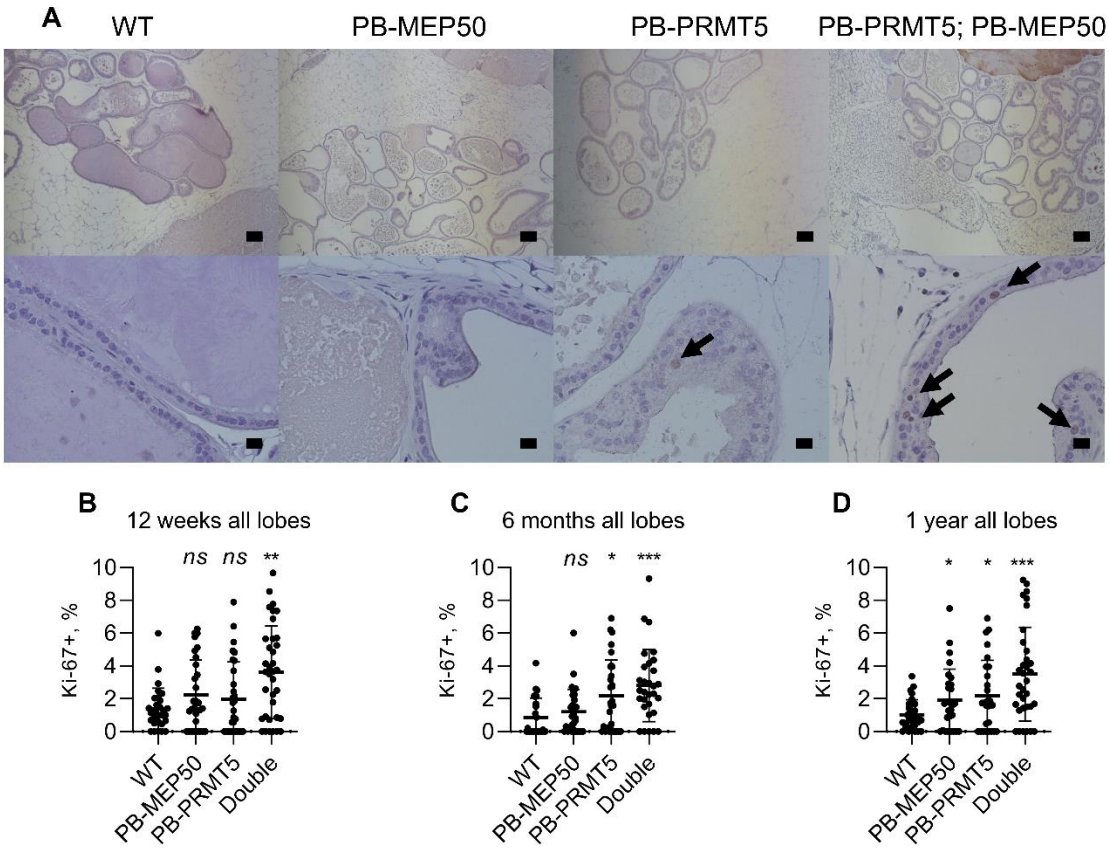

Figure 4.4. Ki-67 staining in prostate tissues of PB-PRMT5; PB-MEP50, PB-PRMT5, PB-MEP50, and WT mice.

A, GU organs of 1-year old mice with indicated genotypes were harvested and probed for Ki-67 presence. Scale bar indicates 200 μm for the top row and 20 μm for the bottom row. Arrows indicate Ki-67-positive cells. B-D, GU organs of 12-weeks, 6-months, and 1-year old mice (n = 10) with indicated genotypes were harvested and probed for Ki-67 presence. Presented are the average percentage of Ki-67-positive cells in the field (3 fields/lobe) for all lobes. Stars indicate difference compare to WT control. Brown-Forsythe and Welch ANOVA followed by Dunnett's T3 multiple comparisons test was used to determine statistical significance of group difference. ns $P > 0.05$, * $P < 0.05$, ** $P < 0.01$, *** $P < 0.001$.

Consistently with observed increase of proliferative index in prostate epithelium of double-transgenic mice, the total and normalized to mice body weight of GU organs (recorded at the moment of GU organs harvesting) did not significantly differ between genotypes at 12 weeks and 6 months (Figure 4.6) but was significantly higher for double-transgenic mice compared to WT control at 1 year (Figure 4.6A and C)

Figure 4.5. Co-overexpression of PRMT5 and MEP50 promotes proliferation of prostate epithelial cells differently in AP, VP, and DLP.

GU organs of 12-weeks, 6-months, and 1-year old mice (n = 10) with indicated genotypes were harvested and probed for Ki-67 presence. A, Representative images of Ki-67 staining in different lobes of 1-year PB-PRMT5; PB-MEP50 mouse. B-J, Presented are the average percentages of Ki-67-positive cells in the field (3 fields/lobe) separately in different lobes. AP, anterior prostate lobe; DLP, dorso-lateral prostate lobe; VP, ventral prostate lobe. Stars indicate difference compare to WT control. Brown-Forsythe and Welch ANOVA followed by Dunnett's T3 multiple comparisons test was used to determine statistical significance of group difference. ns $P > 0.05$, * $P < 0.05$, ** $P < 0.01$, *** $P < 0.001$.

Figure 4.5 continued

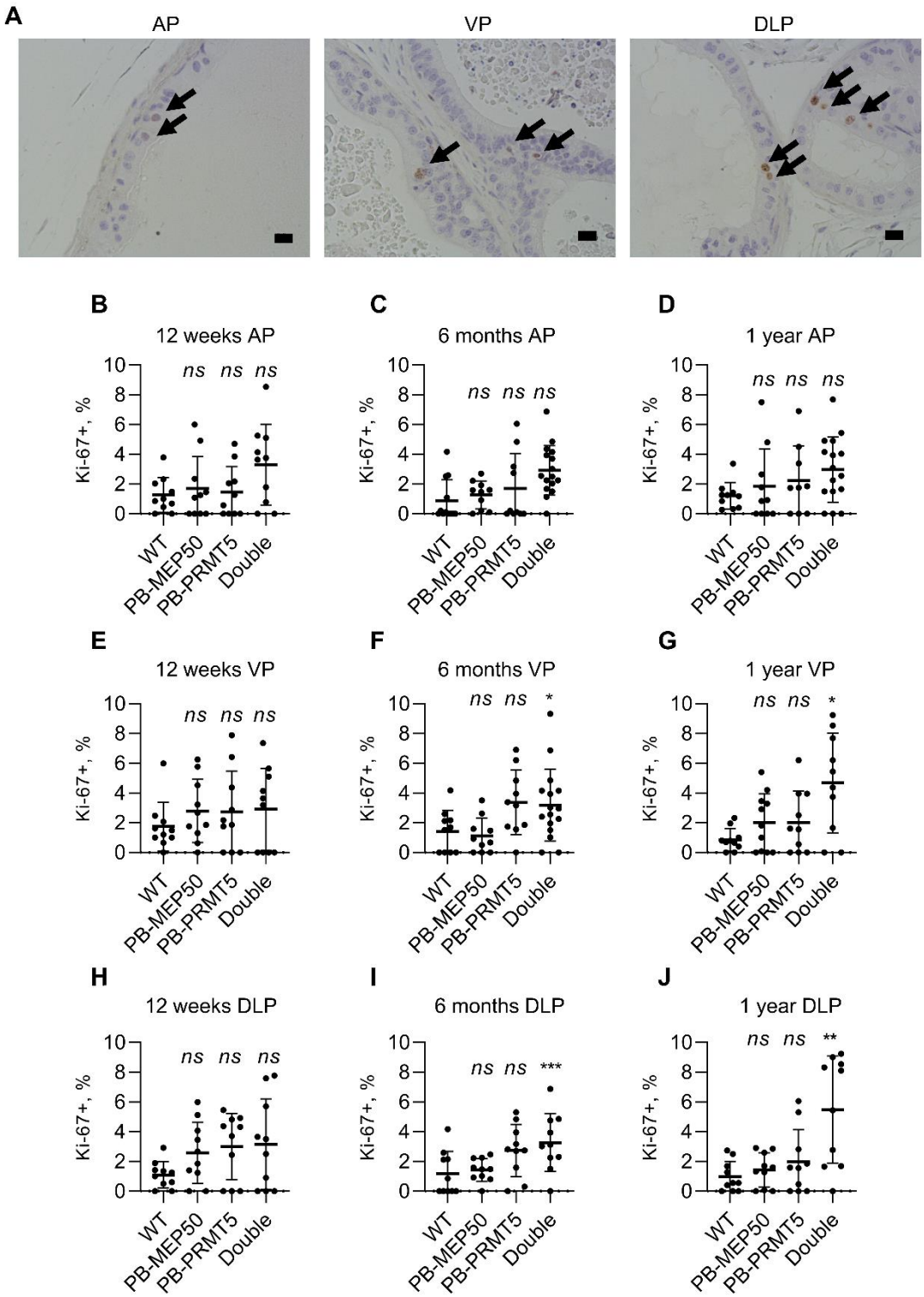

Figure 4.6. Co-overexpression of PRMT5 and MEP50 leads to increase in mouse GU organs weight.

Body weight and weight of GU organs of 12-weeks, 6-months, and 1-year old mice (n = 10) with indicated genotypes were recorded at the moment of GU organs harvesting. Stars indicate difference compare to WT control. Brown-Forsythe and Welch ANOVA followed by Dunnett's T3 multiple comparisons test was used to determine statistical significance of group difference. ns $P > 0.05$, * $P < 0.05$.

Figure 4.6 continued

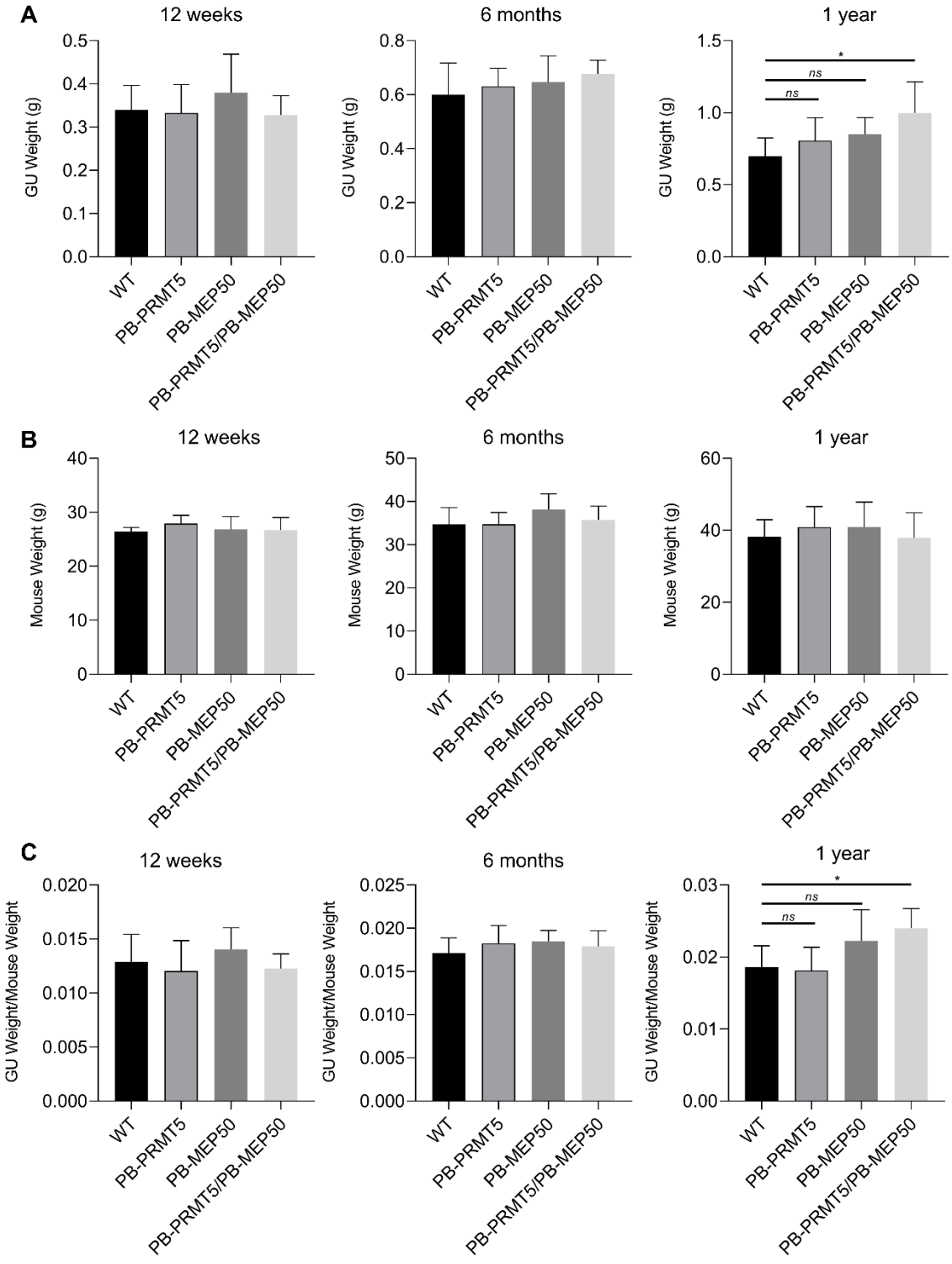

4.3.4 Co-overexpression of PRMT5 and MEP50 increases presence of prostate intraepithelial neoplasia

Knowing that PRMT5 and MEP50 together promote cell proliferation *in vivo*, I then aimed to investigate whether co-overexpression of these proteins can promote cancer formation. As I was not able to observe development of cancer (defined by presence of undifferentiated cells and the loss of basal cells in prostate glands), I analyzed the presence of prostate intraepithelial neoplasia (PIN) defined by loss of monolayer growth and abnormal morphology of prostate epithelial luminal cells (Figure 4.7).

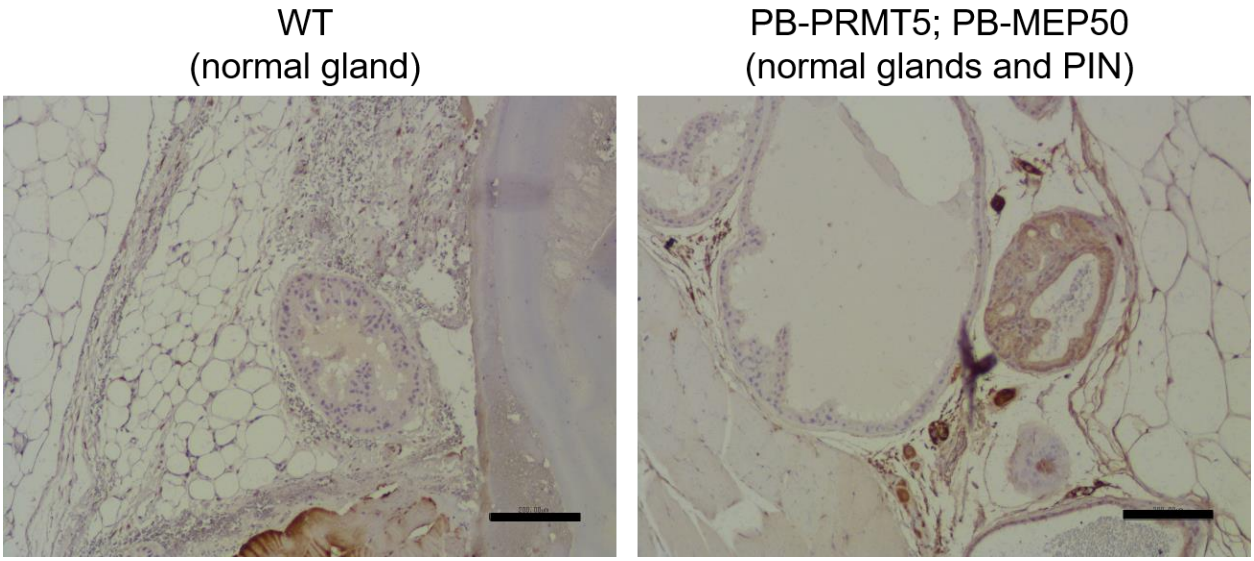

Figure 4.7. Representative images of normal prostate glands and PIN.

GU organs of 1-year old mice with indicated genotypes were harvested and probed for myc presence. Scale bar indicates 200 μm.

Analysis of PIN presence indicated that co-overexpression of PRMT5 and MEP50 can increase presence of PINs in prostate tissues, and the trend is the same for 12 weeks, 6 months, and 1 year old mice (Figure 4.8) further confirming that co-overexpression of PRMT5 and MEP50 promotes proliferation within the prostate.

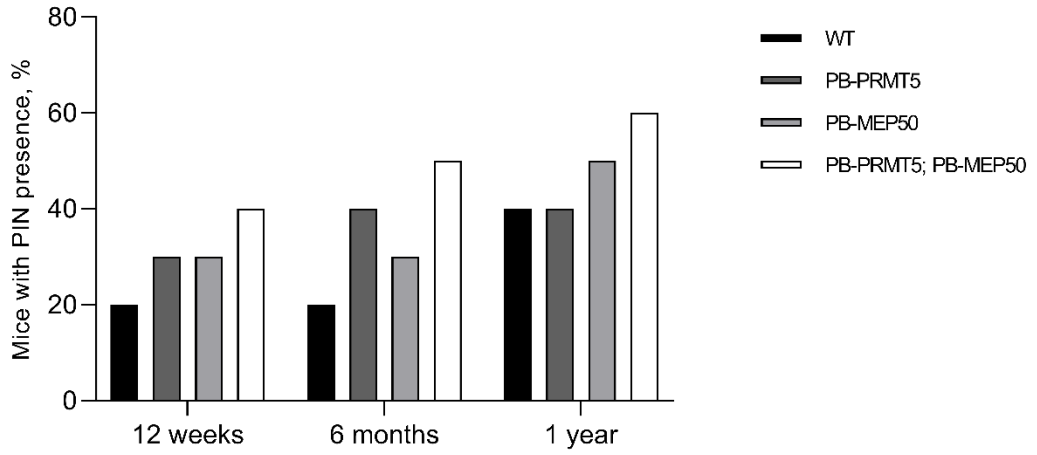

Figure 4.8. Co-overexpression of PRMT5 and MEP50 promotes PIN development in mouse prostates.

GU organs of 12-weeks, 6-months, and 1-year old mice (n = 10) with indicated genotypes were harvested and analyzed for presence of PIN. Presented are the proportions of prostates with PIN presence.

4.3.5 Co-overexpression of PRMT5 and MEP50 increases the number of NE-like cells in mice prostates

Based on the preliminary observations that co-overexpression of PRMT5 and MEP50 in LNCaP cells induces NED, I expected to observe similar effect in double-transgenic mice prostates. In line with this, I probed transgenic mice prostates for CgA and NSE, classic markers of NED. As I did not observe any cancer growth, I also did not detect NEPC tumors. However, 1-year old double-transgenic mice prostates had notable presence of NE-like cell focal growth defined by areas with increased number of CgA- or NSE-positive cells (Figure 4.9A and B). Importantly, none of WT mice had these NE-like cells foci (Figure 4.10). Furthermore, NED foci with high myc staining (indicating high PRMT5/MEP50 expression) tended to have higher CgA and NSE staining (Figure 4.11A), although not significant statistically (Figure 4.11B and C). These observations suggest that co-overexpression of PRMT5 and MEP50 can promote focal NED *in vivo*, similarly to the *in vitro* observations (Figure 4.1).

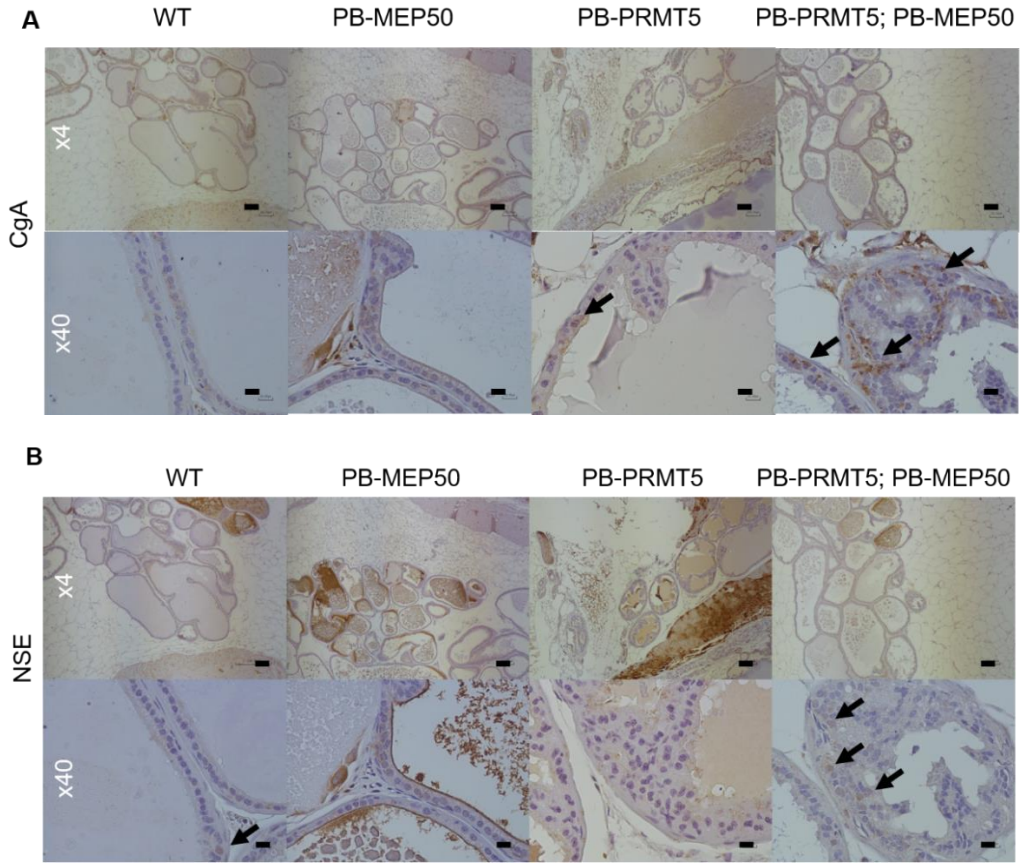

Figure 4.9. CgA and NSE staining in prostate tissues of PB-PRMT5; PB-MEP50, PB-PRMT5, PB-MEP50, and WT mice.

GU organs of 1-year old mice with indicated genotypes were harvested and probed for CgA (A) and NSE (B) presence. Scale bar indicates 200 μm for the top row and 20 μm for the bottom row. Arrows indicate positive cells.

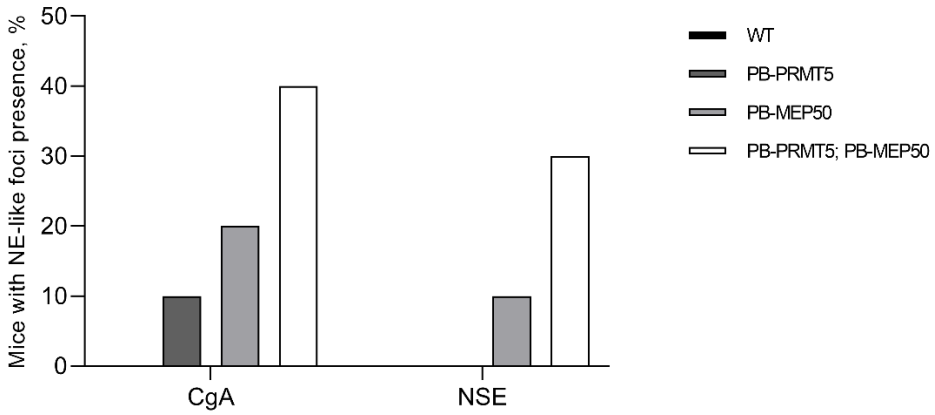

Figure 4.10. Co-overexpression of PRMT5 and MEP50 promotes local NED.

GU organs of 1-year old mice (n = 10) with indicated genotypes were harvested and analyzed for the presence of groups of CgA- and NSE-positive cells (local NED). Presented are the proportions of prostates with local NED.

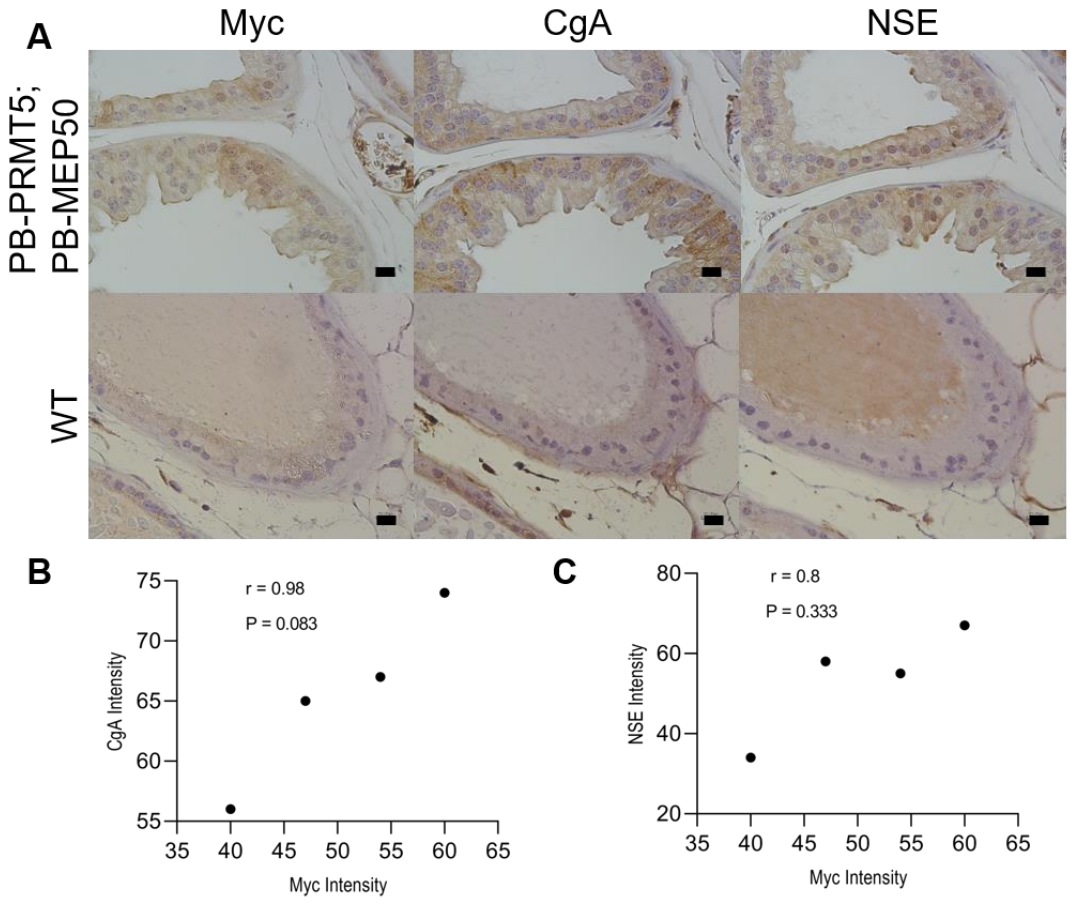

Figure 4.11. PRMT5 and MEP50 expression tend to correlate with NE markers expression.

GU organs of 1-year old mice with indicated genotypes were harvested and probed for myc, CgA and NSE. Presented are representative images of staining (A) and the Spearman correlation analysis of corresponding staining intensities in the NED foci (B and C). Scale bar indicates 200 μm.

4.4 Discussion

4.4.1 Reprograming of PRMT5 binding to the chromatin during NED

During NED, prostate cancer cells undergo significant epigenetic reprograming acquiring NE-like properties and losing classical prostate luminal markers such as AR and PSA [257,260]. Although significant research effort was devoted to elucidating the molecular mechanism of this differentiation, the exact underlying mechanism is still being debated. Here, I present some evidence that PRMT5 dissociates from AR promoter during NED and because of that does not function as activator of AR expression in NE-like cells.

It is well-demonstrated that AR signaling inhibition through the course of ADT or ASI treatment is associated with the increase in presence of cells with NE-like features compared to untreated tumors [264]: for example, in untreated intermediate- and high-risk cohort, the presence of NE-like features was detected on about 9% of tumors, while tumors from CRPC patients treated with ASI displayed NE-like features in 29% of cases [265]. Yet, it is still not clear in the field whether decrease of AR signaling and AR expression is a cause or a mere side effect of NED, although some *in vitro* evidence favors the former without significant *in vivo* evidence [266–268].

Previously, my group has demonstrated that PRMT5 functions as an epigenetic activator of AR expression in HNPC cells, and I demonstrate here that a similar mechanism of AR transcription activation is present in CRPC. Because of these observations, it is tempting to speculate that the dissociation of PRMT5 from the AR promoter could be contributing to the progression of NED via downregulation of AR transcription followed by decreased AR signaling. However, some evidence suggested that NED is dependent on the AR-EZH2-N-Myc interaction [111] and re-wiring of present AR signaling. Thus, it is possible that the loss of AR in NEPC which can be mediated by the dissociation of PRMT5 from the AR promoter, and NED are two independent events.

It is notable that PRMT5 dissociated both from the *AR* promoter that is activated by PRMT5 and from the *IVL* promoter that is repressed by PRMT5. Likely, the epigenetic reprograming during NED affects both activating and repressive PRMT5-containing complexes of different composition (either PRMT5/pICln or PRMT5/pICln/MEP50).

Further, many questions still remain unresolved. PRMT5 does not have a DNA binding domain and is recruited to the chromatin by other DNA-binding proteins. In case of HNPC and

CRPC, Sp1 is the transcription factor that recruits PRMT5 to the proximal promoter region of AR gene. It is unclear whether Sp1 binding or expression changes during NED. It was shown in acute myeloid leukemia cells that PRMT5 promotes Sp1 expression via epigenetic repression of the miRNA targeting Sp1 mRNA [128]. If a similar mechanism is present in prostate cancer, de-repression of this miRNA that is possible due to the epigenetic reprogramming during NED could cause downregulation of Sp1. This, in turn, would further alter the PRMT5 binding. Analysis of Sp1 chromatin binding during NED will help to shed a light on this question.

Additionally, it is not clear at the moment whether NED-related activity of PRMT5 has epigenetic or post-translational regulation nature. Given that PRMT5 can regulate AR activity at multiple levels (see Chapter 1.5), both mechanisms can be significant. Furthermore, it is possible that role of PRMT5 in NED is mediated not exclusively through regulation of AR expression and activity but also has AR-independent component, for example, through epigenetic suppression of REST. Future analysis of genome-wide PRMT5 binding and other non-chromatin PRMT5 binding partners and substrates will provide further mechanistic evidence for the role of PRMT5 in NED.

4.4.2 Co-overexpression of PRMT5 and MEP50 in vitro and in vivo

Here, I demonstrate that PB-driven co-overexpression of PRMT5 and MEP50 can promote focal NED in mouse prostates. My group observed similar effect upon co-transfection of PRMT5 and MEP50 in LNCaP cell culture. However, NED induced *in vitro* typically promotes a slow growing phenotype [93] while here I observed that NED in mouse prostates was accompanied by increased proliferative index in prostate tissues. At the same time the Ki-67 presence was not elevated in the detected NE-like foci which is consistent with previous observations that NE-like cells in NEPC models are Ki-67-negative [70].

One possible explanation for this phenomenon is paracrine signaling of NE-like cells. It was demonstrated previously that NE-like cells produce a variety of neuropeptides and signaling molecules [82] and are able to promote xenograft growth *in vivo* distantly. Thus, it is possible that the observed in my experiments increase of the number of proliferating cells is mediated indirectly through paracrine signaling of NE-like cells that were induced by the PRMT5/MEP50 overexpression.

Here, I did not observe development of NEPC while observing local NED. It was suggested previously that in NEPC development, PTEN inactivation is required to initiate tumor formation,

while additional genetic alterations are required for NED [76]. Thus, it is likely that prostate-specific co-overexpression of PRMT5 and MEP50 on the background of PTEN loss will lead to robust NEPC development. Additionally, it will be necessary to confirm whether both transgenes get expressed equally as myc staining detects both PRMT5 and MEP50 simultaneously without differentiating between two proteins. Analysis of transgenes mRNA or protein expression in prostates will provide additional details for this matter.

4.4.3 Targeting PRMT5/MEP50 as a potential approach for NEPC therapy

NEPC is the terminal lethal stage of prostate cancer without cure or treatment that can prolong patients' survival by more than a few months [109]. Moreover, existing therapies based on taxanes and platinum-based chemotherapy are associated with multiple adverse effects [90]. Thus, there is an urgent need to develop novel treatment approaches for NEPC therapy.

Based on the preliminary *in vitro* observations, it appears that PRMT5 enzymatic activity is required for the NED. Thus, one possible approach could be usage of PRMT5 enzymatic inhibitors as adjuvant or neoadjuvant therapy for ADT and ASI treatment in order to prevent NED in prostate tumors. As discussed above in Chapter 1.7.3, several PRMT5 enzymatic inhibitors are currently in clinical trials (clinicaltrials.gov).

Another specific approach for NEPC therapy can be disruption of PRMT5-MEP50 protein-protein interaction, as this interaction is also required for NED induction. Disruption of protein-protein interactions in NEPC could provide more specific approach rather than targeting all PRMT5 methyltransferase activity. Future development and testing of such inhibitors is warranted.

4.5 Materials and Methods

4.5.1 Cell cultures

LNCaP cells were purchased from ATCC (Manassas, VA, US). Frozen aliquots were stored in the liquid nitrogen vapor. For maintenance, cells were cultured in complete media (RPMI1640 (Corning, NY, US) supplemented with 10% fetal bovine serum (FBS, Atlanta Biologicals, Lawrenceville, GA, US), 2 mM L-glutamine (Corning, NY, US), and 100 units/mL penicillin and 100 µg/mL streptomycin (Gibco, Gaithersburg, MD, US)). For NED induction, cells were cultured for 7 days in RPMI1640 without phenol red (Corning, NY, US) supplemented with

charcoal-stripped FBS (Corning, NY, US), 2 mM L-glutamine, and 100 units/mL penicillin and 100 μg/mL streptomycin. Cells were not passaged more than 30 times.

4.5.2 Chromatin immunoprecipitation (ChIP)-qPCR

First, cross-linking was performed by adding 270 μL of 37% formaldehyde per 10 mL media directly into cell culture media and incubating plates at room temperature for 10 min. Then, 1.12 mL of 1.25 M glycine was added per 10 mL media to stop the cross-linking, and plates were incubated at room temperatures for additional 5 min. All next steps were performed on ice. Cells were scraped off the plates, washed twice in cold PBS, and resuspended in the immunoprecipitation (IP) buffer with protease and phosphatase inhibitors: 50 mM Tris-HCl pH 7.4, 150 mM NaCl, 5 mM EDTA, 1% Triton X-100, 0.5% NP-40, 0.5 mM DTT, 5 μg/mL of each chymostatin, leupeptin, pepstatin A, and antipan, 0.5 mM PMSF, 30 mM PNPP, 10 mM NaF, 0.1 mM Na_3VO_4, 0.1 mM Na_3MoO_4, 10 mM β-glycerophosphate. Cells were sonicated using Branson Model 250 Sonifier at Output 4, 90% duty cycle to generate ~500 base pairs chromatin fragments. Chromatin fragments size was verified using agarose/ethidium bromide gel.

Two micrograms of each of antibodies against PRMT5 (Millipore), MEP50 (Cell Signaling Technology), pICln (Abcam), H2AR3me2s (Abcam), H3R2me2s (EpiGentek), H3R8me2s (Abcam), H4R3me2s (Abcam), was used to immunoprecipitate protein-DNA complexes for the subsequent isolation of DNA using Chelex [233]. DNA immunoprecipitated with naïve rabbit or mouse IgG served as a control. The co-immunoprecipitated DNA was quantified by qPCR using gene-specific primers. All used antibodies are listed in the Appendix A, and ChIP-qPCR primers are listed in the Appendix B.

qPCR was conducted using FastStart Universal SYBR Green Master Mix (Thermo Fisher Scientific, Waltham, MA, US) in a QuantStudio 6 system (Applied Biosystems, Foster City, CA).

4.5.3 Generation of PB-PRMT5; PB-MEP50 transgenic mice

The use of animals and animal-related experimental procedures were approved by the Purdue University Animal Care and Use Committee.

The sequences for myc-PRMT5 and myc-MEP50 were cloned into pBlueScript II SK (+)-ARR2PB-Intron-bGHPolyA using NheI and EcoRV (for myc-PRMT5) and BmtI and EagI sites

(for myc-MEP50). The androgen-dependent expression of both transgenes was separately confirmed in LNCaP cells using Fugene HD (Promega, Madison, WI, US) -mediated plasmid transfection with and without addition of R1881 (synthetic analog of androgen).

Transgenic mice were generated at the Purdue Transgenic Mouse Core Facility in C57BL/6N mice. Transgenic founders were identified by the PCR screening of tail tip DNA using PRMT5-bGH-Fw and PRMT5-bGH-Rv (for PRMT5 detection, 312 bp product) and MEP50-bGH-Fw and MEP50-bGH-Rv (for MEP50 detection, 332 bp) primer pairs for transgene detection and TCR-Fw and TCR-Rv primer pair (206 bp product) for internal PCR control. All primers used are listed in the Appendix B.

Male transgenic founders were bred with WT C57BL/6N females to confirm that transgenes are passed for at least 3 generation. After confirming the stability of transgenes, male and female PB-PRMT5 and PB-MEP50 mice were bred to generate double-transgenic (PB-PRMT5; PB-MEP50), single-transgenic (PB-PRMT5 and PB-MEP50), and WT mice.

4.5.4 DNA isolation for mice genotyping

DNA isolation was performed using HotSHOT method [269]. Tail tip or ear clip materials were incubated in 80 μL per sample of 25 mM NaOH, 0.2 mM EDTA (pH 12) at 95^{o}C for 90 min. Then, reactions were incubated at 4^{o}C for 30 min, and 80 μL of 40 mM Tris-HCl pH 5 was added to the tubes. The supernatant was used as a template in the PCR reactions.

4.5.5 Genotyping PCR

Genotyping mixes were prepared on ice as follows:

Ear/tail DNA 2 μL,

each primer 0.5 μL (final concentration 1 mM, two primer pairs for internal control and transgene),

2^{x} GoTaq Green Master Mix (Promega, Madison, WI, US) 12.5 μL,

Millie-Q water 8.5 μL (25 μL total).

PCR was run in the following program:

(1) 95^{o}C for 3 min;

(2) 95^{o}C for 30 sec;

(3) 55°C for 30 sec;

(4) 72°C for 30 sec;

repeat steps (2) – (4) for 35 cycles;

(5) 72°C for 10 min.

PCR products were resolved on 2% agarose/ethidium bromide gel and visualized in UV light to confirm the presence of transgenes.

4.5.6 Immunohistochemistry

GU organs were isolated and fixed in formalin for 48 h, and then stored in 70% ethanol at 4°C. Paraffin embedment and slide preparation were performed at the Purdue Histology Research Laboratory.

Samples were deparaffinized and rehydrated by incubating slides overnight at 37°C, and then for 2 h at 65°C, followed by incubation in Xylenes solution and a range of ethanol concentration from 100% to 30%, and finally in Millie-Q water at room temperature. Endogenous peroxides were inactivated by incubation of slides in 3% H_2O_2 for 10 min at room temperature. Antigen retrieval was performed by incubating slides soaked in 10 mM Tris pH 10 on boiling water bath for 30 min. Slides were then blocked with 5% non-fat milk solution in PBS for 1 h at room temperature with shaking. Primary antibodies were applied overnight in 5% milk at 4°C: anti-myc (1:100, Abcam), anti-Ki-67 (1:500, BD Biosciences), anti-CgA (1:200, Abcam), anti-NSE (1:200, Abcam). The full list of antibodies and their sources is in the Appendix A. After washing slides in PBS 3 times, secondary HRP-conjugated antibody was applied on samples in 5% milk solution for 1 h. Following another triple washing of slides with PBS, the chromogenic reaction was performed with DAB peroxidase kit (Vector Laboratories, Inc., Burlingame, CA, US), and then slides were counter-stained with hematoxylin-eosin (HE) solution (Vector Laboratories, Inc.). The slides were subsequently dehydrated and mounted using VectaMount™ permanent mounting medium (Vector Laboratories, Inc.).

4.5.7 Statistical analysis

No statistical method was used to predetermine sample size. Image analysis was performed using free software QuPath 0.2 [270]. All statistical analyses were performed using GraphPad

Prism 8 (GraphPad Software, La Jolla, CA, US, www.graphpad.com). For ChIP-qPCR experiments, statistical analysis was performed on ΔC_T values (C_T value for the gene normalized to the C_T value of IgG control). For other experiments, analysis was performed using non-normalized data. Student t-test with Welch's correction was performed to determine statistical significance of group difference when comparing two samples. When comparing multiple sample groups, Brown-Forsythe and Welch ANOVA followed by Dunnett's T3 multiple comparisons test was used.

CHAPTER 5. FUTURE DIRECTIONS

5.1 Summary

Prostate cancer is one of the most frequently diagnosed non-skin cancers and a second-leading cause of cancer-related death in males in United States. Since the most common cause of prostate cancer-related death is metastasis that is often developed with the acquired therapeutic resistance, improving the efficiency of existing therapies and developing novel approaches for the treatment will significantly improve patients' survival.

The first-line treatment option for metastatic prostate cancer and localized prostate cancer with high risk of recurrence is androgen deprivation therapy (ADT) that decreases androgen receptor (AR) signaling. However, targeting AR signaling inevitably leads to AR reactivation and cancer progression to the castration-resistant prostate cancer (CRPC) that has no curable treatment option. Moreover, about 30% of CRPC cases progress to neuroendocrine prostate cancer (NEPC), highly aggressive and lethal type of prostate cancer.

Recently my group has shown that protein arginine methyltransferase 5 (PRMT5) functions as activator of AR expression in hormone-naïve prostate cancer (HNPC). In this research, I demonstrated that PRMT5 also functions as an epigenetic activator of *AR* transcription in CRPC via methylation of H4R3 at the *AR* promoter, and that this epigenetic activation is dependent on pICln, a novel epigenetic partner of PRMT5, and independent of MEP50, canonical cofactor of PRMT5. At the same time, PRMT5 and MEP50 co-overexpression in mouse prostates promotes neuroendocrine differentiation. I show that during NED PRMT5 dissociates from *AR* promoter which is also associated with decrease in H4R3 methylation and binding of pICln. Overall, my results suggest the potential use of targeting PRMT5 or its interaction with PRMT5 binding partners for the treatment of CRPC and NEPC. Results of my work are summarized in the Figure 5.1.

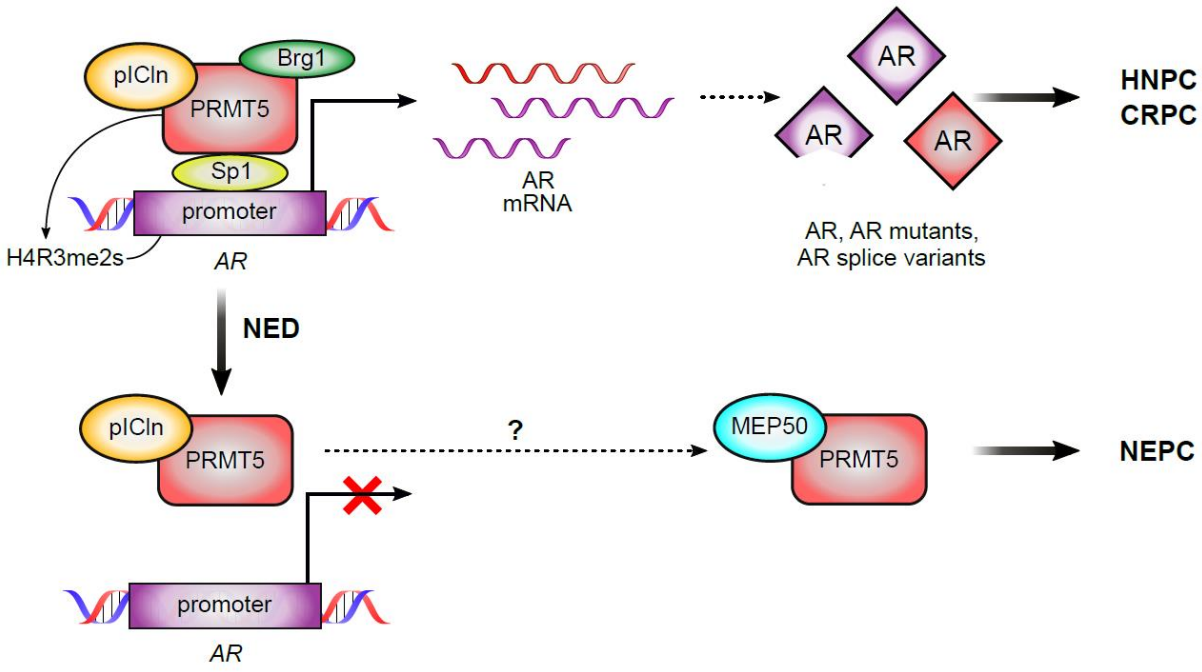

Figure 5.1. Proposed model of PRMT5 function in prostate cancer.

5.2 Elucidate additional mechanisms of PRMT5 function in CRPC

In Chapter 2 I demonstrate using various methods that PRMT5 promotes CRPC cell proliferation at least partially via epigenetic activation of *AR* transcription. Targeting PRMT5 using small-molecule inhibitors BLL3.3 or JNJ-64619178 or two different shRNAs decreased proliferation of several cell lines representing different modes of AR reactivation, and re-expression of AR upon PRMT5 knockdown restored proliferation in 22Rv1 cells. However, at this point it cannot be definitely concluded whether PRMT5 promotes CRPC cell proliferation only through epigenetic regulation of *AR* transcription. In fact, as it was discussed above in Chapter 1, PRMT5 may regulate AR signaling via multiple mechanisms. Furthermore, PRMT5 may epigenetically activate and suppress multiple genes involved in AR signaling or participating in AR-independent pathways. In addition to epigenetic regulation, PRMT5 can regulate multiple signaling molecules via post-translational arginine methylation. Thus, future studies need to focus on PRMT5 interactome and identification of substrates coupled with identification of PRMT5 target genes in CRPC.

5.2.1 How does PRMT5 activate AR transcription in CRPC?

In Chapter 1.1 I show that PRMT5 binds to the *AR* proximal promoter region to methylate H4R3 and H3R2, and that decrease of PRMT5 activity via enzymatic inhibition or shRNA-driven knockdown down-regulate AR expression. However, it is not clear at the moment why these events promote the transcription of *AR*. Previously, it was demonstrated that PRMT5-driven methylation of H3R2 enhances binding of WDR5 to recruit H3K4 methyltransferase complexes MLL1-4 thus promoting H3K4 trimethylation and activation of target gene transcription [129,145,171,183]. However, using ChIP-qPCR with WDR5-specific antibody and AR promoter-specific primers, I was not able to detect WDR5 binding to the AR promoter (data not shown) suggesting that observed activation of AR transcription is not mediated by WDR5/MLL. Thus, further elucidation of recruitment of transcription activators by PRMT5 is required.

One possible method to analyze the composition of the whole epigenetic complex bound to the specific region of chromatin is enChIP [271]. This method involves expression of recombinant Cas9 lacking endonuclease enzymatic activity alongside with expression of short guiding RNA specific to the target gene region. Guiding RNA drives binding of Cas9 to specific region of DNA. Following crosslinking, affinity purification tag within the recombinant Cas9 protein is used to precipitate the proteins bound to AR promoter. enChIP can be coupled with mass spectrometry analysis which will identify the proteins in the PRMT5 transcription activation complex. It will be particularly interesting to compare the composition of proteins precipitated from AR promoter (activated by PRMT5) to the complex at the IVL promoter (suppressed by PRMT5).

5.2.2 What are the target genes of PRMT5 in CRPC?

The RNA-seq analysis described in Chapter 3 identified 6,730 DETs that were differentially up- and down-regulated upon PRMT5 knockdown. However, it cannot be simply assumed that every single one of these identified differentially expressed genes is a direct target of PRMT5-driven epigenetic regulation because the observed differences in gene expression could be as result of secondary effects of PRMT5 knockdown and/or effect of PRMT5-mediate regulation of splicing as it was shown before that PRMT5 plays a role in the alternative splicing events [227,272].

Analysis of genome-wide PRMT5 binding sites using ChIP-seq coupled with ChIP-seq-guided analysis of H4R3 and H3R2 methylation sites will allow to specifically identify direct PRMT5 targets among genes identified using RNA-seq. It was established by my group on HNPC cells and confirmed by me in CRPC cells that Sp1 is the transcription factor recruiting PRMT5 to the AR promoter. Genome-wide analysis of Sp1 binding in prostate cancer cells will help to identify genes that are regulated by PRMT5 in a similar to *AR* transcription regulation manner.

5.2.3 Does PRMT5 activity contribute to the AR pre-mRNA splicing?

Previous report by Braun et al. has demonstrated that pharmacological inhibition of PRMT5 promotes introns detention in glioma cells [272]. Additionally, recently Tan et al. reported that knockout of PRMT5 in hematopoietic stem cells leads to increased introns detention and exon skipping events [227]. Thus, it appears that PRMT5 promotes constitutive splicing. This seems counter-intuitive as in Chapter 2 I demonstrate that knockdown or pharmacological inhibition of PRMT5 decreases AR-V7 mRNA expression that is formed as a result of alternative splicing at 3'-splice site of a cryptic exon 3 instead of 3'-splice site of exon 4 [273]. Furthermore, the preliminary analysis of splicing events in the RNA-seq samples described in Chapter 3.3.4 indicated that the emergence of mutually exclusive exons was the most common event for AR pre-mRNA upon PRMT5 knockdown. Thus, it is possible that in the context of prostate cancer PRMT5 can regulate epigenetically splicing factors that promote formation of AR-V7 mRNA.

One such factor that was suggested to be implicated in AR-V7 expression is splicing factor, proline- and glutamine-rich (SFPQ, also known as PSF). Elevated expression of SFPQ was found in CRPC tissues compared to HNPC samples, and SFPQ association with AR transcript was higher in CRPC cells compared to HNPC cells [273]. Notably, study by Radzisheuskaya et al. in AML cells identified SFPQ as one of the substrates of PRMT5, although arginine methylation of SFPQ in these cells appeared not essential for cell survival [274]. Another splicing factor that was a functionally important PRMT5 substrate in AML cells in this study was serine and arginine-rich splicing factor 1 (SRSF1). Importantly, in prostate cancer SRSF1 association with *AR* transcript is enhanced during ADT leading to higher AR-V7 expression [273]. Role of PRMT5-driven methylation or potential epigenetic regulation by PRMT5 of these splicing factors was not investigated in the context of prostate cancer. It will be interesting to examine the level of SRSF1 and SFPQ association with *AR* transcript before and after PRMT5 knockdown. RNA

immunoprecipitation assay (which is similar to ChIP but involves isolation of RNA after immunoprecipitation step) can be used to evaluate this association. Additionally, ChIP-seq analysis described above would help identifying these splicing factors as direct targets of PRMT5 epigenetic regulation.

5.3 Establish if targeting PRMT5 is an effective approach for prostate cancer treatment

In Chapter 2, I determine that knockdown of PRMT5 alone decreases growth of xenograft tumors and prolongs tumor-specific survival of mice. In this experiment, I used the homogenous pool of cultured cells grafted in immunocompromised mice to test the hypothesis in the setting more similar to the patient tumor compared to simple 2D cell culture. It will be necessary to evaluate the effect of PRMT5 targeting in more advanced models of prostate cancer closer resembling patients' tumor progression.

5.3.1 Do PRMT5 inhibitors effectively suppress xenograft growth in mice?

It will be useful to evaluate the targeting of PRMT5 in prostate cancer models using orally-delivered PRMT5 small molecule inhibitors. Given that five PRMT5 inhibitors are already in clinical trials, there is no concern about general toxicity of these inhibitors. As at least one of these PRMT5 inhibitors (JNJ-64619178) is effective in suppressing 22Rv1 cell proliferation and AR expression *in vitro*, future experiments can evaluate whether administering JNJ-64619178 decreases xenograft growth and AR expression in mice similar to experiments described in Chapter 2.3.3 and 2.3.4.

5.3.2 Does PRMT5 targeting suppress tumor growth in other models of prostate cancer?

After evaluation of JNJ-64619178 treatment effect in xenograft model, it will be important to evaluate whether PRMT5 targeting also suppresses tumor growth in more clinically relevant models of prostate cancer. Patient-derived xenografts (PDXs) and patient-derived cells organoids and spheroids all have advantage of maintaining heterogeneity and mutation profile similar to patients' samples compared to cultured cell lines. Multiple PDXs series are available for prostate cancer, modeling either HNPC, CRPC, or NEPC, including those that can be grafted subcutaneously and in renal capsule [275]. My group already has some of these PDXs lines and

plans to use them in future experiments. These results will provide a strong evidence for clinical potential of PRMT5 targeting for prostate cancer therapy.

5.4 Determine the mechanism of regulation of PRMT5 activity by PRMT5-interacting proteins

In Chapter 3 I provide the evidence demonstrating that pICln and not MEP50 promote PRMT5-driven activation of *AR* transcription in CRPC cells. First, MEP50 knockdown did not affect AR expression in 22Rv1 cells and did not change PRMT5-driven methylation level. Second, MEP50 was detected at the AR promoter using ChIP-qPCR. Third, MEP50 knockdown did not decrease presence of AR signaling pathway genes. On the opposite, pICln was bound to the AR promoter in PRMT5-dependent manner and was required for the PRMT5-driven methylation of H4R3 and expression. Furthermore, the BiFC analysis suggested that pICln and MEP50 can at least partially compete for PRMT5 binding. However, the fine details of PRMT5-pICln interaction and pICln-mediated regulation of PRMT5 enzymatic activity are not elucidated yet.

5.4.1 What are the structures of PRMT5:pICln, PRMT5:MEP50:pICln complexes?

The results of BiFC competition assay suggest that pICln may interact with PRMT5 in a similar to MEP50 manner. However, the structure of PRMT5:pICln or PRMT5:MEP50:pICln has not been solved yet. The structure of PRMT5:MEP50 complex has been solved several times using crystallography [119] and cryoelectronic microscopy [276]. Structurally, PRMT5:MEP50 complex is a heterooctamer consisting of four PRMT5 and four MEP50 molecules. Previously, several reports demonstrated that PRMT5, MEP50 and pICln can be present in the same complex [236,237,277]. Thus, taken together with the BiFC analysis data, it is possible that pICln may replace one or more MEP50 molecules in PRMT5:MEP50:pICln complex. However, at this point it is hard to predict the exact stoichiometry of the complex. Furthermore, as RIOK1 can compete with pICln for PRMT5 binding, the existence of PRMT5:MEP50:pICln:RIOK1 complex is also possible. The current collaboration of my group with Dr. Jiang group at Purdue University is working on elucidation of these complexes structure using recombinant proteins expressed in insect culture and cryoelectronic microscopy approach. Because the system to express and purify recombinant proteins has been established, the first results are expected very soon. Elucidation of PRMT5:pICln complex structure will allow to design novel drugs targeting this interaction and

may provide an insight on the mechanism of enzymatic activation and substrate selection by PRMT5:pICln.

Additionally, as PRMT5 does not have DNA-binding domain and is recruited to the DNA by other chromatin-binding proteins, it will be interesting to elucidate the structure of larger complex containing Sp1 and histone substrates or the whole nucleosome. These results may shed light on the differential gene transcription activation and repression by PRMT5 and different interacting partners.

5.4.2 How does the presence of interacting proteins change enzymatic activity of PRMT5?

It was demonstrated *in vitro* that PRMT5 enzymatic activity is low in the absence of interacting proteins, and presence of interacting proteins can alter the substrate specificity of PRMT5 [131,135,277]. However, most of the biochemical studies described in literature used bacterially expressed proteins that might not recapitulate proteins expressed in eukaryotic cells. To fully characterize the effect of different PRMT5-binding partners on the PRMT5 methyltransferase activity, my group plans to utilize recombinant proteins expressed in insect cells as whole complexes (PRMT5:pICln, PRMT5:MEP50:pICln, and others) and a variety of substrates (free histones, nucleosomes, nucleosomes in the presence of Sp1 and DNA). These results can provide further evidence that MEP50 might not be an obligate cofactor of PRMT5. However, as epigenetic regulation happens in the context of larger epigenetic complexes, experiments in live cells, for example, utilizing specific PPI inhibitors, would provide evidence for potential MEP50 requirement for the PRMT5-driven histone methylation.

5.4.3 How do MEP50 and pICln contribute to the chromatin status?

Interestingly, results of my ChIP-qPCR assays demonstrate that PRMT5:pICln binds to the PRMT5-activated promoter (*AR*) while PRMT5:MEP50:pICln binds to PRMT5-repressed promoter (*IVL*). To fully characterize how PRMT5-interacting proteins contribute to gene expression regulation by PRMT5, it will be necessary to determine genome loci occupied by these interacting proteins and relate it to the results of the RNA-seq analysis described in Chapter 3. One possible approach for that purpose is ChIP-seq. Coupling ChIP-seq with rapid immunoprecipitation mass spectrometry of endogenous protein (RIME) method will allow to

identify other interacting proteins within pICln- or MEP50-containing complexes [278]. Implementation of assay for transposase-accessible chromatin (ATAC)-seq upon PRMT5, MEP50, and pICln knockdown will allow us to evaluate how each of these proteins contribute to the chromatin accessibility thus informing how PRMT5:MEP50 and PRMT5:pICln can activate and repress gene transcription.

5.5 Further validate how PRMT5 and MEP50 contribute to NEPC development

My results from Chapter 4 strongly suggest that PRMT5/MEP50 are required for NED. I show that co-overexpression of PRMT5 and MEP50 in mouse prostates significantly promotes cell proliferation and NED. However, the mechanism of PRMT5/MEP50 contribution to the NED is still poorly understood.

5.5.1 What are the molecular targets and pathways of PRMT5/MEP50 during NED?

It is not clear at the moment whether PRMT5/MEP50 complex regulates NED via epigenetic or post-translational regulation mechanism. Given that PRMT5 can regulate AR activity at multiple levels (see Chapter 1.5), both mechanisms can be significant. Furthermore, it is possible that regulatory function of PRMT5/MEP50 complex in NED is mediated through AR-independent mechanisms, for example, through epigenetic suppression of REST. Future analysis of genome-wide PRMT5 and MEP50 binding and other non-chromatin PRMT5/MEP50 binding partners and substrates will provide further mechanistic evidence for the role of PRMT5/MEP50 in NED.

Additionally, my group received results of RNA-seq analysis in ADT-induced NED-LNCaP cells with and without PRMT5 knockdown and with and without MEP50 knockdown. In collaboration with Dr. Wan group at the Indiana University, using these results, we will identify pathways and genes that are regulated by PRMT5/MEP50.

5.5.2 Can co-overexpression of PRMT5/MEP50 on the background of PTEN knockout promote NEPC?

In Chapter 4 I demonstrate that PRMT5/MEP50 co-overexpression did not promote cancer growth beyond PIN formation. Thus, it will be interesting to investigate whether PRMT5/MEP50 can promote NEPC in mouse prostate cancer model. PTEN inactivation through deletion or loss-

of-function mutations is one of the most common alterations for HNPC, CRPC, and NEPC [97]. As prostate-specific deletion of *PTEN* led to the quick development of metastatic prostate cancer in mouse model [101], this model is suitable for investigation of additional alterations required for NEPC development. I have already set up breeding for the generation of *PB-PRMT5; PB-MEP50; PTEN$^{loxP/loxP}$; PB-Cre4* mice using the breeding scheme detailed below (Figure 5.2) and obtained few GU organs for further analysis using IHC.

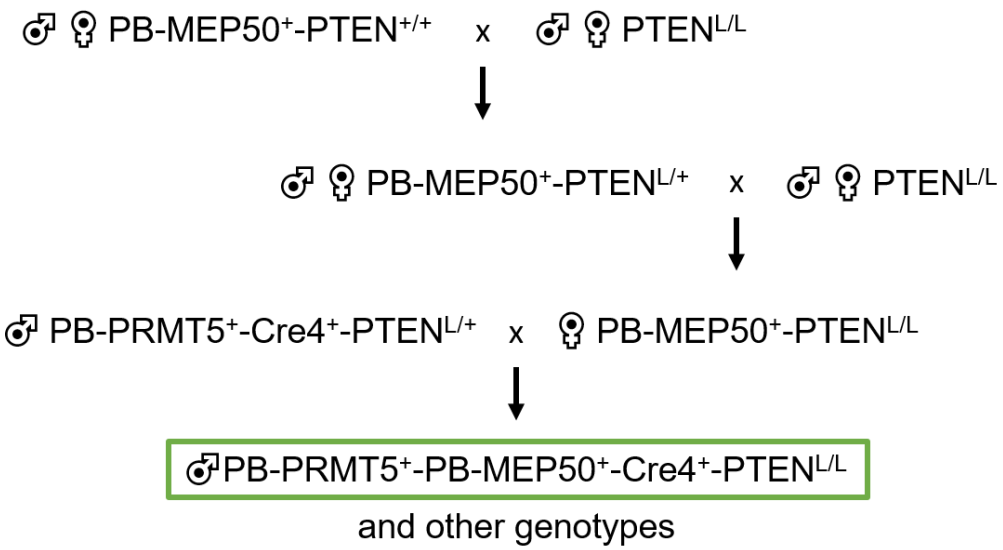

Figure 5.2. Breeding scheme to generate mice with prostate co-overexpression of PRMT5/MEP50 on the background of prostate-specific PTEN loss.

5.5.3 Can targeting PRMT5 or PRMT5/MEP50 complex prevent treatment-induced NED?

Treatment-induced NED is a major challenge of prostate cancer treatment. NED can be induced by the majority of prostate cancer treatments including ADT and ASI [279,280]. Thus, it was predicted that the increased usage of ASIs such as abiraterone acetate and enzalutamide is likely to cause increased number of NEPC cases.

During the co-targeting experiment described in Chapter 2.3.4 I collected tumor samples and blood samples for the subsequent analysis of potential NED in the 22Rv1 xenograft tumors and NED markers such as CgA in blood serum. Thus, it will be possible to use these samples to evaluate whether abiraterone acetate or enzalutamide treatment induced NED in 22Rv1 xenograft

tumors, and whether targeting PRMT5 prevented NED in these tumors. Although it is possible that neither ASI treatment induced NED, as induction or lack of such was not previously reported.

Alternative approach to validate targeting PRMT5 or PRMT5/MEP50 for NED prevention would be usage of GEM model of treatment-induced NED. Zou et al. reported a model in which mice with prostate-specific loss of PTEN and p53 develop CRPC [70]. These mice develop castration-resistant prostate tumors at the age of 10 months. Notably, when treated with ASI abiraterone acetate, 39% of mice developed NEPC features. Thus, this model can represent ASI-induced NED and can be used for evaluation of PRMT5 targeting (for example, via administration PRMT5 small molecule inhibitor JNJ-64619178) or PRMT5/MEP50 targeting (for example, via administration of PRMT5/MEP50 PPI inhibitor) for the prevention or treatment of NEPC.

APPENDIX A. LIST OF ANTIBODIES

Antibody target	Manufacturer	Catalog # and identifier
Rabbit Anti-Androgen Receptor	Santa Cruz	sc-816, RRID AB_1563391
Mouse Anti-Androgen Receptor	Agilent	Cat# M3562, RRID: AB_2060174
Rabbit Anti-Androgen Receptor-V7	Abcam	Cat# ab198394
Rabbit Anti-Androgen Receptor-V7	RevMAb Biosciences	Cat# 31-1109-00, RRID: AB_2716436
Mouse Anti-beta-Actin Monoclonal, Clone AC-15	Sigma-Aldrich	Cat# A1978, RRID: AB_476692
Rabbit Anti-Cleaved Caspase-3 (Asp175) (5A1E) Monoclonal	Cell Signaling Technology	Cat# 9664, RRID: AB_2070042
Rabbit Anti-Chromogranin A	Abcam	Cat# ab15160
Rabbit Anti-CLNS1A (C-term)	Abcam	Cat# T1435, RRID: AB_10704366
Rabbit Anti-COPR5	Novus Biological	Cat# NBP2-30884
Rabbit Anti-Histone H2A (symmetric di methyl R3)	Abcam	Cat# ab22397, RRID: AB_880431
Rabbit Anti-Histone H3 (symmetric di methyl R2)	EpiGentek	Cat# A-3705-100
Rabbit Anti-Histone H3 (symmetric di methyl R8)	Abcam	Cat# ab130740
Rabbit Anti-Histone H4 (symmetric di methyl R3)	Abcam	Cat# ab5823, RRID: AB_10562795
Rabbit Anti-Ki67 Monoclonal, SP6	GeneTex	Cat# GTX16667, RRID: AB_422351
Rabbit Anti-Human MEP50	Cell Signaling Technology	Cat# 2823S, RRID: AB_2215724
Mouse Anti-Myc tag Monoclonal, 9E10	Abcam	Cat# ab32, RRID: AB_303599
Rabbit Anti-NSE antibody	Abcam	Cat# ab227301
Normal rabbit IgG antibody	Santa Cruz Biotechnology	Cat# sc-2027, RRID: AB_737197
Normal mouse IgG antibody	Santa Cruz Biotechnology	Cat# sc-2025, RRID: AB_737182
Rabbit Anti-PRMT5 Polyclonal	Millipore	Cat# 07-405, RRID: AB_310589
Rabbit Anti-RIOK1	Bethyl	Cat# A302-457A, RRID: AB_1944259
Sheep Anti-Mouse IgG ECL Antibody, HRP Conjugated	GE Healthcare	Cat# NA9310-1mL, RRID: AB_772193
Donkey Anti-Rabbit IgG ECL Antibody, HRP Conjugated	GE Healthcare	Cat# NA9340-1mL, RRID: AB_772191

APPENDIX B. LIST OF OLIGONUCLEOTIDES

shRNA sequences

shRNA name	shRNA target	shRNA sequence
shPRMT5#1	PRMT5	5′-CCCATCCTCTTCCCTATTAAG-3′
shPRMT5#2	PRMT5	5’-GCCCAGTTTGAGATGCCTTAT-3′
shSC	None	5’- CAACAAGATGAAGAGCACCAA-3’
shMEP50#1	MEP50	5’- CCTCACAAGGACTCTGTGTTT-3’
shMEP50#2	MEP50	5'-CCTCAGCAAAGTGAAGTCTTT-3'
shpICln#1	pICln	5’-CCAACAGTTGCTGGACAGTTT-3’
shpICln#2	pICln	5'-ATGATGATGTTGAACCTATTA-3'

qPCR primers

Gene	Forward primer	Reverse primer
AR-FL	5’-GTGGAAGCTGCAAGGTCTTC-3’	5’-CGAAGACGACAAGATGGACA-3’
AR-V7	5'-GGATGACTCTGGGAGAAAAATTCCG-3'	5'-GTCTGGTCATTTTGAGATGCTTGCA-3'
BRCA1	5’-GTTGTTATGAAAACAGATGCTGAGTTTG-3’	5’-CTGGGTCACCCAGAAATAGCTAAC-3’
CCNE1	5'-GATTGCAGAGCTGTTGGA-3'	5'-ACCACTGATACCCTGAAACC-3'
DDX17	5'-GACCACAAGTTGATCCAACTA-3'	5'-TAGCTGGCCAACCATCT-3'
EP300	5'-CCAACCAGAGGAGAGTATACATAT-3'	5'-TGTTGTGTAACCTAATTTCTTGAC-3'
GAPDH	5’-CTGACTTCAACAGCGACACC-3’	5’-CCCTGTTGCTGTAGCCAAAT-3’
IVL	5’-CCTCAGCCTTACTGTGAG-3’	5’-GGGAGGCAGTGGAGTTGG-3’
MEP50	5'-GCCTCTCCTCACAAGGACTC-3'	5'-CCAGCGAGGTAGGAAGGTAG-3'
NCOR1	5'-CATCTCACAGGGAACACC-3'	5'-CAAAGTAGCTGATTTGGCA-3'
NCOR2	5'-ATCTCCCAAGGAATGTCG-3'	5'-TGAAGGGTGCCAGCTT-3'
NRIP1	5'-GCCAGAAGATGCACACTTG-3'	5'-AATATCAGTGTTCGTCTGTCTCC-3'
pICln	5'-TCAGCGTTGGAGGCAATGTT-3'	5'-CCCTGTCCTTGTTCATGTGCTTC-3'
PRMT5	5’-CAGAGAAGGAGTTCTGCTCCTAC-3’	5’-ATGGCCTGCTGGTACTGAGAGT-3′
RNF4	5'-ACAATGAGTACAAGAAAGCGTC-3'	5'-TTCATCTCCAGCAGTTTCC-3'
RNF6	5'-CACCCCTGGAGAAATAACAT-3'	5'-GGGACTTCTGAGTCTCTGTAATT-3'
TRIM68	5' - TAAACAGGAGCAAATCTTGG - 3'	5'-GCACATCAGCTGCATAAGT-3'

ChIP-qPCR primers

Gene	Forward primer	Reverse primer
AR distal	5’-AGGAAGAGGTGTGAGAAGAGGCT-3’	5’-AGTTTATGGGCTGCCAGTCTGC-3’
AR proximal	5’-TATCTGCTGGCTTGGTCATGGCTTG-3’	5’-CTGCTTCCTGAATAGCTCCTGCTT-3’
IVL	5’-TCAGCTGTATCCACTGCCCTCTTT-3’	5’-TCACACCGGTCTTATGGGTTAGCA-3’

Mouse genetics primers

Target	Forward primer	Reverse primer
MEP50-bGH	5'-TGGTGTTCTCCCCACACAGTGTT-3'	5'-CAACTAGAAGGCACAGTCGAGGCT-3'
PRMT5-bGH	5'-TCTGCTATTCATAACCCCACAGG-3'	5-GCCTGCTATTGTCTTCCCAATCCTC-3'
TCR	5'-CAAATGTTGCTTGTCTGGTG-3'	5'-GTCAGTCGAGTGCACAGTTT-3'

APPENDIX C. DATASETS USED FOR MRNA EXPRESSION ANALYSIS

dataset	PMID	Sample size
GSE126078	PMID: 31361600	98
GSE74685	PMID: 26667932	149
GSE50630	PMID: 25189356	8
GSE70285	PMID: 26842848	20
GSE31528	PMID: 25189356	8
GSE74367	PMID: 26990456	56
GSE70768	PMID: 26501111	125
GSE32269	PMID: 23426182	51
GSE72220	PMID: 26945428	57
GSE141551	PMID: 25990700, PMID: 28145099, PMID: 28496006	503
GSE107299	PMID: 30889379	213
GSE6956	PMID: 18245496	59
GSE3933	PMID: 14711987,	71
GSE2109	PMID: 21629784	60
GSE21034	PMID: 20579941	150
GSE8402	PMID: 18505969	455
GSE29650	PMID: 21552559	30
GSE28403	PMID: 21919029	9
GSE41192	PMID: 25544761, PMID: 25859291, PMID: 24589457	3
GSE66187	PMID: 26071481	71
GSE101607	PMID: 27497761	48
Glinsky	PMID: 15067324	79
E_TABM_26	PMID: 16618720	44
nepc_wcm_2016	PMID: 26855148	34
prad_broad	PMID: 22610119	31
prad_eururol_2017	PMID: 28927585	65
prad_fhcrc	PMID: 26928463	171
prad_mich	PMID: 22722839	94
prad_mskcc	PMID: 20579941	150
prad_su2c_2015	PMID: 26000489	118
prad_su2c_2019	PMID: 31061129	270
prad_tcga	https://www.cancer.gov/tcga	498
prad_tcga_pan_can_atlas_2018	PMID: 29625048,29596782,29622463,29617662,29625055,29625050,29617662,30643250	493
prad_tcga_pub	PMID: 26544944	333
Sum		4624

REFERENCES

1. Verze P, Cai T, Lorenzetti S. The role of the prostate in male fertility, health and disease. Nat Rev Urol. 2016 Jul 1;13:379–86.

2. Lee CH, Akin-Olugbade O, Kirschenbaum A. Overview of Prostate Anatomy, Histology, and Pathology. Endocrinol Metab Clin North Am. 2011 Sep;40:565–75.

3. McNeal JE. The zonal anatomy of the prostate. Prostate. 1981 Jan 1;2:35–49.

4. Henry GH, Malewska A, Joseph DB, Malladi VS, Lee J, Torrealba J, et al. A Cellular Anatomy of the Normal Adult Human Prostate and Prostatic Urethra. Cell Rep. 2018 Dec 18;25:3530-3542.e5.

5. Levesque C, Nelson PS. Cellular constituents of the prostate stroma: Key contributors to prostate cancer progression and therapy resistance. Cold Spring Harb Perspect Med. 2018 Aug 1;8:a030510.

6. Kurita T, Medina RT, Mills AA, Cunha GR. Role of p63 and basal cells in the prostate. Development. 2004 Oct 15;131:4955–64.

7. Sun Y, Niu J, Huang J. Neuroendocrine differentiation in prostate cancer. Am J Transl Res. 2009 Feb 5;1:148–62.

8. Mirosevich J, Bentel JM, Zeps N, Redmond SL, D'Antuono MF, Dawkins HJS. Androgen receptor expression of proliferating basal and luminal cells in adult murine ventral prostate. J Endocrinol. 1999;162:341–50.

9. Siiteri PK, Wilson JD. Testosterone formation and metabolism during male sexual diflferentiation in the human embryo. J Clin Endocrinol Metab. 1974;38:113–25.

10. Cunha GR, Cooke PS, Kurita T. Role of stromal-epithelial interactions in hormonal responses. Vol. 67, Archives of Histology and Cytology. International Society of Histology and Cytology; 2004. p. 417–34.

11. Wilson JD, Griffin JE, Russell DW. Steroid 5α-reductase 2 deficiency. Endocr Rev. 1993;14:577–93.

12. Quigley CA, De Bellis A, Marschke KB, El-Awady MK, Wilson EM, French FS. Androgen Receptor Defects: Historical, Clinical, and Molecular Perspectives*. Vol. 16. 1995.

13. Heinlein CA, Chang C. Androgen receptor in prostate cancer. Endocr Rev. 2004;25:276–308.

14. Isaacs JT. Antagonistic effect of androgen on prostatic cell death. Prostate. 1984;5:545–57.

15. Shafi AA, Yen AE, Weigel NL. Androgen receptors in hormone-dependent and castration-resistant prostate cancer. Vol. 140, Pharmacology and Therapeutics. Elsevier Inc.; 2013. p. 223–38.

16. Kim Y, Alarcon S, Lee S, Lee M-J, Giaccone G, Neckers L, et al. Update on Hsp90 Inhibitors in Clinical Trial. Curr Top Med Chem. 2009;9:1479–92.

17. Mangelsdorf DJ, Thummel C, Beato M, Herrlich P, Schütz G, Umesono K, et al. The nuclear receptor superfamily: The second decade. Cell. 1995;83:835–9.

18. Lubahn DB, Joseph DR, Sullivan PM, Willard HF, French FS, Wilson EM. Cloning of human androgen receptor complementary DNA and localization to the X chromosome. Science (80-). 1988;240:327–30.

19. Tan MHE, Li J, Xu HE, Melcher K, Yong E. Androgen receptor: structure, role in prostate cancer and drug discovery. Acta Pharmacol Sin. 2015 Jan;36:3–23.

20. Heemers H V., Tindall DJ. Androgen receptor (AR) coregulators: A diversity of functions converging on and regulating the AR transcriptional complex. Vol. 28, Endocrine Reviews. 2007. p. 778–808.

21. Siegel RL, Miller KD, Jemal A. Cancer statistics, 2020. CA Cancer J Clin. 2020 Jan 1;70:7–30.

22. Rebbeck TR. Prostate Cancer Genetics: Variation by Race, Ethnicity, and Geography. Vol. 27, Seminars in Radiation Oncology. W.B. Saunders; 2017. p. 3–10.

23. Kaiser A, Haskins C, Siddiqui MM, Hussain A, D'Adamo C. The evolving role of diet in prostate cancer risk and progression. Vol. 31, Current Opinion in Oncology. Lippincott Williams and Wilkins; 2019. p. 222–9.

24. Zeegers MPA, Jellema A, Ostrer H. Empiric risk of prostate carcinoma for relatives of patients with prostate carcinoma: A meta-analysis. Cancer. 2003 Apr 15;97:1894–903.

25. Papsidero LD, Wang MC, Valenzuela LA, Murphy GP, Chu TM. A Prostate Antigen in Sera of Prostatic Cancer Patients. Cancer Res. 1980;40:2428–32.

26. Wolf AMD, Wender RC, Etzioni RB, Thompson IM, D'Amico A V., Volk RJ, et al. American Cancer Society Guideline for the Early Detection of Prostate Cancer: Update 2010. CA Cancer J Clin. 2010 Mar 1;60:70–98.

27. Humphrey PA. Histopathology of prostate cancer. Cold Spring Harb Perspect Med. 2017;7:1–22.

28. Chang AJ, Autio KA, Roach M, Scher HI. High-risk prostate cancer-Classification and therapy. Vol. 11, Nature Reviews Clinical Oncology. Nature Publishing Group; 2014. p. 308–23.

29. Eggener SE, Mueller A, Berglund RK, Ayyathurai R, Soloway C, Soloway MS, et al. A Multi-Institutional Evaluation of Active Surveillance for Low Risk Prostate Cancer. J Urol. 2009 Apr;181:1635–41.

30. Huggins C, Hodges C V. Studies on prostatic cancer i. the effect of castration, of estrogen and of androgen injection on serum phosphatases in metastatic carcinoma of the prostate. Cancer Res. 1941;1:293–7.

31. Crawford ED, Eisenberger MA, Mcleod DG, Spaulding JT, Benson R, Dorr FA, et al. A Controlled Trial of Leuprolide with and without Flutamide in Prostatic Carcinoma. N Engl J Med. 1989 Aug 17;321:419–24.

32. Sciarra A, Fasulo A, Ciardi A, Petrangeli E, Gentilucci A, Maggi M, et al. A meta-analysis and systematic review of randomized controlled trials with degarelix versus gonadotropin-releasing hormone agonists for advanced prostate cancer. Med (United States). 2016 Jul 1;95.

33. Stuchbery R, McCoy PJ, Hovens CM, Corcoran NM. Androgen synthesis in prostate cancer: Do all roads lead to Rome? Vol. 14, Nature Reviews Urology. Nature Publishing Group; 2017. p. 49–58.

34. Nevedomskaya E, Baumgart SJ, Haendler B. Recent advances in prostate cancer treatment and drug discovery. Int J Mol Sci. 2018;19.

35. Crawford ED, Heidenreich A, Lawrentschuk N, Tombal B, Pompeo ACL, Mendoza-Valdes A, et al. Androgen-targeted therapy in men with prostate cancer: evolving practice and future considerations. Vol. 22, Prostate Cancer and Prostatic Diseases. Nature Publishing Group; 2019. p. 24–38.

36. Boulos S, Mazhar D. The evolving role of chemotherapy in prostate cancer. Futur Oncol. 2017;1091–5.

37. Mulders PF, De Santis M, Powles T, Fizazi K. Targeted treatment of metastatic castration-resistant prostate cancer with sipuleucel-T immunotherapy. Vol. 64, Cancer Immunology, Immunotherapy. Springer Science and Business Media Deutschland GmbH; 2015. p. 655–63.

38. Turajlic S, Litchfield K, Xu H, Rosenthal R, McGranahan N, Reading JL, et al. Insertion-and-deletion-derived tumour-specific neoantigens and the immunogenic phenotype: a pan-cancer analysis. Lancet Oncol. 2017 Aug 1;18:1009–21.

39. Wilson JM, Parker C. The safety and efficacy of radium-223 dichloride for the treatment of advanced prostate cancer. Expert Rev Anticancer Ther. 2016;16:911–8.

40. Antonarakis ES, Gomella LG, Petrylak DP. When and How to Use PARP Inhibitors in Prostate Cancer: A Systematic Review of the Literature with an Update on On-Going Trials. Eur Urol Oncol. 2020 Aug 17;

41. Saad F, Fizazi K. Androgen Deprivation Therapy and Secondary Hormone Therapy in the Management of Hormone-sensitive and Castration-resistant Prostate Cancer. Urology. 2015;86:852–61.

42. Ylitalo EB, Thysell E, Jernberg E, Lundholm M, Crnalic S, Egevad L, et al. Subgroups of Castration-resistant Prostate Cancer Bone Metastases Defined Through an Inverse Relationship Between Androgen Receptor Activity and Immune Response. Eur Urol. 2017 May 1;71:776–87.

43. Park SW, Kim JH, Lee HJ, Shin DH, Lee SD, Yoon S. The expression of androgen receptor and its variants in human prostate cancer tissue according to disease status, and its prognostic significance. World J Men?s Heal. 2019 Jan 1;37:68–77.

44. Djusberg E, Jernberg E, Thysell E, Golovleva I, Lundberg P, Crnalic S, et al. High levels of the AR-V7 Splice Variant and Co-Amplification of the Golgi Protein Coding YIPF6 in AR Amplified Prostate Cancer Bone Metastases. Prostate. 2017 May 1;77:625–38.

45. Robinson D, Van Allen EM, Wu Y-M, Schultz N, Lonigro RJ, Mosquera J-M, et al. Integrative Clinical Genomics of Advanced Prostate Cancer. Cell. 2015 May;161:1215–28.

46. Chen CD, Welsbie DS, Tran C, Baek SH, Chen R, Vessella R, et al. Molecular determinants of resistance to antiandrogen therapy. Nat Med. 2004 Jan 21;10:33–9.

47. Rokhlin OW, Scheinker VS, Taghiyev AF, Bumcrot D, Glover RA, Cohen MB. MicroRNA-34 mediates AR-dependent p53-induced apoptosis in prostate cancer. Cancer Biol Ther. 2008;7:1288–96.

48. Sikand K, Slaibi JE, Singh R, Slane SD, Shukla GC. MiR 488* inhibits androgen receptor expression in prostate carcinoma cells. Int J Cancer. 2011 Aug 15;129:810–9.

49. Nadiminty N, Tummala R, Lou W, Zhu Y, Zhang J, Chen X, et al. MicroRNA let-7c Suppresses Androgen Receptor Expression and Activity via Regulation of Myc Expression in Prostate Cancer Cells * □ S. ASBMB. 2011;

50. Grasso CS, Wu YM, Robinson DR, Cao X, Dhanasekaran SM, Khan AP, et al. The mutational landscape of lethal castration-resistant prostate cancer. Nature. 2012 Jul 12;487:239–43.

51. Jernberg E, Bergh A, Wikström P. Clinical relevance of androgen receptor alterations in prostate cancer. Vol. 6, Endocrine Connections. BioScientifica Ltd.; 2017. p. R146–61.

52. Hermanson O, Glass CK, Rosenfeld MG. Nuclear receptor coregulators: Multiple modes of modification. Trends Endocrinol Metab. 2002;13:55–60.

53. Vellky JE, Ricke WA. Development and prevalence of castration-resistant prostate cancer subtypes. Neoplasia. 2020 Nov;22:566–75.

54. Mohler JL, Gregory CW, Ford H, Kim D, Weaver CM, Petrusz P, et al. The Androgen Axis in Recurrent Prostate Cancer. Clin Cancer Res. 2004 Jan 15;10:440–8.

55. Montgomery RB, Mostaghel EA, Vessella R, Hess DL, Kalhorn TF, Higano CS, et al. Maintenance of intratumoral androgens in metastatic prostate cancer: A mechanism for castration-resistant tumor growth. Cancer Res. 2008 Jun 1;68:4447–54.

56. Dehm SM, Tindall DJ. Alternatively spliced androgen receptor variants. Endocr Relat Cancer. 2011;18:183–96.

57. Lu C, Luo J. Decoding the androgen receptor splice variants. Transl Androl Urol. 2013;2:178–86.

58. Watson PA, Chen YF, Balbas MD, Wongvipat J, Socci ND, Viale A, et al. Constitutively active androgen receptor splice variants expressed in castration-resistant prostate cancer require full-length androgen receptor. Proc Natl Acad Sci U S A. 2010 Sep 28;107:16759–65.

59. Sun S, Sprenger CCT, Vessella RL, Haugk K, Soriano K, Mostaghel EA, et al. Castration resistance in human prostate cancer is conferred by a frequently occuring androgen receptor splice variant. J Clin Invest. 2010;120.

60. Sciarra A, Gentilucci A, Silvestri I, Salciccia S, Cattarino S, Scarpa S, et al. Androgen receptor variant 7 (AR-V7) in sequencing therapeutic agents for castratrion resistant prostate cancer: A critical review. Medicine (Baltimore). 2019 May 1;98:e15608.

61. Hu R, Dunn TA, Wei S, Isharwal S, Veltri RW, Humphreys E, et al. Ligand-independent androgen receptor variants derived from splicing of cryptic exons signify hormone-refractory prostate cancer. Cancer Res. 2009 Jan 1;69:16–22.

62. Hu R, Lu C, Mostaghel EA, Yegnasubramanian S, Gurel M, Tannahill C, et al. Distinct transcriptional programs mediated by the ligand-dependent full-length androgen receptor and its splice variants in castration-resistant prostate cancer. Cancer Res. 2012;72:3457–62.

63. Chan SC, Selth LA, Li Y, Nyquist MD, Miao L, Bradner JE, et al. Targeting chromatin binding regulation of constitutively active AR variants to overcome prostate cancer resistance to endocrine-based therapies. Nucleic Acids Res. 2015;43:5880–97.

64. Lu J, Lonergan PE, Nacusi LP, Wang L, Schmidt LJ, Sun Z, et al. The cistrome and gene signature of androgen receptor splice variants in castration resistant prostate cancer cells. J Urol. 2015 Feb 1;193:690–8.

65. Li Y, Chan SC, Brand LJ, Hwang TH, Silverstein KAT, Dehm SM. Androgen receptor splice variants mediate enzalutamide resistance in castration-resistant prostate cancer cell lines. Cancer Res. 2013 Jan 15;73:483–9.

66. Cheng MA, Chou F-J, Wang K, Yang R, Ding J, Zhang Q, et al. Androgen receptor (AR) degradation enhancer ASC-J9 ® in an FDA-approved formulated solution suppresses castration resistant prostate cancer cell growth. Cancer Lett. 2018 Mar 28;417:182–91.

67. Vanaja DK, Mitchell SH, Toft DO, Young CYF. Effect of geldanamycin on androgen receptor function and stability. Cell Stress Chaperones. 2002;7:55–64.

68. Mullard A. First targeted protein degrader hits the clinic. Nat Rev Drug Discov. 2019 Mar 6;18:237–9.

69. Shen MM, Abate-Shen C. Molecular genetics of prostate cancer: New prospects for old challenges. Vol. 24, Genes and Development. Cold Spring Harbor Laboratory Press; 2010. p. 1967–2000.

70. Zou M, Toivanen R, Mitrofanova A, Floch N, Hayati S, Sun Y, et al. Transdifferentiation as a Mechanism of Treatment Resistance in a Mouse Model of Castration-Resistant Prostate Cancer. Cancer Discov. 2017 Jul 1;7:736–49.

71. Packer JR, Maitland NJ. The molecular and cellular origin of human prostate cancer. Vol. 1863, Biochimica et Biophysica Acta - Molecular Cell Research. Elsevier B.V.; 2016. p. 1238–60.

72. Lee SH, Shen MM. Cell types of origin for prostate cancer. Vol. 37, Current Opinion in Cell Biology. Elsevier Ltd; 2015. p. 35–41.

73. Sievert KD, Stenzl A. Re: Lineage analysis of basal epithelial cells reveals their unexpected plasticity and supports a cell-of-origin model for prostate cancer heterogeneity. Eur Urol. 2013;64:340–1.

74. Wang X, Julio MK De, Economides KD, Walker D, Yu H, Halili MV, et al. A luminal epithelial stem cell that is a cell of origin for prostate cancer. Nature. 2009;461:495–500.

75. Park JW, Lee JK, Phillips JW, Huang P, Cheng D, Huang J, et al. Prostate epithelial cell of origin determines cancer differentiation state in an organoid transformation assay. Proc Natl Acad Sci U S A. 2016 Apr 19;113:4482–7.

76. Park JW, Lee JK, Sheu KM, Wang L, Balanis NG, Nguyen K, et al. Reprogramming normal human epithelial tissues to a common, lethal neuroendocrine cancer lineage. Science (80-). 2018 Oct 5;362:91–5.

77. Jin RJ, Wang Y, Masumori N, Ishii K, Tsukamoto T, Shappell SB, et al. NE-10 neuroendocrine cancer promotes the LNCaP xenograft growth in castrated mice. Cancer Res. 2004;64:5489–95.

78. Xing N, Qian J, Bostwick D, Bergstralh E, Young CYF. Neuroendocrine cells in human prostate over-express the anti-apoptosis protein survivin. Prostate. 2001 Jun 15;48:7–15.

79. Segal NH, Cohen RJ, Haffejee Z, Savage N. BCL-2 proto-oncogene expression in prostate cancer and its relationship to the prostatic neuroendocrine cell. Arch Pathol Lab Med. 1994;118:616–8.

80. Moch H, Cubilla AL, Humphrey PA, Reuter VE, Ulbright TM. The 2016 WHO Classification of Tumours of the Urinary System and Male Genital Organs—Part A: Renal, Penile, and Testicular Tumours. Eur Urol. 2016;70:93–105.

81. Epstein JI, Amin MB, Beltran H, Lotan TL, Mosquera J-M, Reuter VE, et al. Proposed morphologic classification of prostate cancer with neuroendocrine differentiation. Am J Surg Pathol. 2014 Jun;38:756–67.

82. Hu J, Han B, Huang J. Morphologic spectrum of neuroendocrine tumors of the prostate an updated review. Arch Pathol Lab Med. 2020;144:320–5.

83. Hoang DT, Iczkowski KA, Kilari D, See W, Nevalainen MT. Androgen receptor-dependent and -independent mechanisms driving prostate cancer progression: Opportunities for therapeutic targeting from multiple angles. Oncotarget. 2017;8:3724–45.

84. Santoni M, Conti A, Burattini L, Berardi R, Scarpelli M, Cheng L, et al. Neuroendocrine differentiation in prostate cancer: novel morphological insights and future therapeutic perspectives. Biochim Biophys Acta. 2014;1846:630–7.

85. Aggarwal R, Huang J, Alumkal JJ, Zhang L, Feng FY, Thomas G V., et al. Clinical and genomic characterization of treatment-emergent small-cell neuroendocrine prostate cancer: A multi-institutional prospective study. J Clin Oncol. 2018 Aug 20;36:2492–503.

86. Abida W, Cyrta J, Heller G, Prandi D, Armenia J, Coleman I, et al. Genomic correlates of clinical outcome in advanced prostate cancer. Proc Natl Acad Sci U S A. 2019;166:11428–36.

87. Carver BS. Defining and Targeting the Oncogenic Drivers of Neuroendocrine Prostate Cancer. Cancer Cell. 2016 Apr 11;29:431–2.

88. Wang HT, Yao YH, Li BG, Tang Y, Chang JW, Zhang J. Neuroendocrine Prostate Cancer (NEPC) progressing from conventional prostatic adenocarcinoma: factors associated with time to development of NEPC and survival from NEPC diagnosis-a systematic review and pooled analysis. J Clin Oncol. 2014 Oct 20;32:3383–90.

89. Marcus DM, Goodman M, Jani AB, Osunkoya AO, Rossi PJ. A comprehensive review of incidence and survival in patients with rare histological variants of prostate cancer in the United States from 1973 to 2008. Prostate Cancer Prostatic Dis. 2012 Sep 21;15:283–8.

90. Culine S, El Demery M, Lamy PJ, Iborra F, Avancès C, Pinguet F. Docetaxel and Cisplatin in Patients With Metastatic Androgen Independent Prostate Cancer and Circulating Neuroendocrine Markers. J Urol. 2007 Sep 1;178:844–8.

91. Deng X, Elzey BD, Poulson JM, Morrison WB, Ko S-C, Hahn NM, et al. Ionizing radiation induces neuroendocrine differentiation of prostate cancer cells in vitro, in vivo and in prostate cancer patients. Am J Cancer Res. 2011;1:834–44.

92. Deng X, Liu H, Huang J, Cheng L, Keller ET, Parsons SJ, et al. Ionizing Radiation Induces Prostate Cancer Neuroendocrine Differentiation through Interplay of CREB and ATF2: Implications for Disease Progression. Cancer Res. 2008;68:9663–70.

93. Hu CD, Choo R, Huang J. Neuroendocrine differentiation in prostate cancer: A mechanism of radioresistance and treatment failure. Vol. 5, Frontiers in Oncology. Frontiers Media S.A.; 2015.

94. Offin M, Chan JM, Tenet M, Rizvi HA, Shen R, Riely GJ, et al. Concurrent RB1 and TP53 Alterations Define a Subset of EGFR-Mutant Lung Cancers at risk for Histologic Transformation and Inferior Clinical Outcomes. J Thorac Oncol. 2019 Oct 1;14:1784–93.

95. Beltran H, Tagawa ST, Park K, MacDonald T, Milowsky MI, Mosquera JM, et al. Challenges in recognizing treatment-related neuroendocrine prostate cancer. J Clin Oncol. 2012;30.

96. Davies AH, Beltran H, Zoubeidi A. Cellular plasticity and the neuroendocrine phenotype in prostate cancer. Vol. 15, Nature Reviews Urology. Nature Publishing Group; 2018. p. 271–86.

97. Jamaspishvili T, Berman DM, Ross AE, Scher HI, De Marzo AM, Squire JA, et al. Clinical implications of PTEN loss in prostate cancer. Vol. 15, Nature Reviews Urology. Nature Publishing Group; 2018. p. 222–34.

98. Krohn A, Diedler T, Burkhardt L, Mayer PS, De Silva C, Meyer-Kornblum M, et al. Genomic deletion of PTEN is associated with tumor progression and early PSA recurrence in ERG fusion-positive and fusion-negative prostate cancer. Am J Pathol. 2012;181:401–12.

99. Yoshimoto M, Cunha IW, Coudry RA, Fonseca FP, Torres CH, Soares FA, et al. FISH analysis of 107 prostate cancers shows that PTEN genomic deletion is associated with poor clinical outcome. Br J Cancer. 2007;97:678–85.

100. Ramaswamy S, Nakamura N, Vazquez F, Batt DB, Perera S, Roberts TM, et al. Regulation of G1 progression by the PTEN tumor suppressor protein is linked to inhibition of the phosphatidylinositol 3-kinase/akt pathway. Proc Natl Acad Sci U S A. 1999;96:2110–5.

101. Wang S, Gao J, Lei Q, Rozengurt N, Pritchard C, Jiao J, et al. Prostate-specific deletion of the murine Pten tumor suppressor gene leads to metastatic prostate cancer. Cancer Cell. 2003 Sep 1;4:209–21.

102. Tomlins SA, Rhodes DR, Perner S, Dhanasekaran SM, Mehra R, Sun XW, et al. Recurrent fusion of TMPRSS2 and ETS transcription factor genes in prostate cancer. Science (80-). 2005;310:644–8.

103. Blee AM, He Y, Yang Y, Ye Z, Yan Y, Pan Y, et al. TMPrSS2-ERG controls luminal epithelial lineage and antiandrogen sensitivity in PTEN and TP53-mutated prostate cancer. Clin Cancer Res. 2018;24:4551–65.

104. Scheble VJ, Braun M, Beroukhim R, Mermel CH, Ruiz C, Wilbertz T, et al. ERG rearrangement is specific to prostate cancer and does not occur in any other common tumor. Mod Pathol. 2010;23:1061–7.

105. Carceles-Cordon M, Kelly WK, Gomella L, Knudsen KE, Rodriguez-Bravo V, Domingo-Domenech J. Cellular rewiring in lethal prostate cancer: the architect of drug resistance. Nat Rev Urol. 2020;17:292–307.

106. Zhou Z, Flesken-Nikitin A, Corney DC, Wang W, Goodrich DW, Roy-Burman P, et al. Synergy of p53 and Rb Deficiency in a Conditional Mouse Model for Metastatic Prostate Cancer. Cancer Res. 2006;66:7889–98.

107. Zou M, Toivanen R, Mitrofanova A, Floch N, Hayati S, Sun Y, et al. !!!Transdifferentiation as a Mechanism of Treatment Resistance in a Mouse Model of Castration-Resistant Prostate Cancer. Cancer Res. 2020;

108. Ku SY, Rosario S, Wang Y, Mu P, Seshadri M, Goodrich ZW, et al. *Rb1* and *Trp53* cooperate to suppress prostate cancer lineage plasticity, metastasis, and antiandrogen resistance. Science (80-). 2017;355:78–83.

109. Quintanal-Villalonga Á, Chan JM, Yu HA, Pe'er D, Sawyers CL, Sen T, et al. Lineage plasticity in cancer: a shared pathway of therapeutic resistance. Vol. 17, Nature Reviews Clinical Oncology. Nature Research; 2020. p. 360–71.

110. Bai S, Cao S, Jin L, Kobelski M, Schouest B, Wang X, et al. A positive role of c-Myc in regulating androgen receptor and its splice variants in prostate cancer. Oncogene. 2019 Jun 20;38:4977–89.

111. Dardenne E, Beltran H, Benelli M, Gayvert K, Berger A, Puca L, et al. N-Myc Induces an EZH2-Mediated Transcriptional Program Driving Neuroendocrine Prostate Cancer. Cancer Cell. 2016 Oct;30:563–77.

112. Stoyanova T, Cooper AR, Drake JM, Liu X, Armstrong AJ, Pienta KJ, et al. Prostate cancer originating in basal cells progresses to adenocarcinoma propagated by luminal-like cells. Proc Natl Acad Sci U S A. 2013;110:20111–6.

113. Lee JK, Phillips JW, Smith BA, Park JW, Stoyanova T, McCaffrey EF, et al. N-Myc Drives Neuroendocrine Prostate Cancer Initiated from Human Prostate Epithelial Cells. Cancer Cell. 2016;29:536–47.

114. Karkhanis V, Hu YJ, Baiocchi RA, Imbalzano AN, Sif S. Versatility of PRMT5-induced methylation in growth control and development. Trends Biochem Sci. 2011;36:633–41.

115. Fuhrmann J, Clancy KW, Thompson PR. Chemical Biology of Protein Arginine Modifications in Epigenetic Regulation. Vol. 115, Chemical Reviews. American Chemical Society; 2015. p. 5413–61.

116. Krause CD, Yang ZH, Kim YS, Lee JH, Cook JR, Pestka S. Protein arginine methyltransferases: Evolution and assessment of their pharmacological and therapeutic potential. Pharmacol Ther. 2007;113:50–87.

117. Lorton BM, Shechter D. Cellular consequences of arginine methylation. Vol. 76, Cellular and Molecular Life Sciences. Birkhauser Verlag AG; 2019. p. 2933–56.

118. Blanc RS, Richard S. Arginine Methylation: The Coming of Age. Vol. 65, Molecular Cell. Cell Press; 2017. p. 8–24.

119. Antonysamy S, Bonday Z, Campbell RM, Doyle B, Druzina Z, Gheyi T, et al. Crystal structure of the human PRMT5:MEP50 complex. Proc Natl Acad Sci U S A. 2012 Oct 30;109:17960–5.

120. Stopa N, Krebs JE, Shechter D. The PRMT5 arginine methyltransferase: many roles in development, cancer and beyond. Cell Mol Life Sci. 2015 Jun;72:2041–59.

121. Kim S, Günesdogan U, Zylicz JJ, Hackett JA, Cougot D, Bao S, et al. PRMT5 protects genomic integrity during global DNA demethylation in primordial germ cells and preimplantation embryos. Mol Cell. 2014 Nov 20;56:564–79.

122. Kim H, Ronai ZA. PRMT5 function and targeting in cancer. Vol. 4, Cell Stress. Shared Science Publishers OG; 2020. p. 199–215.

123. Wei X, Yang J, Adair SJ, Ozturk H, Kuscu C, Lee KY, et al. Targeted CRISPR screening identifies PRMT5 as synthetic lethality combinatorial target with gemcitabine in pancreatic cancer cells. Proc Natl Acad Sci. 2020 Oct 23;202009899.

124. Bao X, Zhao S, Liu T, Liu Y, Liu Y, Yang X. Overexpression of PRMT5 promotes tumor cell growth and is associated with poor disease prognosis in epithelial ovarian cancer. J Histochem Cytochem. 2013;61:206–17.

125. Győrffy B, Surowiak P, Budczies J, Lánczky A, Higashiyama M. Online Survival Analysis Software to Assess the Prognostic Value of Biomarkers Using Transcriptomic Data in Non-Small-Cell Lung Cancer. Chellappan SP, editor. PLoS One. 2013 Dec 18;8:e82241.

126. Shailesh H, Zakaria ZZ, Baiocchi R, Sif S. Protein arginine methyltransferase 5 (PRMT5) dysregulation in cancer. Oncotarget. 2018 Nov 30;9:36705–18.

127. Fan Z, Kong X, Xia J, Wu X, Li H, Xu H, et al. The arginine methyltransferase PRMT5 regulates CIITA-dependent MHC II transcription. Biochim Biophys Acta - Gene Regul Mech. 2016 May 1;1859:687–96.

128. Tarighat SS, Santhanam R, Frankhouser D, Radomska HS, Lai H, Anghelina M, et al. The dual epigenetic role of PRMT5 in acute myeloid leukemia: gene activation and repression via histone arginine methylation. Leukemia. 2015;30:1–11.

129. Chen H, Lorton B, Gupta V, Shechter D. A TGFβ-PRMT5-MEP50 axis regulates cancer cell invasion through histone H3 and H4 arginine methylation coupled transcriptional activation and repression. Oncogene. 2017 Jan 19;36:373–86.

130. Ho MC, Wilczek C, Bonanno JB, Xing L, Seznec J, Matsui T, et al. Structure of the Arginine Methyltransferase PRMT5-MEP50 Reveals a Mechanism for Substrate Specificity. PLoS One. 2013;8:p.e57008.

131. Friesen WJ, Paushkin S, Wyce A, Massenet S, Pesiridis GS, Van Duyne G, et al. The methylosome, a 20S complex containing JBP1 and pICln, produces dimethylarginine-modified Sm proteins. Mol Cell Biol. 2001 Dec;21:8289–300.

132. Guderian G, Peter C, Wiesner J, Sickmann A, Schulze-Osthoff K, Fischer U, et al. RioK1, a New Interactor of Protein Arginine Methyltransferase 5 (PRMT5), Competes with pICln for Binding and Modulates PRMT5 Complex Composition and Substrate Specificity. J Biol Chem. 2011 Jan 21;286:1976–86.

133. Yang M, Lin X, Segers F, Suganthan R, Hildrestrand GA, Rinholm JE, et al. OXR1A, a Coactivator of PRMT5 Regulating Histone Arginine Methylation. Cell Rep. 2020 Mar 24;30:4165–78.

134. Lacroix M, Messaoudi S El, Rodier G, Le Cam A, Sardet C, Fabbrizio E. The histone-binding protein COPR5 is required for nuclear functions of the protein arginine methyltransferase PRMT5. EMBO Rep. 2008 May 11;9:452–8.

135. Pesiridis GS, Diamond E, Van Duyne GD. Role of pICLn in methylation of Sm proteins by PRMT5. J Biol Chem. 2009;284:21347–59.

136. Owens JL, Beketova E, Liu S, Tinsley SL, Asberry AM, Deng X, et al. PRMT5 Cooperates with pICln to Function as a Master Epigenetic Activator of DNA Double-Strand Break Repair Genes. iScience. 2020 Jan 24;23:100750.

137. Deng X, Shao G, Zhang H-T, Li C, Zhang D, Cheng L, et al. Protein arginine methyltransferase 5 functions as an epigenetic activator of the androgen receptor to promote prostate cancer cell growth. Oncogene. 2016;36:1–9.

138. Saha K, Adhikary G, Eckert RL. MEP50/PRMT5 reduces gene expression by histone arginine methylation and this is reversed by PKCd/p38d signaling. J Invest Dermatol. 2016 Jan;136:214–24.

139. La Vignera S, Condorelli RA, Russo GI, Morgia G, Calogero AE. Endocrine control of benign prostatic hyperplasia. Andrology. 2016 May 1;4:404–11.

140. Snow O, Lallous N, Singh K, Lack N, Rennie P, Cherkasov A. Androgen receptor plasticity and its implications for prostate cancer therapy. Cancer Treat Rev. 2019 Dec 1;81:101871.

141. Watson PA, Arora VK, Sawyers CL. Emerging mechanisms of resistance to androgen receptor inhibitors in prostate cancer. Nat Rev Cancer. 2015 Nov 24;15:701–11.

142. Cucchiara V, Yang JC, Mirone V, Gao AC, Rosenfeld MG, Evans CP. Epigenomic regulation of androgen receptor signaling: Potential role in prostate cancer therapy. Cancers (Basel). 2017 Jan 1;9:9.

143. Nakayama T, Watanabe M, Suzuki H, Toyota M, Sekita N, Hirokawa Y, et al. Epigenetic regulation of androgen receptor gene expression in human prostate cancers. Lab Investig. 2000 Dec 1;80:1789–96.

144. Shiota M, Takeuchi A, Yokomizo A, Kashiwagi E, Tatsugami K, Naito S. Methyltransferase inhibitor adenosine dialdehyde suppresses androgen receptor expression and prostate cancer growth. J Urol. 2012 Jul;188:300–6.

145. Migliori V, Müller J, Phalke S, Low D, Bezzi M, Mok WC, et al. Symmetric dimethylation of H3R2 is a newly identified histone mark that supports euchromatin maintenance. Nat Struct Mol Biol. 2012 Feb 8;19:136–45.

146. Faber PW, Van Rooij HCJ, Schipper HJ, Brinkmann AO, Trapman J. Two different, overlapping pathways of transcription initiation are active on the TATA-less human androgen receptor promoter. The role of Sp1. J Biol Chem. 1993;268:9296–301.

147. Zhu C, Hou X, Zhu J, Jiang C, Wei W. Expression of miR-30c and miR-29b in prostate cancer and its diagnostic significance. Oncol Lett. 2018 Sep 1;16:3140–4.

148. Mongiardi MP, Savino M, Bartoli L, Beji S, Nanni S, Scagnoli F, et al. Myc and Omomyc functionally associate with the Protein Arginine Methyltransferase 5 (PRMT5) in glioblastoma cells. Sci Rep. 2015 Nov 13;5:15494.

149. Koh CM, Bezzi M, Low DHP, Ang WX, Teo SX, Gay FPH, et al. MYC regulates the core pre-mRNA splicing machinery as an essential step in lymphomagenesis. Nature. 2015 Jul 2;523:96–100.

150. Karkhanis V, Alinari L, Ozer HG, Chung J, Zhang X, Sif S, et al. Protein arginine methyltransferase 5 represses tumor suppressor miRNAs that down-regulate CYCLIN D1 and c-MYC expression in aggressive B-cell lymphoma. J Biol Chem. 2020 Jan 31;295:1165–80.

151. Berger A, Brady NJ, Bareja R, Robinson B, Conteduca V, Augello MA, et al. N-Myc-mediated epigenetic reprogramming drives lineage plasticity in advanced prostate cancer. J Clin Invest. 2019 Sep 3;129:3924–40.

152. Park JH, Szemes M, Vieira GC, Melegh Z, Malik S, Heesom KJ, et al. Protein arginine methyltransferase 5 is a key regulator of the MYCN oncoprotein in neuroblastoma cells. Mol Oncol. 2015;9:617–27.

153. Zhang L, Altuwaijri S, Deng F, Chen L, Lal P, Bhanot UK, et al. NF-κB regulates androgen receptor expression and prostate cancer growth. Am J Pathol. 2009 Aug 1;175:489–99.

154. Thomas-Jardin SE, Dahl H, Nawas AF, Bautista M, Delk NA. NF-κB signaling promotes castration-resistant prostate cancer initiation and progression. Pharmacol Ther. 2020 Mar 19;19:107538.

155. Harris DP, Chandrasekharan UM, Bandyopadhyay S, Willard B, DiCorleto PE. PRMT5-mediated methylation of NF-κB p65 at Arg174 is required for endothelial CXCL11 gene induction in response to TNF-α and IFN-γ costimulation. PLoS One. 2016 Feb 1;11:e0148905.

156. Wei H, Wang B, Miyagi M, She Y, Gopalan B, Huang D Bin, et al. PRMT5 dimethylates R30 of the p65 subunit to activate NF-kappaB. Proc Natl Acad Sci U S A. 2013 Aug 13;110:13516–21.

157. Alimirah F, Panchanathany R, Cheny J, Zhang X, Ho SM, Choubey D. Expression of androgen receptor is negatively regulated by p53. Neoplasia. 2007;9:1152–9.

158. Li Y, Chitnis N, Nakagawa H, Kita Y, Natsugoe S, Yang Y, et al. PRMT5 is required for lymphomagenesis triggered by multiple oncogenic drivers. Cancer Discov. 2015;5:288–303.

159. Hosohata K, Li P, Hosohata Y, Qin J, Roeder RG, Wang Z. Purification and identification of a novel complex which is involved in androgen receptor-dependent transcription. Mol Cell Biol. 2003 Oct;23:7019–29.

160. Mounir Z, Korn JM, Westerling T, Lin F, Kirby CA, Schirle M, et al. ERG signaling in prostate cancer is driven through PRMT5-dependent methylation of the androgen receptor. Elife. 2016 May 16;5:e13964.

161. Zhou L, Wu H, Lee P, Wang Z. Roles of the androgen receptor cofactor p44 in the growth of prostate epithelial cells. J Mol Endocrinol. 2006 Oct;37:283–300.

162. Liu S, Kumari S, Hu Q, Senapati D, Venkadakrishnan VB, Wang D, et al. A comprehensive analysis of coregulator recruitment, androgen receptor function and gene expression in prostate cancer. Elife. 2017 Aug 18;6:e28482.

163. Yang Y, Bedford MT. Protein arginine methyltransferases and cancer. Nat Rev Cancer. 2013;13:37–50.

164. Jahan S, Davie JR. Protein arginine methyltransferases (PRMTs): Role in chromatin organization. Adv Biol Regul. 2015;57:173–84.

165. Li M, An W, Xu L, Lin Y, Su L, Liu X. The arginine methyltransferase PRMT5 and PRMT1 distinctly regulate the degradation of anti-apoptotic protein CFLARL in human lung cancer cells. J Exp Clin Cancer Res. 2019 Dec 8;38:64.

166. Favia A, Salvatori L, Nanni S, Iwamoto-Stohl LK, Valente S, Mai A, et al. The Protein Arginine Methyltransferases 1 and 5 affect Myc properties in glioblastoma stem cells. Sci Rep. 2019 Dec 1;9:15925.

167. Gao G, Zhang L, Villarreal OD, He W, Su D, Bedford E, et al. PRMT1 loss sensitizes cells to PRMT5 inhibition. Nucleic Acids Res. 2019;47:5038–48.

168. Collins CC, Volik S V., Lapuk A V., Wang Y, Gout PW, Wu C, et al. Next generation sequencing of prostate cancer from a patient identifies a deficiency of methylthioadenosine phosphorylase, an exploitable tumor target. Mol Cancer Ther. 2012 Mar;11:775–81.

169. Almeida-Rios D, Graça I, Vieira FQ, Ramalho-Carvalho J, Pereira-Silva E, Martins AT, et al. Histone methyltransferase PRMT6 plays an oncogenic role of in prostate cancer. Oncotarget. 2016 Aug 1;7:53018–28.

170. Xu Z, He Y, Ju J, Rank G, Cerruti L, Ma C, et al. The role of WDR5 in silencing human fetal globin gene expression. Haematologica. 2012 Nov 1;97:1632–40.

171. Lorton BM, Harijan RK, Burgos ES, Bonanno JB, Almo SC, Shechter D. A Binary Arginine Methylation Switch on Histone H3 Arginine 2 Regulates Its Interaction with WDR5. Biochemistry. 2020 Mar 31;e-pub ahead of print 31 March 2020.

172. Jain K, Jin CY, Clarke SG. Epigenetic control via allosteric regulation of mammalian protein arginine methyltransferases. Proc Natl Acad Sci U S A. 2017 Sep 19;114:10101–6.

173. Dhar SS, Lee SH, Kan PY, Voigt P, Ma L, Shi X, et al. Trans-tail regulation of MLL4-catalyzed H3K4 methylation by H4R3 symmetric dimethylation is mediated by a tandem PHD of MLL4. Genes Dev. 2012 Dec 15;26:2749–62.

174. Majumder S, Liu Y, Ford OH, Mohler JL, Whang YE. Involvement of arginine methyltransferase CARM1 in androgen receptor function and prostate cancer cell viability. Prostate. 2006 Sep 1;66:1292–301.

175. Husmann D, Gozani O. Histone lysine methyltransferases in biology and disease. Nat Struct Mol Biol. 2019 Oct 1;26:880–9.

176. Deb G, Thakur VS, Gupta S. Multifaceted role of EZH2 in breast and prostate tumorigenesis: Epigenetics and beyond. Epigenetics. 2013;8:464–76.

177. Tae S, Karkhanis V, Velasco K, Yaneva M, Erdjument-Bromage H, Tempst P, et al. Bromodomain protein 7 interacts with PRMT5 and PRC2, and is involved in transcriptional repression of their target genes. Nucleic Acids Res. 2011;39:5424–38.

178. Chung J, Karkhanis V, Tae S, Yan F, Smith P, Ayers LW, et al. Protein arginine methyltransferase 5 (PRMT5) inhibition induces lymphoma cell death through reactivation of the retinoblastoma tumor suppressor pathway and polycomb repressor complex 2 (PRC2) Silencing. J Biol Chem. 2013;288:35534–47.

179. Furuno K, Masatsugu T, Sonoda M, Sasazuki T, Yamamoto K. Association of Polycomb group SUZ12 with WD-repeat protein MEP50 that binds to histone H2A selectively in vitro. Biochem Biophys Res Commun. 2006 Jul 7;345:1051–8.

180. Liu F, Xu Y, Lu X, Hamard P-J, Karl DL, Man N, et al. PRMT5-mediated histone arginine methylation antagonizes transcriptional repression by polycomb complex PRC2. Nucleic Acids Res. 2020 Feb 6;48:2956–68.

181. Liu Q, Wang G, Li Q, Jiang W, Kim J-S, Wang R, et al. Polycomb group proteins EZH2 and EED directly regulate androgen receptor in advanced prostate cancer. Int J Cancer. 2019 Jul 15;145:415–26.

182. Kim JY, Banerjee T, Vinckevicius A, Luo Q, Parker JB, Baker MR, et al. A Role for WDR5 in Integrating Threonine 11 Phosphorylation to Lysine 4 Methylation on Histone H3 during Androgen Signaling and in Prostate Cancer. Mol Cell. 2014 May 22;54:613–25.

183. Cao L, Wu G, Zhu J, Tan Z, Shi D, Wu X, et al. Genotoxic stress-triggered β-catenin/JDP2/PRMT5 complex facilitates reestablishing glutathione homeostasis. Nat Commun. 2019 Dec 1;10:3761.

184. Verdone L, Agricola E, Caserta M, Di Mauro E. Histone acetylation in gene regulation. Briefings Funct Genomics Proteomics. 2006;5:209–21.

185. Jin L, Garcia J, Chan E, De La Cruz C, Segal E, Merchant M, et al. Therapeutic targeting of the CBP/p300 bromodomain blocks the growth of castration-resistant prostate cancer. Cancer Res. 2017 Oct 15;77:5564–75.

186. Shin SH, Lee GY, Lee M, Kang J, Shin HW, Chun YS, et al. Aberrant expression of CITED2 promotes prostate cancer metastasis by activating the nucleolin-AKT pathway. Nat Commun. 2018 Dec 1;9:4113.

187. Feng Y, Wang J, Asher S, Hoang L, Guardiani C, Ivanov I, et al. Histone H4 acetylation differentially modulates arginine methylation by an in cis mechanism. J Biol Chem. 2011 Jun 10;286:20323–34.

188. Pal S, Yun R, Datta A, Lacomis L, Erdjument-Bromage H, Kumar J, et al. mSin3A/histone deacetylase 2- and PRMT5-containing Brg1 complex is involved in transcriptional repression of the Myc target gene cad. Mol Cell Biol. 2003 Nov;23:7475–87.

189. Scaglione A, Patzig J, Liang J, Frawley R, Bok J, Mela A, et al. PRMT5-mediated regulation of developmental myelination. Nat Commun. 2018 Dec 1;9:2840.

190. Joseph DB, Strand DW, Vezina CM. DNA methylation in development and disease: an overview for prostate researchers. Am J Clin Exp Urol. 2018;6:197–218.

191. Feinberg AP, Tycko B. The history of cancer epigenetics. Nat Rev Cancer. 2004;4:143–53.

192. Zhao Q, Rank G, Tan YT, Li H, Moritz RL, Simpson RJ, et al. PRMT5-mediated methylation of histone H4R3 recruits DNMT3A, coupling histone and DNA methylation in gene silencing. Nat Struct Mol Biol. 2009 Mar;16:304–11.

193. Liu X, Zhang J, Liu L, Jiang Y, Ji J, Yan R, et al. Protein arginine methyltransferase 5-mediated epigenetic silencing of IRX1 contributes to tumorigenicity and metastasis of gastric cancer. Biochim Biophys Acta - Mol Basis Dis. 2018 Sep 1;1864:2835–44.

194. Le Guezennec X, Vermeulen M, Brinkman AB, Hoeijmakers WAM, Cohen A, Lasonder E, et al. MBD2/NuRD and MBD3/NuRD, Two Distinct Complexes with Different Biochemical and Functional Properties. Mol Cell Biol. 2006 Feb 1;26:843–51.

195. Lu C, Brown LC, Antonarakis ES, Armstrong AJ, Luo J. Androgen receptor variant-driven prostate cancer II: advances in laboratory investigations. Prostate Cancer Prostatic Dis. 2020 Mar 5;3:1–17.

196. Chang AJ, Autio KA, Roach M, Scher HI. High-risk prostate cancer-Classification and therapy. Nat Rev Clin Oncol. 2014;11:308–23.

197. Polkinghorn WR, Parker JS, Lee MX, Kass EM, Spratt DE, Iaquinta PJ, et al. Androgen receptor signaling regulates DNA repair in prostate cancers. Cancer Discov. 2013 Nov;3:1245–53.

198. Goodwin JF, Schiewer MJ, Dean JL, Schrecengost RS, de Leeuw R, Han S, et al. A hormone-DNA repair circuit governs the response to genotoxic insult. Cancer Discov. 2013 Nov;3:1254–71.

199. Asim M, Tarish F, Zecchini HI, Sanjiv K, Gelali E, Massie CE, et al. Synthetic lethality between androgen receptor signalling and the PARP pathway in prostate cancer. Nat Commun. 2017 Dec 1;8:374.

200. Shen Y, Gao G, Yu X, Kim H, Wang L, Xie L, et al. Discovery of First-in-Class Protein Arginine Methyltransferase 5 (PRMT5) Degraders. J Med Chem. 2020 Sep 10;63:9977–89.

201. Jin J, Liu J, Shen Y. PROTEIN ARGININE METHYLTRANSFERASE 5 (PRMT5) DEGRADATION / DISRUPTION COMPOUNDS AND METHODS OF USE. 2019. p. WO2019165189A1.

202. Beketova E, Fang S, Owens JL, Liu S, Chen X, Zhang Q, et al. Protein arginine methyltransferase 5 promotes pICln-dependent androgen receptor transcription in castration-resistant prostate cancer. Cancer Res. 2020 Sep 30;canres.1228.2020.

203. Siegel RL, Miller KD, Jemal A. Cancer statistics, 2018. CA Cancer J Clin. 2018 Jan 1;68:7–30.

204. Loh KP, Mohile SG, Kessler E, Fung C. Treatment of Metastatic Prostate Cancer in Older Adults. Curr Oncol Rep. 2016 Oct 1;18:63.

205. Morris MJ, Bryan Rumble R, Basch E, Hotte SJ, Loblaw A, Rathkopf D, et al. Optimizing anticancer therapy in metastatic non-castrate prostate cancer: American society of clinical oncology clinical practice guideline. J Clin Oncol. 2018 May 20;36:1521–39.

206. Chandrasekar T, Yang JC, Gao AC, Evans CP. Mechanisms of resistance in castration-resistant prostate cancer (CRPC). Transl Androl Urol. 2015;4:365–80.

207. Alinari L, Mahasenan K V., Yan F, Karkhanis V, Chung JH, Smith EM, et al. Selective inhibition of protein arginine methyltransferase 5 blocks initiation and maintenance of B-cell transformation. Blood. 2015;125:2530–43.

208. Wu T, Millar H, Gaffney D, Beke L, Mannens G, Vinken P, et al. Abstract 4859: JNJ-64619178, a selective and pseudo-irreversible PRMT5 inhibitor with potent in vitro and in vivo activity, demonstrated in several lung cancer models. Cancer Res. 2018 Jul 1;78:4859.

209. Liu W, Xie CC, Zhu Y, Li T, Sun J, Cheng Y, et al. Homozygous deletions and recurrent amplifications implicate new genes involved in prostate cancer. Neoplasia. 2008 Aug;10:897–907.

210. Liu LL, Xie N, Sun S, Plymate S, Mostaghel E, Dong X. Mechanisms of the androgen receptor splicing in prostate cancer cells. Oncogene. 2014;33:3140–50.

211. Pal S, Vishwanath SN, Erdjument-Bromage H, Tempst P, Sif S. Human SWI/SNF-Associated PRMT5 Methylates Histone H3 Arginine 8 and Negatively Regulates Expression of ST7 and NM23 Tumor Suppressor Genes. Mol Cell Biol. 2004 Nov 1;24:9630–45.

212. Scoumanne A, Zhang J, Chen X. PRMT5 is required for cell-cycle progression and p53 tumor suppressor function. Nucleic Acids Res. 2009;37:4965–76.

213. Gu Z, Li Y, Lee P, Liu T, Wan C, Wang Z. Protein arginine methyltransferase 5 functions in opposite ways in the cytoplasm and nucleus of prostate cancer cells. PLoS One. 2012;7:e44033.

214. Giatromanolaki A, Fasoulaki V, Kalamida D, Mitrakas A, Kakouratos C, Lialiaris T, et al. CYP17A1 and Androgen-Receptor Expression in Prostate Carcinoma Tissues and Cancer Cell Lines. Curr Urol. 2019 Nov 1;13:157–65.

215. Sekhar KR, Wang J, Freeman ML, Kirschner AN. Radiosensitization by enzalutamide for human prostate cancer is mediated through the DNA damage repair pathway. Budunova I, editor. PLoS One. 2019 Apr 1;14:e0214670.

216. Liu C, Armstrong C, Zhu Y, Lou W, Gao AC. Niclosamide enhances abiraterone treatment via inhibition of androgen receptor variants in castration resistant prostate cancer. Oncotarget. 2016 May 31;7:32210–20.

217. Yu J, Yu J, Mani RS, Cao Q, Brenner CJ, Cao X, et al. An Integrated Network of Androgen Receptor, Polycomb, and TMPRSS2-ERG Gene Fusions in Prostate Cancer Progression. Cancer Cell. 2010 May 18;17:443–54.

218. Tee W-W, Pardo M, Theunissen TW, Yu L, Choudhary JS, Hajkova P, et al. Prmt5 is essential for early mouse development and acts in the cytoplasm to maintain ES cell pluripotency. Genes Dev. 2010 Dec 15;24:2772–7.

219. Shilo K, Wu X, Sharma S, Welliver M, Duan W, Villalona-Calero M, et al. Cellular localization of protein arginine methyltransferase-5 correlates with grade of lung tumors. Diagn Pathol. 2013 Dec 10;8.

220. Pak MG, Lee HW, Roh MS. High nuclear expression of protein arginine methyltransferase-5 is a potentially useful marker to estimate submucosal invasion in endoscopically resected early colorectal carcinoma. Pathol Int. 2015 Oct 1;65:541–8.

221. Kumar B, Yadav A, Brown N V., Zhao S, Cipolla MJ, Wakely PE, et al. Nuclear PRMT5, cyclin D1 and IL-6 are associated with poor outcome in oropharyngeal squamous cell carcinoma patients and is inversely associated with p16-status. Oncotarget. 2017;8:14847–59.

222. Yang F, Wang J, Ren H yan, Jin J, Wang A lian, Sun L li, et al. Proliferative role of TRAF4 in breast cancer by upregulating PRMT5 nuclear expression. Tumor Biol. 2015 Aug 24;36:5901–11.

223. Ancelin K, Lange UC, Hajkova P, Schneider R, Bannister AJ, Kouzarides T, et al. Blimp1 associates with Prmt5 and directs histone arginine methylation in mouse germ cells. Nat Cell Biol. 2006;8:623–30.

224. Hou Z, Peng H, Ayyanathan K, Yan K-P, Langer EM, Longmore GD, et al. The LIM Protein AJUBA Recruits Protein Arginine Methyltransferase 5 To Mediate SNAIL-Dependent Transcriptional Repression. Mol Cell Biol. 2008;28:3198–207.

225. Teng Y, Girvan AC, Casson LK, Pierce WM, Qian M, Thomas SD, et al. AS1411 alters the localization of a complex containing protein arginine methyltransferase 5 and nucleolin. Cancer Res. 2007;67:10491–500.

226. Braadland PR, Urbanucci A. Chromatin reprogramming as an adaptation mechanism in advanced prostate cancer. Endocr Relat Cancer. 2019 Apr 1;26:R211–35.

227. Tan DQ, Li Y, Yang C, Li J, Tan SH, Chin DWL, et al. PRMT5 Modulates Splicing for Genome Integrity and Preserves Proteostasis of Hematopoietic Stem Cells. Cell Rep. 2019;26:2316–28.

228. Kanade SR, Eckert RL. Protein arginine methyltransferase 5 (PRMT5) signaling suppresses protein kinase Cδ- and p38δ-dependent signaling and keratinocyte differentiation. J Biol Chem. 2012 Mar 2;287:7313–23.

229. Wüstemann T, Haberkorn U, Babich J, Mier W. Targeting prostate cancer: Prostate-specific membrane antigen based diagnosis and therapy. Med Res Rev. 2019 Jan 1;39:40–69.

230. Gross A, Schoendube J, Zimmermann S, Steeb M, Zengerle R, Koltay P. Technologies for Single-Cell Isolation. Int J Mol Sci. 2015 Jul 24;16:16897–919.

231. Fox MH. A model for the computer analysis of synchronous DNA distributions obtained by flow cytometry. Cytometry. 1980;1:71–7.

232. Livak KJ, Schmittgen TD. Analysis of Relative Gene Expression Data Using Real-Time Quantitative PCR and the 2−ΔΔCT Method. Methods. 2001 Dec;25:402–8.

233. Nelson JD, Denisenko O, Sova P, Bomsztyk K. Fast chromatin immunoprecipitation assay. Nucleic Acids Res. 2006;34:1–7.

234. Tuominen VJ, Ruotoistenmäki S, Viitanen A, Jumppanen M, Isola J. ImmunoRatio: A publicly available web application for quantitative image analysis of estrogen receptor (ER), progesterone receptor (PR), and Ki-67. Breast Cancer Res. 2010 Jul;12:177–202.

235. Faul F, Erdfelder E, Lang AG, Buchner A. G*Power 3: A flexible statistical power analysis program for the social, behavioral, and biomedical sciences. In: Behavior Research Methods. Psychonomic Society Inc.; 2007. p. 175–91.

236. Meister G, Eggert C, Bühler D, Brahms H, Kambach C, Fischer U. Methylation of Sm proteins by a complex containing PRMT5 and the putative U snRNP assembly factor pICln. Curr Biol. 2001 Dec 11;11:1990–4.

237. Friesen WJ, Wyce A, Paushkin S, Abel L, Rappsilber J, Mann M, et al. A novel WD repeat protein component of the methylosome binds Sm proteins. J Biol Chem. 2002 Mar 8;277:8243–7.

238. Saha K, Adhikary G, Eckert RL. MEP50/PRMT5 Reduces Gene Expression by Histone Arginine Methylation and this Is Reversed by PKCδ/p38δ Signaling. J Invest Dermatol. 2016 Jan;136:214–24.

239. Kodama Y, Hu CD. Bimolecular Fluorescence Complementation (BiFC) Analysis of Protein-Protein Interaction. How to Calculate Signal-to-Noise Ratio. Methods Cell Biol. 2013;113:107–21.

240. LeBlanc SE, Konda S, Wu Q, Hu Y-J, Oslowski CM, Sif S, et al. Protein Arginine Methyltransferase 5 (Prmt5) Promotes Gene Expression of Peroxisome Proliferator-Activated Receptor γ2 (PPARγ2) and Its Target Genes during Adipogenesis. Mol Endocrinol. 2012 Apr;26:583–97.

241. Serio J, Ropa J, Chen W, Mysliwski M, Saha N, Chen L, et al. The PAF complex regulation of Prmt5 facilitates the progression and maintenance of MLL fusion leukemia. Oncogene. 2018 Jan 25;37:450–60.

242. Pu WT, Krapivinsky GB, Krapivinsky L, Clapham DE. pICln Inhibits snRNP Biogenesis by Binding Core Spliceosomal Proteins. Mol Cell Biol. 1999 Jun 1;19:4113–20.

243. Hong X, Huang H, Qiu X, Ding Z, Feng X, Zhu Y, et al. Targeting posttranslational modifications of RIOK1 inhibits the progression of colorectal and gastric cancers. Elife. 2018 Jan 31;7.

244. Weinberg F, Reischmann N, Fauth L, Taromi S, Mastroianni J, Köhler M, et al. The Atypical Kinase RIOK1 Promotes Tumor Growth and Invasive Behavior. EBioMedicine. 2017 Jun 1;20:79–97.

245. Barrett T, Wilhite SE, Ledoux P, Evangelista C, Kim IF, Tomashevsky M, et al. NCBI GEO: Archive for functional genomics data sets - Update. Nucleic Acids Res. 2013 Jan;41:D991-5.

246. Cerami E, Gao J, Dogrusoz U, Gross BE, Sumer SO, Aksoy BA, et al. The cBio Cancer Genomics Portal: An open platform for exploring multidimensional cancer genomics data. Cancer Discov. 2012 May;2:401–4.

247. Gao J, Aksoy BA, Dogrusoz U, Dresdner G, Gross B, Sumer SO, et al. Integrative analysis of complex cancer genomics and clinical profiles using the cBioPortal. Sci Signal. 2013 Apr 2;6:PL1.

248. Rhodes DR, Yu J, Shanker K, Deshpande N, Varambally R, Ghosh D, et al. ONCOMINE: A Cancer Microarray Database and Integrated Data-Mining Platform. Neoplasia. 2004 Jan;6:1–6.

249. Xu Y, Song Q, Pascal LE, Zhong M, Zhou Y, Zhou J, et al. DHX15 is up-regulated in castration-resistant prostate cancer and required for androgen receptor sensitivity to low DHT concentrations. Prostate. 2019 May 3;79:657–66.

250. Dobin A, Davis CA, Schlesinger F, Drenkow J, Zaleski C, Jha S, et al. STAR: ultrafast universal RNA-seq aligner. Bioinformatics. 2013 Jan 1;29:15–21.

251. Liao Y, Smyth GK, Shi W. featureCounts: an efficient general purpose program for assigning sequence reads to genomic features. Bioinformatics. 2014 Apr 1;30:923–30.

252. Robinson MD, McCarthy DJ, Smyth GK. edgeR: A Bioconductor package for differential expression analysis of digital gene expression data. Bioinformatics. 2009 Nov 11;26:139–40.

253. McCarthy DJ, Chen Y, Smyth GK. Differential expression analysis of multifactor RNA-Seq experiments with respect to biological variation. Nucleic Acids Res. 2012 May;40:4288–97.

254. Dennis G, Sherman BT, Hosack DA, Yang J, Gao W, Lane HC, et al. Genome-wide distribution of 5-formylcytosine in embryonic stem cells is associated with transcription and depends on thymine DNA glycosylase. Genome Biol. 2003;4:P3.

255. Huang DW, Sherman BT, Lempicki RA. Systematic and integrative analysis of large gene lists using DAVID bioinformatics resources. Nat Protoc. 2009 Dec 18;4:44–57.

256. Boorjian SA, Karnes RJ, Viterbo R, Rangel LJ, Bergstralh EJ, Horwitz EM, et al. Long-term survival after radical prostatectomy versus external-beam radiotherapy for patients with high-risk prostate cancer. Cancer. 2011 Jul 1;117:2883–91.

257. Davies A, Zoubeidi A, Selth LA. The epigenetic and transcriptional landscape of neuroendocrine prostate cancer. Endocr Relat Cancer. 2020;27:R35–50.

258. Suarez CD, Deng X, Hu C-D. Targeting CREB inhibits radiation-induced neuroendocrine differentiation and increases radiation-induced cell death in prostate cancer cells. Am J Cancer Res. 2014;4:850–61.

259. Berman-Booty LD, Knudsen KE. Models of neuroendocrine prostate cancer. Endocr Relat Cancer. 2015;22:R33–49.

260. Beltran H, Prandi D, Mosquera JM, Benelli M, Puca L, Cyrta J, et al. Divergent clonal evolution of castration-resistant neuroendocrine prostate cancer. Nat Med. 2016 Mar;22:298–305.

261. Shen R, Dorai T, Olsson CA, Buttyan R, Katz AE. Transdifferentiation of cultured human prostate cancer cells to a neuroendocrine cell phenotype in a hormone-depleted medium. Urol Oncol Semin Origical Investig. 1997;1439:67–75.

262. Zhang J, Thomas TZ, Kasper S, Matusik RJ. A Small Composite Probasin Promoter Confers High Levels of Prostate-Specific Gene Expression through Regulation by Androgens and Glucocorticoids *in Vitro* and *in Vivo* [1]. Endocrinology. 2000 Dec;141:4698–710.

263. Sales Gil R, Vagnarelli P. Ki-67: More Hidden behind a 'Classic Proliferation Marker.' Vol. 43, Trends in Biochemical Sciences. Elsevier Ltd; 2018. p. 747–8.

264. Terry S, Beltran H. The many faces of neuroendocrine differentiation in prostate cancer progression. Vol. 4 MAR, Frontiers in Oncology. Frontiers Research Foundation; 2014. p. 60.

265. Kaur H, Samarska I, Lu J, Faisal F, Maughan BL, Murali S, et al. Neuroendocrine differentiation in usual-type prostatic adenocarcinoma: Molecular characterization and clinical significance. Prostate. 2020 Sep 10;80:1012–23.

266. Svensson C, Ceder J, Iglesias-Gato D, Chuan Y-C, Pang ST, Bjartell A, et al. REST mediates androgen receptor actions on gene repression and predicts early recurrence of prostate cancer. Nucleic Acids Res. 2014 Jan 1;42:999–1015.

267. Zhang Y, Zheng D, Zhou T, Song H, Hulsurkar M, Su N, et al. Androgen deprivation promotes neuroendocrine differentiation and angiogenesis through CREB-EZH2-TSP1 pathway in prostate cancers. J Urol. 2019;202:32.

268. Bishop JL, Thaper D, Vahid S, Davies A, Ketola K, Kuruma H, et al. The Master Neural Transcription Factor BRN2 Is an Androgen Receptor-Suppressed Driver of Neuroendocrine Differentiation in Prostate Cancer. AACR. 2016;

269. Truett GE, Heeger P, Mynatt RL, Truett AA, Walker JA, Warman ML. Preparation of PCR-quality mouse genomic dna with hot sodium hydroxide and tris (HotSHOT). Biotechniques. 2000;29:52–4.

270. Bankhead P, Loughrey MB, Fernández JA, Dombrowski Y, McArt DG, Dunne PD, et al. QuPath: Open source software for digital pathology image analysis. Sci Rep. 2017 Dec 1;7:1–7.

271. Fujita T, Fujii H. Isolation of Specific Genomic Regions and Identification of Associated Molecules by enChIP. J Vis Exp. 2016 Jan 20;e53478.

272. Braun CJ, Stanciu M, Boutz PL, Patterson JC, Calligaris D, Higuchi F, et al. Coordinated Splicing of Regulatory Detained Introns within Oncogenic Transcripts Creates an Exploitable Vulnerability in Malignant Glioma. Cancer Cell. 2017 Oct 9;32:411–26.

273. Takayama KI. Splicing factors have an essential role in prostate cancer progression and androgen receptor signaling. Biomolecules. 2019 Apr 1;9.

274. Radzisheuskaya A, Shliaha P V., Grinev V, Lorenzini E, Kovalchuk S, Shlyueva D, et al. PRMT5 methylome profiling uncovers a direct link to splicing regulation in acute myeloid leukemia. Nat Struct Mol Biol. 2019 Nov 1;26:999–1012.

275. Namekawa T, Ikeda K, Horie-Inoue K, Inoue S. Application of Prostate Cancer Models for Preclinical Study: Advantages and Limitations of Cell Lines, Patient-Derived Xenografts, and Three-Dimensional Culture of Patient-Derived Cells. Cells. 2019 Jan 20;8:74.

276. Timm DE, Bowman V, Madsen R, Rauch C. Cryo-electron microscopy structure of a human PRMT5:MEP50 complex. Fotiadis D, editor. PLoS One. 2018 Mar 8;13:e0193205.

277. Martin G, Ostareck-Lederer A, Chari A, Neuenkirchen N, Dettwiler S, Blank D, et al. Arginine methylation in subunits of mammalian pre-mRNA cleavage factor I. RNA. 2010 Aug 1;16:1646–59.

278. Mohammed H, Taylor C, Brown GD, Papachristou EK, Carroll JS, D'Santos CS. Rapid immunoprecipitation mass spectrometry of endogenous proteins (RIME) for analysis of chromatin complexes. Vol. 11, Nature Protocols. Nature Publishing Group; 2016. p. 316–26.

279. Hirano D, Okada Y, Minei S. Neuroendocrine Differentiation in Hormone Refractory Prostate Cancer Following Androgen Deprivation Therapy. Eur Urol. 2004 May 1;45:586–92.

280. Buttigliero C, Tucci M, Bertaglia V, Vignani F, Bironzo P, Di Maio M, et al. Understanding and overcoming the mechanisms of primary and acquired resistance to abiraterone and enzalutamide in castration resistant prostate cancer. Cancer Treat Rev. 2015 Dec;41:884–92.